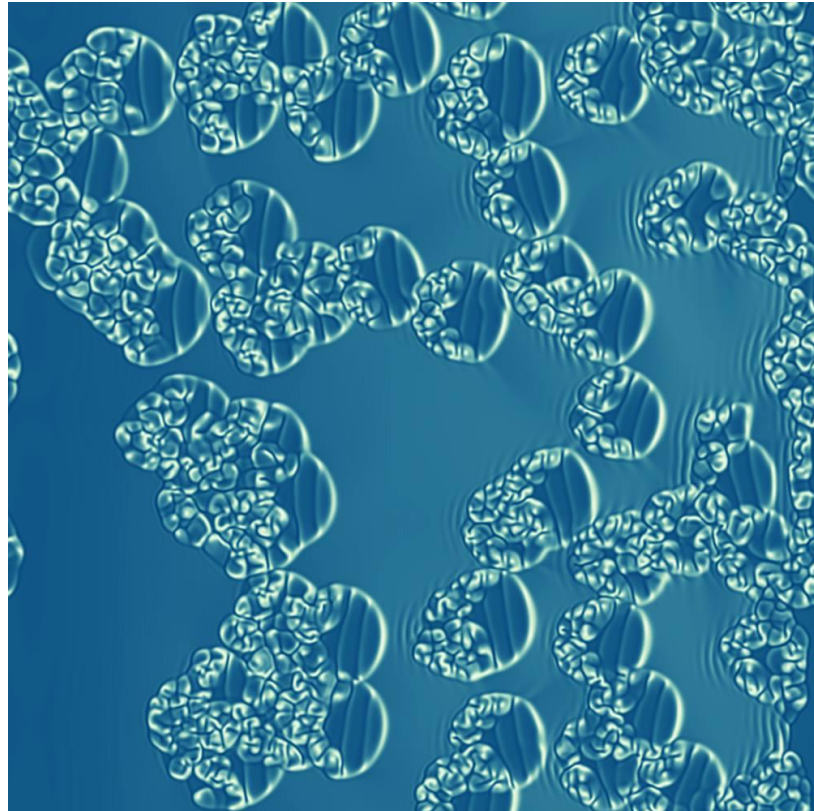


UNIVERSITÉ DE NICE-SOPHIA ANTIPOLIS
THESE EN SCIENCES PHYSIQUES



Strong Resonances in a Field of Oscillators
and
Bifurcations of Defects

Presented by

KJARTAN PIERRE EMILSSON

To obtain the 'Grade de Docteur en Sciences'

june 1994, Sophia-Antipolis, FRANCE

ABSTRACT

There are two subjects in this thesis. In the first part, a qualitative method to classify and predict the structure of defects in reaction-diffusion systems is introduced. This qualitative approach makes it easier to analyze the behavior of defects in complex systems. It also gives us information about the inner structure of the defect, and from that point of view, it makes it possible to approach the concept of defect bifurcation in a novel manner. In the second part, we study the normal form governing the evolution of a spatially extended homogeneous temporal instability, in the presence of a temporal forcing. This is equivalent to studying strong resonances of a field of nonlinear oscillators. A detailed analysis of the phase space of this normal form reveals a rich dynamical structure, which gives rise to a variety of spatial structures. These include excitable pulses, excitable spirals, fronts and spatially periodic structures. These structures are studied and their possible bifurcations are analyzed from a qualitative point of view.

KEYWORDS

Bifurcations and Instability. Strong Resonances. Nonlinear Physics. Topological Defects. Turbulence. Excitability. Chaos. Ginzburg-Landau.

1 INTRODUCTION

In these last 30 years, there has been great progress in the modeling of instabilities emerging in spatially extended systems. The biggest breakthrough was the introduction of amplitude equations describing the evolution of a system's unstable modes, allowing for a macroscopic description of the instability which in general is less complex than a microscopic one [1, 2, 3]. The discovery of universality in the complex temporal behavior of dynamical systems [4, 5] twenty years ago led to hopes that a unified description of spatiotemporal instabilities would be possible. Today, we see an approach to unify the description of instabilities in spatially extended systems using amplitude equations and the qualitative analysis of dynamical systems. We can hope that this approach will lead one day to a qualitative theory of partial differential equations.

The starting point of this approach is that at the onset of instability in a physical system, be it spatially extended or not, we can describe the asymptotic dynamic of the system using a few amplitude equations slowly varying in space and time. An example is fluid convection between two plates with a temperature gradient. Above a certain gradient, the transmission of heat by diffusion becomes less efficient than transmission by fluid movement. We then witness the emergence of convection rolls with a given wavelength. To describe this qualitative change, the amplitude of the unstable mode of the conductive solution is introduced. This amplitude, also called the *order parameter*, actually measures the amount of symmetry breaking induced by the instability. As an example, in his theory of magnetism, Landau writes an equation that describes the transition between paramagnetic and ferromagnetic states. In the 1970s, similar approaches were used successfully in problems involving fluid convection [2, 6, 7, 8]. Since then, numerous works have followed this approach in various domains including Chemistry [9] to describe the oscillating Belousov-Zhabotinsky chemical reaction [10], Optics [11] and Biology [12] (for general review articles see [13, 14, 15, 16, 17, 18])

An approach that has proven very fruitful is the use of the so-called Ginzburg-Landau model. This model arises through the observation that when studying the linear stability of spatially extended systems close to the onset of instabilities, we can identify three generic instability mechanisms. These mechanisms correspond on one hand to temporal instabilities with the emergence of an oscillation with a given frequency ω_0 of a physical observable (e.g. the concentration of a given chemical) and on the other hand spatial instabilities with the emergence of a spatial wavelength k_0 in the system. The third case being the combination of both.

For all three cases ($[\omega_0 \neq 0, k_0 = 0]$, $[\omega_0 = 0, k_0 \neq 0]$ and $[\omega_0 \neq 0, k_0 \neq 0]$), it is possible to derive equations which do not depend on the detailed microscopic mechanisms of the instability but which take into account the symmetry spontaneously broken by the instability. The three *normal forms* that govern the evolution of the marginal amplitudes are the following:

- Spatially homogeneous instability with a non-zero temporal frequency. In this case we describe our physical observable in the form:

$$U(x, t) = Ae^{i\omega_0 t}\psi + \bar{A}e^{-i\omega_0 t}\bar{\psi} + \dots$$

And the corresponding normal form is [9]:

$$\partial_t A = (\mu + iv)A - (1 + i\beta)|A|^2A + (1 + i\alpha)\nabla^2 A \quad (1-1)$$

This equation is known as the complex Ginzburg-Landau equation. This is the canonical form associated with the breaking of the time translation symmetry.

- **Spatially periodic instability with zero temporal frequency.** In this case we describe our physical observable in the form:

$$U(x, t) = (Ae^{ik_0 x} + \bar{A}e^{-ik_0 x})\psi + \dots$$

And the corresponding normal form is [2, 7, 6]:

$$\partial_t A = \mu A - |A|^2 A + \left(\partial_x - \frac{i}{2k_0} \partial_y^2 \right)^2 A \quad (1-2)$$

This equation is known as the Newell-Whitehead-Segel equation. This is the canonical form associated with the breaking of the space-translation symmetry.

- **Spatially periodic instability with a non-zero temporal frequency.** In this case we describe our physical observable as the sum of two progressive waves:

$$U(x, t) = Ae^{i(k_0 x - \omega_0 t)} + Be^{-i(k_0 x + \omega_0 t)} + c.c. + \dots$$

And the corresponding normal form is [19, 20]:

$$\begin{aligned} \partial_t A + c\partial_x A &= (\mu + iv)A - (1 + i\beta)|A|^2A + (\delta + i\gamma)|B|^2A + (1 + i\alpha)\nabla^2 A \\ \partial_t B - c\partial_x B &= (\mu + iv)B - (1 + i\beta)|B|^2B + (\delta + i\gamma)|A|^2B + (1 + i\alpha)\nabla^2 B \end{aligned} \quad (1-3)$$

Which are basically two coupled complex Ginzburg-Landau equations. Depending on the case whether the transition to the spatial wavelength happens in an isotropic manner or not, the spatial derivatives can be more complicated. Here we have chosen the simpler isotropic case.

For a review of all these cases, see for example [18, 17, 10].

Following this description of the elementary symmetry breakings, we can pursue this same approach for secondary instabilities. We then need to study the breaking of the symmetries of the bifurcated states. For example, in the case of cellular structures, an analogous classification of normal forms can be obtained [21].

This approach of describing the instability as slowly varying amplitudes is valid only near the onset of the instability. Farther from the threshold, analysis

is more complicated and the model cited here are no longer valid. It is then possible to describe the bifurcated structure as a slowly varying phase [18].

An important domain of research concerning the Ginzburg-Landau equations and more generally reaction-diffusion equations is the study of defects in the bifurcated structures. These defects happen to have a primordial role in the transition towards spatiotemporal disorder and have led to the notion of defect mediated turbulence or *topological turbulence* [22, 23].

The subject of this thesis is divided in two parts. In the first part (Chapter 2), a qualitative method to classify and predict the structure and dynamic of defects in reaction-diffusion equations is introduced. This method complements existing topological classifications of defects [24, 25, 26, 27, 28, 29]. This qualitative approach facilitates the analysis and prediction of the existence and dynamical behavior of defects in complex systems. It also gives us an insight into the internal structure of the defect and as such allows us to consider the concept of defect bifurcation in a new light. This is especially important considering that defects play a major role in the selection of patterns in spatially extended systems [15, 30].

In the second part, we study the normal form arising from a temporal instability in a spatially homogeneous system Eq.(1-1) subject to temporal forcing. This amounts to the study the resonances in a field of non-linear oscillators. A similar study had been done in the case of spatial forcing of a spatially periodic instability Eq.(1-2) [31, 32]. The dynamical system corresponding to the temporal forcing had also been studied [33, 34]. The forcing introduces new terms in Eq.(1-1), corresponding to the symmetry breaking induced by it while the spatial coupling remains a diffusion-dispersion term. The dynamical system part of these equations define a very rich two-dimensional phase space dependent on 3 parameters. The complexity of this system justifies the use of qualitative methods in order to attempt to classify all the possible phenomenon and instabilities that can arise.

To start with, we perform a detailed analysis of the phase space corresponding to the dynamical system, which gives us the roadmap allowing us to explore this system. Secondly, we will study phenomenon that arise in a limit where the dynamic is reduced to a simpler phase dynamic. Third and last we will study specific instabilities in the case of parametric resonance. In that case, the generic form of defects are *fronts* and these illustrate most of the dynamic observed. We also see how these defects can bifurcate in various ways, sometimes affecting the global state of the system in a very significant manner.

More specifically, in Chapter 3 we have a recall of the notions of temporal forcing and phase locking that ensues. The notion of strong resonances is reviewed and the normal forms for instabilities in a spatially extended system subject to strong resonances are derived. We then do a detailed analysis of the phase space of the dynamical system part of the equations and draw the corresponding bifurcation diagrams.

In Chapter 4, the equations derived in the preceding chapter are studied in the regime where they can be reduced to a simple phase equation. In this regime, we find basically two different type of dynamics: An excitable dynamic,

characteristic of chemical and biological systems and a dynamic leading to the emergence of a spatial wavelength. The latter can be directly attributed to the stabilizing effect of the forcing and phase instability characteristic of Eq.(1-1). We show that in the excitable regime we can have pulses that can travel. These pulses can become the source of excitable spirals in two dimensions. In the regime of the emergence of a spatial wavelength, we show that in two dimensions it leads to the emergence of hexagonal patterns that can become transitionally turbulent.

In Chapter 5, we limit ourselves to the study of parametric temporal forcing. In this case, an analogy with magnetic systems had already been studied [35, 36] but in addition it has been shown that it can describe behavior of nematic liquid crystal in a rotating magnetic field [37]. The richness of this system is substantial such that the methods introduced in Chapter 2 along with the phase diagrams derived in Chapter 3 come as a great help for classifying and explain the phenomenon observed. Two generic structures of these systems are described: fronts and periodical structures.

The front structures come in two essential types: Ising and Bloch domain walls [36], using analogies with magnetism. The transition between these two fronts can be explained as bifurcation of the defect core which breaks the chiral symmetry. For certain parameter values, Bloch fronts can move. It is shown that this leads to the formation of spirals, which have been observed in liquid crystals [38, 39] and whose dynamic can be reduced to a normal form corresponding to a parametric resonance [37, 40]. It is also shown that for other parameter values, the core of the defects can develop a temporal instability, leading to a regular oscillation of the defect core. Secondary instabilities can then occur in the form of period-doubling cascades eventually leading to chaos. In the chaotic regime, we show numerically that the front then undergoes a diffusive and chaotic movement. This is a remarkable manifestation of low-dimensional chaos in a system with a large number of degrees of freedom.

The spatially periodic structures can be considered as a periodic network of fronts. In certain cases, these structures are the result of a competition between a homogenous temporal instability and a spatial instability with a given wavelength. The normal form of the codimension-2 bifurcation is derived. This competition leads to regimes where we observe hexagonal patterns, a transition to hexagons/rolls, a transition to rolls/oscillations and a Ising/Bloch transition of rolls. We present here what amounts to a phenomenological description of these instabilities, thus underlining their richness. Such a study would have been inconceivable without the recourse to massive computing power allowing the interactive study of the system through a wide range of parameter values. Such an approach has the benefit of quickly giving ideas about models that could be interesting to adapt to specific experimental setups.

In this thesis we emphasize the qualitative description of the normal form that describes the strong temporal resonances and we try to understand the mechanisms which lead to instabilities for the various parameter values as well as their relation to the bifurcations of the dynamical system. It is worth

noting though that in these last couple of years, the description of certain physical system, e.g. in liquid crystals and in Chemistry [38, 10] have been reduced to amplitude equations of the form presented here and that numerous instabilities described here have been observed experimentally in these systems. This confirms the interest of these equations that capture a large variety of behaviors. A variety that extend far more than what has been described here. We can hope that many of the instabilities omitted here will be able to be understood as the combination of the basic instabilities described here.

2 A QUALITATIVE THEORY OF DEFECTS

In the introduction we saw how primary spatial and temporal instabilities could be described by simple amplitude equations. These equations are found by projecting the original system down on its center manifold, and removing non-secular terms in the resulting equations by change of variables, such that it takes the simplest form possible. We would now be interested in knowing what kind of qualitative features these simplified equations possess [41].

2.1 THE CONCEPT OF GENERICITY

We will in what follows often refer to the concept of genericity. To illustrate this concept in a more concrete manner, let us take the classical example of codimension 1 bifurcations in dynamical systems [42]. The usual assumption is that we have some dynamical system in the form:

$$\begin{aligned}\partial_t U &= f_\mu(U) \\ f_0(0) &= 0\end{aligned}\tag{2-1}$$

Where U is a N -dimensional vector, and μ an M -dimensional parameter vector. The stability of the zero solution can then be determined by the linearized operator $L_\mu(U)$, as long as it has no eigenvalue with zero real part. Assuming this to be the case, we are interested in knowing under what general condition the matrix L_μ will acquire eigenvalues with zero real part as a function of μ .

Assuming that there exists a μ_0 such that $f_{\mu_0}(p)$ is a hyperbolic fixed point, then the implicit function theorem guarantees that we can find an expression $p(\mu)$, such that $p(\mu)$ is an equilibrium point. If μ is M -dimensional, $p(\mu)$ will define an M -dimensional manifold \mathcal{M} in (x, μ) space. We can now associate to each point of \mathcal{M} the corresponding linearized operator for that point. This operator can be represented as a point in the space of $N \times N$ matrices, so \mathcal{M} will be mapped to an M -dimensional manifold in matrix space.

But in the space of $N \times N$ matrices, we can define manifolds which represent matrices fulfilling some specific condition. We can for example define the set of $N \times N$ matrices fulfilling the condition of having exactly one zero eigenvalue, or the set having exactly one pure imaginary pair of eigenvalues. It can be easily shown that these sets both form $N \times N - 1$ dimensional manifolds, i.e. of codimension 1 in $N \times N$ space.

But one very important result of differential topology is that two manifolds in n -dimensional space will generically have a non-empty intersection if the sum of their respective dimensions is higher or equal to the dimension of the embedding space (see Figure 1).

This gives us the very general result that if our system f depends on at least one parameter, then there generically exists values of the parameter(s) such that the linearized operator has a zero eigenvalue (or a pure imaginary conjugate pair).

More physically speaking, we can formulate this result as: Any system with at least one control parameter will generically undergo a codimension 1 bifurcation for some value of that parameter.

This simple example illustrates the vagueness of the genericity concept, as it is hidden in the complicated realm of differential topology, but at the same time it shows us how general the results can be once it is applied to some specific example. Another consequence of this general result is that to observe bifurcations of higher codimension, we will need as many parameters more to obtain genericity of that bifurcation.

To come back to the example of codimension 1 bifurcation, we can actually push our result even farther. By virtue of the center manifold theorem, it is clear that near the bifurcation value, we can reduce the dimension of our system by projecting it on the center manifold (e.g. by averaging out rapidly oscillating modes). Furthermore, we can choose our projection in such a way as to choose the simplest possible form of the resulting equations, thus leading to a normal form presentation of our reduced system. For the codimension 1 bifurcations these are often represented as:

- One real zero eigenvalue:

$$\partial_t U = \mu U - U^3, \quad U \in \mathbb{R} \quad (2-2)$$

- One conjugate pair of pure imaginary eigenvalues:

$$\partial_t A = (\mu + iv)A - (1 + i\beta)|A|^2A, \quad A \in \mathbb{C} \quad (2-3)$$

These two bifurcations are named the *pitchfork bifurcation* and the *Hopf bifurcation* respectively.

To sum it up: Any physical system, described by a dynamical system depending on at least one parameter, will have parameter values where its behavior is described by either one of the above equations. So much for that.

Now we can ask ourselves how this carries over to partial differential equations. The answer to that question lies behind much of the work which has been done in the field of amplitude equations in this last decade, but was in fact known much before that in the domain of phase transitions.

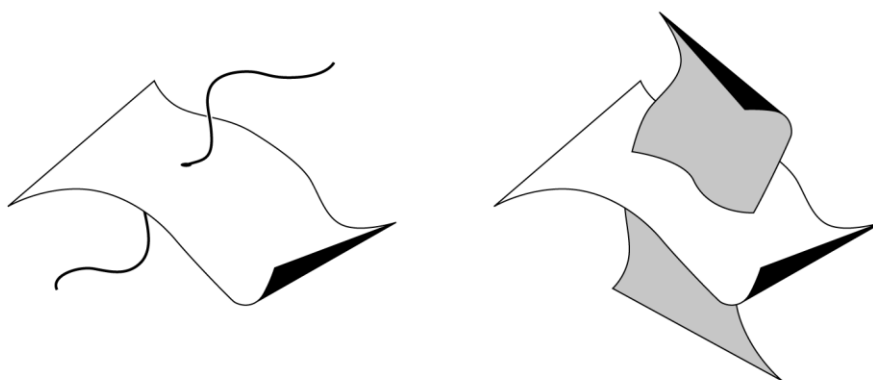


Figure 1: Generic intersection of manifolds in three-dimensional space. The first is codimension 3 and the second codimension 2.

First of all, the notion of center manifold can in some cases still be defined. Thus whenever there is a separation of scales in the system, be it temporal or spatial scales, we can sometimes average out the fast scales, to obtain an equation in the slow variables. Assuming this to be the case, the relevant question is then whether the separation of spatial scales occurs in some generic manner, as it does in the temporal domain for codimension 1 bifurcations.

For some general classes of systems this is indeed the case. If we consider for example the large class of reaction-diffusion systems, with a linear diffusion part:

$$\partial_t U = f(U) + D(\nabla)U \quad (2-4)$$

Where the operator ∇ can be in 1,2 or 3 spatial dimensions, and D is polynomial. Transforming the linearized equation to Fourier modes gives us:

$$\partial_t \tilde{U}_k = L(\tilde{U}_k) + D(-i\vec{k})\tilde{U}_k \quad (2-5)$$

Writing the real part of the growth rate as $\sigma(\vec{k})$, and assuming there is a parameter μ such that for some μ we have $\sigma(\vec{k}) < 0$ for all \vec{k} . In a similar manner as for temporal bifurcations, we ask ourselves how this growth rate can become positive. Generically, by varying μ , there will be a value μ_0 such that $\sigma(\vec{k}_0) = 0$ (or $\sigma(|\vec{k}_0|) = 0$ if the system is assumed isotropic). If $\vec{k}_0 = 0$ then we have a natural separation of scales in the system, as a continuous band of low frequency spatial modes get excited around zero, while the remaining modes are linearly stable. We can then locally estimate the growth rate by a Taylor expansion, which yields at first order:

$$\tilde{\sigma}(k) = \mu - \mu_0 - \vec{k} \cdot \vec{k} \quad (2-6)$$

In the case that $|\vec{k}_0| > 0$, we have the appearance of a wavelength in the system, but a continuous band of wavevectors are being excited around \vec{k}_0 . Intuitively, the interaction of these nearby modes leads to very long scale modulations, thus we are led to consider these slow modulations of the pattern. This is basically done by rewriting the system centered around \vec{k}_0 with the growth rate expanded as a Taylor series. In the anisotropic case, this yields the same estimation as above, but in the isotropic case the result is (in two dimensions $\vec{k}_0 = (k_x, k_y)$):

$$\tilde{\sigma}(k) = \mu - \mu_0 - (k_x + \frac{k_y}{2k_0})^2$$

As can be seen, by very general arguments, we are led to write down the equations expressing the form of a system on its central manifold at the onset of a spatial instability. By generalizing even further, nothing prevents us from now including the generic temporal instabilities in this picture, as previously described. We can thus look for the normal forms expressing all possible combinations of the unstable temporal modes (characterized by the eigenvalues 0 or $\pm i\omega_0$) and unstable spatial modes (characterized by the eigenvalues 0 or $\pm k_0$), expressing all possible codimension 1 instabilities possible. This gives us the equations Eq.1-2, Eq.1-1 and Eq.1-3 shown in the introduction.

One other source of richness for spatial structures is their disorder. With disorder, a simple structure like a regular set of rolls in a Rayleigh-Bénard experiment, can show itself under infinitely many aspects. The disorder of patterns can be characterized by the defects of the pattern. The possible defects for a given pattern depend strongly on the genericity of defects, in the sense that there are few elementary ones, which can account for a variety of disorder in patterns.

2.2 THE GENERIC EXISTENCE OF DEFECTS

Let us first note that these equations take the form of reaction-diffusion equations, i.e. a system where we can clearly separate the part responsible for the temporal or dynamical behavior from the spatial behavior characterized by diffusion. This permits us to expect that even though the formal phase space of a partial differential equation is infinitely dimensional, there will occur a rapid contraction of the dimensionality of the system, due to diffusive terms, which will eventually end up on a low-dimensional attractor characterized by a dynamic on a central manifold, obeying the equations of the reaction part.

To make this approach more explicit, we will assume that we have a parameter α which governs the amplitude of the diffusive part, i.e. we assume a system of the form:

$$\partial_t U = f(U) + \alpha D(U, \nabla)$$

In the limit of $\alpha \rightarrow 0$, this system reduces to an infinite set of discrete dynamical systems, where each point of the field $U(x, t)$ corresponds to an initial condition of f , which will evolve independently of its neighboring points. As such we can think of the configuration of the spatial field at a given instant t as being a ‘drop’ of initial conditions of the dynamical system. Alternatively, we could extend the dynamical system with a number of dimension equal to the number of spatial dimensions, i.e. treat the spatial coordinates as variables with no dynamic, shown here for a two-dimensional case:

$$\begin{aligned} \partial_t U &= f(U(x, y)) \\ \partial_t x &= 0 \\ \partial_t y &= 0 \end{aligned} \tag{2-7}$$

Which has the advantage of preserving the internal dimensionality of the ‘drop’. We thus see for example, that for a two-dimensional spatial system, a smooth configuration of the field will be mapped into a smooth two-dimensional manifold in this extended phase space.

We then ask the following question: for an arbitrary initial configuration of the field, can we predict on what attractor, if any, this configuration will relax on in this extended phase space? This turns out to be possible in many cases and under very general conditions.

Indeed, if we consider the phase space of the reaction part of Eq.2-2, we can apply all the usual tools of the qualitative theory of discrete dynamical systems, to end up with a purely topological description of this phase space in terms of elementary invariant limit sets, like fixed points, heteroclinic and homoclinic

orbits and limit cycles. If the dimension of the discrete system is higher than two, and we have a homoclinic orbit, then we will also have to include more complicated attractors, like strange chaotic attractors. We will assume here that we can limit ourselves to the simplest limit sets.

For asymptotic dynamics, the most interesting limit sets are the non-wandering sets such as fixed points and limit cycles, and more specifically the attracting sets, i.e. stable fixed points and attracting limit cycles. These sets have an associated domain of attraction, in which each point will eventually converge to the attracting set. One important feature of these sets is that the domain of attraction of disjoint attracting sets are necessarily non-intersecting and separated by the stable manifolds of non-attracting sets [42].

This feature lies at the basis of a qualitative theory of defects. Indeed, we see that for example if we have a dynamical system with two attracting sets, and if our spatial configuration, when mapped in our extended phase space, is such that one part lies in the domain of attraction of one set, while another part lies in the second domain, we will necessarily have at least one part of the system intersecting the stable manifold of a non-attracting set.

As a stable manifold is an invariant set, any point on it will be trapped there. Subsequent evolution should then lead (for $\alpha = 0$) to the formation of a singularity, where two parts of the field lie on two different stable solutions, separated by a discontinuity lying on an unstable solution. We argue that these discontinuities form the core of the defect.

The whole question is then: Given the topology of phase space, under what general conditions can we expect the formation of discontinuities, and what will be the fate of these discontinuities in the presence of diffusion? The first question can be addressed by using genericity arguments, thus giving us a general method to predict the generic existence and nature of defects. The answer to the second question is subtler, and should be considered case by case. We begin by answering the first question.

Let us assume that our spatial field lives in d spatial dimensions, and is an N -dimensional vector field. The phase space will thus typically be N -dimensional, and our extended phase space will be $N + d$ dimensional. By mapping the field into this extended phase space, it will trace a d -dimensional manifold \mathcal{I} , which we will call the *spatial manifold*.

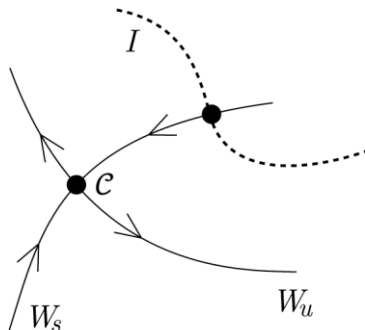


Figure 2: The attracting set \mathcal{C} and its stable and unstable manifold

Let us now assume that there exists a non-attracting set \mathcal{C} . This set will typically have unstable and stable manifolds $W_u(\mathcal{C})$ and $W_s(\mathcal{C})$ respectively. As \mathcal{C} belongs to both sets, we can write the following dimensional relations:

$$\dim W_u(\mathcal{C}) + \dim W_s(\mathcal{C}) = N + \dim(\mathcal{C})$$

We are interested in knowing when an arbitrary configuration \mathcal{I} will intersect the stable manifold $W_s(\mathcal{C})$. Knowing that this will generically happen when the sum of their respective dimensions is equal or greater to the space in which they are embedded, we obtain the condition:

$$\dim W_s(\mathcal{C}) + \dim(\mathcal{C}) \leq N$$

i.e.:

$$d \leq \dim W_u(\mathcal{C}) - \dim(\mathcal{C}) \equiv n_u(\mathcal{C})$$

Where $n_u(\mathcal{C})$ denotes the number of unstable directions of \mathcal{C} . Thus we get a general result which tells us that to know if we can expect the apparition of defects, it suffices to count the unstable directions of non-attracting sets and compare it to the dimension of physical space. We also note that the dimension of phase space does not appear, and does thus not matter (except for the maximum number of unstable directions available of course).

We can now estimate what the dimension of the intersection will be, if it exists. We can write a general expression for this:

$$\dim(\mathcal{I} \cap W_s(\mathcal{C})) = \dim(\mathcal{I}) + \dim W_s(\mathcal{C}) - N$$

i.e.:

$$\dim(\mathcal{I} \cap W_s(\mathcal{C})) = d - n_u(\mathcal{C})$$

This intersection corresponds to the core of the defect, and its dimension in physical space will be the same. We can thus write an expression for the codimension of the defect core \mathcal{D} with respect to physical space as:

$$\text{codim}(\mathcal{D}) = d - \dim(\mathcal{I} \cap W_s(\mathcal{C})) = n_u(\mathcal{C})$$

So the codimension of a defect in physical space is equal to the number of unstable directions of the non-attracting set. This is quite a general result, and can be applied in a variety of ways. It tells us for example that for a scalar field, only codimension 1 defects can be expected. This excludes for example point defects for a two-dimensional scalar field, while they are possible for a complex field.

2.3 THE EFFECT OF DIFFUSION

We now turn to the problem of determining what will happen to the singularity once the diffusion is turned on. The basic idea is that the diffusion amounts to a contraction of the spatial manifold in phase space. This contraction can be either hindered or favored by the underlying dynamics. The whole question is thus in what situation the effect of dynamic cancels out the contracting effect of diffusion, but that is the only possibility for the persistence of a non-trivial spatial structure. One answer to this is the case where there is a presence of

symmetry in phase space, where the defect connects two symmetrically equivalent states. In that case the domain of attraction of the two different states are identical and the diffusion can do nothing except smooth out the singularities.

A typical example of this is the basic kink defect, which can be found for example in the following system:

$$\begin{aligned}\partial_t U &= U - U^3 + \partial_x^2 U \\ \partial_t V &= -V\end{aligned}\tag{2-8}$$

The phase space of this system consists of two stable non-trivial fixed points and the unstable origin.

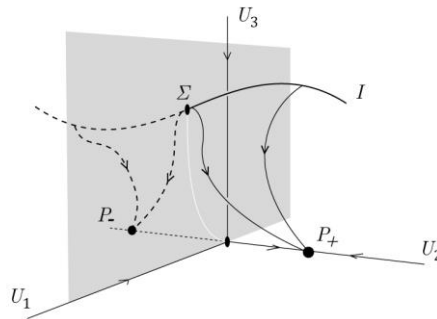


Figure 3: Formation of a kink defect

As can be seen in Figure 3, an arbitrary initial configuration will generically intersect the stable manifold of the unstable point. This point has one unstable direction, thus we expect the formation of a codimension 1 defect. Half of the manifold will thus be attracted to the point P_+ while the other will be attracted to P_- . In one spatial dimension, this is a 0-dimensional defect, i.e. a point defect. Because the two stable states are symmetric, the evolution will create a smooth kink solution joining the two states.

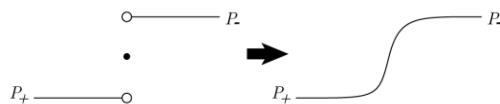


Figure 4: Spatial solution with kink defect, without and with diffusion

Another example is the case where we have a stable limit cycle, which has appeared as a result of a Hopf bifurcation of some fixed point as is shown in Figure 5. In this case, the fixed point has two unstable directions, so we expect a defect of codimension 2. Such defects can occur in for example Eq.(1-2), in two spatial dimensions.

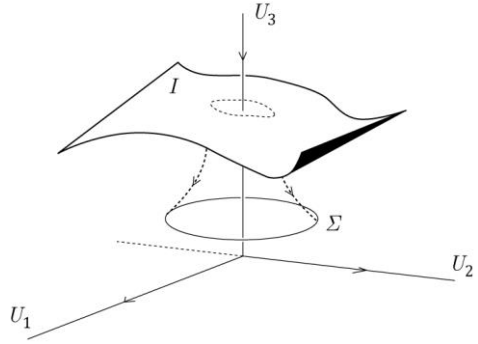


Figure 5: Formation of a vortex defect

In this case we expect a generic intersection of the two dimensional spatial manifold with the origin. For $\nu = \beta = 0$, the limit cycle is in fact a degenerate cycle of fixed points, so we observe the formation of point defect with radial equiphases. The effect of diffusion in this case will be to regularize the equiphases, thus leading to a regular vortex. In the case $\nu \neq 0$, we have a regular limit-cycle with a constant angular velocity. The spatial manifold will thus wind itself around the origin with a constant rotation rate. The diffusion will in this case make the equiphases rotationally invariant and thereby select a constant phase gradient, which corresponds to a wavenumber. We will thus observe the creation of a phase spiral (see Figure 6).



Figure 6: Phase spirals of Eq.(1-2) in two dimensions ($\alpha = 0, \beta = \nu = 1$)

2.4 DEFECT BIFURCATIONS

An important concept which acquires a new aspect in this formalism, is the notion of bifurcation of defects from a qualitative point of view. Indeed, as we have seen, the core of the defect generically lies on an unstable solution of the system. As such one could think that the core would be a sensitive and unstable region. This is usually not so, because the diffusion actually strings the defect across the unstable solution and it actually has little freedom of movement in this topological confinement.

But if any change occurs to the unstable solution, these changes will be immediately reflected in the core of the defect, and we can thus expect that bifurcation of defects follow bifurcations of the unstable solution.

In fact, the situation is a little bit more complex as the defect originally arises by an intersection of the stable manifold with the unstable solution and it may actually happen that the core really stays on the stable manifold instead of converging on the unstable solution. We thus see that the core of the defect is sensitive to both the unstable solutions and its stable manifold. We can thus expect a bifurcation of the defect not only for bifurcations of the unstable

solutions but also for any quantitative change of the flow on the stable manifold of that unstable solution. This gives a wide variety of possible critical situations for the core of the defect.

Another complication arises on how to interpret dispersive effects, and in a more general manner, all non-variational effects. A system is said to be variational if its evolution equation can be derived by a variational principle from a free energy, i.e. we can write:

$$\partial_t A = -\frac{\delta H(A)}{\delta \bar{A}}$$

Where $\delta/\delta\bar{A}$ denotes functional derivation. Such systems are also called gradient flows. An important characteristic of such systems is that, as they are derived from an energy potential, there exists a state of lowest energy, and the system will eventually relax on that state thus reaching a state of static equilibrium. Non-variational systems are systems where we cannot define a free energy and we thus cannot derive an evolution equation from a variational principle.

This is characteristic of non-equilibrium systems, in which energy is constantly pumped into the system to compensate diffusive effects. Such systems will in general have no static equilibrium, though a dynamical equilibrium might be attained.

We will see in the next chapters how non-variational effects lead to the existence of non-static defects, which can have a very complicated behavior at their core, eventually leading to complex spatiotemporal states, which can be considered as weakly turbulent.

3 STRONG RESONANCES IN A FIELD OF OSCILLATORS

Oscillatory behavior is quite common in physical systems and as we have seen this can be understood by the fact that the Hopf bifurcation is a generic instability of dynamical systems depending on one parameter. The question now arises what secondary instabilities can occur in oscillatory systems. A well-known scenario for a secondary instability of a Hopf bifurcation is the period-doubling cascade, eventually leading to chaotic behavior. Oddly enough, this universal behavior of finite dimensional dynamical systems has never been observed in spatially extended systems. In a more general framework, we can note that physical systems can rarely be considered as fully isolated, so we expect to observe phenomenon linked to the interaction between individual systems. For oscillatory systems this leads to the study of interaction between systems oscillating at different frequencies. This is the basis of the phenomenon of *resonances*.

3.1 NORMAL FORMS OF STRONG RESONANCES

The basic approach consists in considering the Poincaré map of a Hopf bifurcation [42, 34, 33]. In the presence of a simple limit cycle of a given period ω_0 , this map consists of a single fixed point Z_0 . The discrete map governing the local stability of this point can be written:

$$Z_{i+1} = \lambda Z_i + N(Z_i) \quad (3-1)$$

with λ a complex parameter and N represents non-linear terms. This same system is obtained when studying the Poincaré map for two coupled oscillators. A classification of all possible instabilities can be made by studying the multiplier λ . In the case that $|\lambda| < 1$, the fixed point is stable so the basic oscillation remains unperturbed (the oscillators are uncoupled). When λ crosses the unit circle, a variety of behaviors occur (see Figure 7), and to make things clearer, we will write $\lambda = (1 + \mu)e^{i(\omega_0/\omega)^2\pi}$.

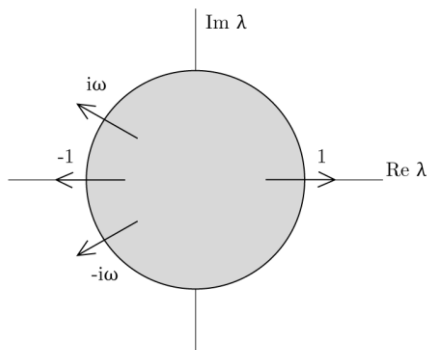


Figure 7: Possible unstable eigenvalues for the perturbation of a limit cycle

First of all, we note that when ω_0/ω is an irrational number, the iterates of Eq.(3-1-1) will be mapped around and invariant circle without ever returning to the same point. The orbit will be dense on the circle. In terms of coupled

oscillators, we can then see that the trajectories in phase space trace out a torus, which they cover densely. The temporal behavior is then said to be *quasi-periodic*.

When the frequency ratio is rational we can write it as an irreducible fraction m/n . In this case we see that the fixed point traces a periodic orbit of period n . Such states are named *phase-locked states*, as it can be understood that there now exists a fixed relation between the phase of the two oscillators. This is also called a *resonance of order n* . This terminology arises from the structure of the normal form constructed for a given frequency ratio.

The normal form of Eq.(3-13-1) will govern the local behavior of the fixed point near the threshold $|\lambda| = 1$, and will define the central manifold on which the bifurcated solutions will evolve. The exact representation of these normal forms is directly related to the symmetries that the system obeys. For a resonance m/n we can state this symmetry requirement as the invariance by rotations $e^{i(m/n)2\pi}$.

In the cases $n \in \{1,2\}$, the multiplier is real, $\lambda = \pm 1$. This has as a consequence that the central manifold will be one-dimensional. We can thus write the normal form as the mappings obeying $X \rightarrow X$ ($n = 1$) and $X \rightarrow -X$ ($n = 2$). At lowest order, the corresponding mappings are:

$$\begin{aligned} (n=1) \quad X_{i+1} &= (1 + \mu)X_i + \delta X_i^2 + \dots \\ (n=2) \quad X_{i+1} &= -(1 + \mu)X_i + \beta X_i^3 + \dots \end{aligned}$$

where X is the coordinate of the iterations along the central manifold.

In the cases $n > 2$, the multiplier is complex and the corresponding complex normal forms obeying the symmetry requirement are found to be:

$$Z_{i+1} = \lambda Z_i + \sum_{j=1}^{(n-1)/2} a_j |Z_i|^{2j} Z_i + \gamma \bar{Z}_i^{n-1} \quad (3-2)$$

which is of order $|\bar{Z}|^n$. The resonances which can be described by a normal form involving only cubic non-linearities are called *strong resonances*, and they correspond to $n < 5$. All other cases are called *weak resonances*. We will see another justification for this division later, but a general argument states that for weak resonances, the additional terms can be safely neglected, thus leaving us with a normal form identical to the non-resonant case.

In the case of strong resonances, the first two cases can be simply interpreted, and are maybe the most commonly studied. They represent for mappings what codimension 1 bifurcations are for flows with a simple eigenvalue zero.

The $n = 1$ resonance occurs for example in oscillators subjected to an additive external forcing. It is well known that the response of such systems is strongest when the internal and external frequency match. This resonance is the equivalent of a pitchfork (or transcritical) bifurcations for flows. It is thus characterized by the loss of stability of the original limit cycle with the apparition of two new stable limit cycles (in the pitchfork case).

The $n = 2$ resonance occurs in oscillators subjected to a parametric forcing at twice the natural frequency, and it is also the basis of the mechanism of period doubling. This bifurcation has no analog to bifurcations in flows. It corresponds to the apparition of a new limit cycle with twice the period as the original one, and as such this is also known as a *subharmonic bifurcation*.

For $n > 2$, we have what is the formal equivalent of a Hopf bifurcation for flows, but the analysis is more complicated and the resulting behavior richer.

3.2 ARNOLD TONGUES

At this point we might ask why resonance phenomena are observed at all in nature, considering the fact that they only occur for rational frequency ratios, which have a measure zero. The answer to that lies in the non-linearity of the dynamic, which guarantees the existence of a central manifold at the bifurcation threshold. On that manifold, the dynamic is governed by the normal forms cited above, which are invariant by rotations of the form $e^{i(m/n)2\pi}$. If we consider how these are affected by a small deviation from a rational frequency ratio of the form $m/n + \nu$, it can be shown that for ν small enough and a finite distance from threshold, the $e^{i\nu 2\pi}$ term can be absorbed through the coefficients of the normal form. This small deviation is called the *detuning* or the *mismatch*. This interesting result thus states that for a small detuning and a given distance above threshold the resonance persists in a finite interval of frequency ratios. Thus the criterion of resonance now exists for a set of non-zero measure, and this set increases with the distance from the bifurcation threshold. If we trace the domain of the detuning as a function of threshold we obtain what is called a *resonance horn* or *Arnold tongue* (see Figure 8).

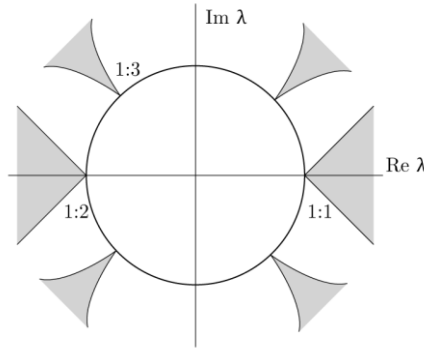


Figure 8: Arnold tongues for a Hopf bifurcation

This leads to the second justification for the terms of strong and weak resonances. Indeed, it can be shown that the form of an Arnold tongue for weak resonances is given by:

$$\Delta\nu \approx \mu^{\frac{n-2}{2}}$$

where μ is the distance from the threshold. The tongues are thus seen to be extremely narrow near the threshold. In a certain manner, strong resonances represent the majority of possible resonances for a given threshold value. But even more important is the fact that when a system has locked on a strong

resonance, then this locking is robust, i.e. persists for small changes of parameters.

To illustrate these concepts, we will now set about to determine the normal form for a weakly non-linear oscillator subject to parametric forcing.

3.3 PARAMETRIC RESONANCE OF A WEAKLY NONLINEAR OSCILLATOR

Given the non-linear oscillator of the form:

$$\partial_t^2 U + (\omega_0^2 + \nu + 2\gamma \cos \omega t)U - \beta U^3 - 2\mu \partial_t U + \alpha \partial_t U U^2 = 0 \quad (3-3)$$

For $\mu < 0$ this oscillator is damped, so we expect the appearance of self-oscillation for $\mu > 0$. These oscillations will be saturated by the non-linear terms and perturbed by the parametric forcing. The form of the non-linear damping is such that the effective damping is negative for small amplitudes, but becomes positive for large amplitudes. To make an analysis of the behavior close to threshold, we assume that all non-linearities are small and that the detuning is small, i.e. we introduce the order relation:

$$\nu \sim \gamma \sim \beta \sim \mu \sim \alpha \sim \epsilon$$

We can now perform a multi-scale analysis by introducing the timescale $\partial_t \rightarrow \partial_t + \epsilon \partial_T$ and writing U as: $U = U_0 + \epsilon U_1 + \dots$. By inserting into Eq.(3-3) and identifying orders of ϵ we obtain:

ϵ^0 :

$$\partial_t^2 U_0 + \omega_0^2 U_0 = 0$$

which has the general solution:

$$U_0 = A(T)e^{i\omega_0 t} + \bar{A}(T)e^{-i\omega_0 t}$$

We now go to the next order:

ϵ^1 :

$$\begin{aligned} \partial_t^2 U_1 + \omega_0^2 U_1 &= -2\partial_T \partial_t U_0 - \nu U_0 - \gamma(e^{i\omega_0 t} + e^{-i\omega_0 t})U_0 + \beta U_0^3 + 2\mu \partial_t U_0 \\ &\quad - \alpha U_0^2 \partial_t U_0 \\ &= -2(i\omega_0 \partial_T A e^{i\omega_0 t} - i\omega_0 \partial_T \bar{A} e^{-i\omega_0 t}) - \nu(A e^{i\omega_0 t} + \bar{A} e^{-i\omega_0 t}) \\ &\quad - \gamma(A e^{i(\omega_0+\omega)t} + A e^{i(\omega_0-\omega)t} + \bar{A} e^{-i(\omega_0+\omega)t} + \bar{A} e^{-i(\omega_0-\omega)t}) \\ &\quad + \beta(A^3 e^{3i\omega_0 t} + 3|A|^2 A e^{i\omega_0 t} + 3|A|^2 \bar{A} e^{-i\omega_0 t} + 3\bar{A}^3 e^{-3i\omega_0 t}) \\ &\quad - \alpha(i\omega_0 A^3 e^{3i\omega_0 t} + i\omega_0 |A|^2 A e^{i\omega_0 t} - 3i\omega_0 |A|^2 \bar{A} e^{-i\omega_0 t} \\ &\quad - i\omega_0 \bar{A}^3 e^{-3i\omega_0 t}) \\ &\quad + 2\mu(i\omega_0 A e^{i\omega_0 t} - i\omega_0 \bar{A} e^{-i\omega_0 t}) \end{aligned}$$

Resonant terms are of the form $e^{i\omega_0 t}$ and $e^{-i\omega_0 t}$. Such terms appear in the forcing term when $\omega = 2\omega_0$. Let's assume this to be the case. Resonant terms with $e^{i\omega_0 t}$ thus yield the following solvability condition:

$$\partial_T A = \left(\mu + i \frac{\nu}{2\omega_0} \right) A - \left(\frac{\alpha}{2} + i \frac{3\beta}{2\omega_0} \right) |A|^2 A + i \frac{\gamma}{2\omega_0} \bar{A}$$

By rescaling time such that $T \rightarrow \frac{1}{\mu}T$ and then scale A such that $A \rightarrow A\sqrt{2\mu/\alpha}$, we get:

$$\partial_T A = \left(1 + i\frac{\nu}{2\mu\omega_0}\right)A - \left(1 + i\frac{3\beta}{\alpha\omega_0}\right)|A|^2 A + i\frac{\gamma}{2\mu\omega_0}A$$

And finally we can make the coefficient of \bar{A} real with the rotation $A \rightarrow Ae^{i\pi/4}$. By writing $\nu' = \nu/2\mu\omega_0$, $\beta' = 3\beta/\alpha\omega_0$ and $\gamma' = \gamma/2\mu\omega_0$ and dropping primes we finally obtain:

$$\partial_T A = (1 + iv)A - (1 + i\beta)|A|^2 A + \gamma\bar{A} \quad (3-4)$$

which is the normal form for the $\omega \approx 2\omega_0$ parametric resonance. The next term in the expansion of U will be of the form:

$$U_1 = B(A, \bar{A})(T)e^{3i\omega_0 t} + \bar{B}(A, \bar{A})e^{-3i\omega_0 t}$$

So the full solution is given by:

$$U = Ae^{i\omega_0 t} + \epsilon B(A, \bar{A})e^{3i\omega_0 t} + c.c. + \dots$$

with B equal to:

$$B = -\frac{((\beta - i\alpha\omega_0)A^2 - \gamma)A}{8\omega_0^2}$$

We note that this term vanishes with A , thus excluding the possibility of a purely forced solution. This is characteristic of the form of the parametric forcing, i.e. components at the forcing frequency never appear by themselves.

Depending on the different form of attractors of the normal form, we can describe different types of physical solutions:

- $A = 0$ No oscillations
- $A = R_0 e^{i\varphi_0}$ Oscillations in phase with the forcing

To extend this analysis to a spatially extended system of coupled non-linear oscillators is straightforward, but to illustrate another approach we will now derive this same equation for a spatially distributed system by using simple symmetry arguments.

3.4 STRONG RESONANCES IN SPATIALLY EXTENDED SYSTEMS

We have already seen that for a homogeneous spatially extended system which undergoes a Hopf bifurcation with a frequency ω_0 (e.g. a chemical reaction), we can write any observable as:

$$U = A(X, T)e^{i\omega_0 t} + c.c. + h.o.t.$$

The invariance of the original system with regards to time translations $t \rightarrow t + \tau$, imposes that A should be invariant by an arbitrary rotation of phase $A \rightarrow Ae^{i\varphi}$. This led to the normal form:

$$\partial_T A = (\mu + iv)A - (1 + i\beta)|A|^2 A + (1 + i\alpha)\nabla^2 A$$

The presence of the external forcing with period T_e introduces a time reference, so we now have the discrete time-translation symmetry $t \rightarrow t + kT_e$ instead of the continuous one. The symmetry requirements thus read:

$$A \rightarrow Ae^{i\omega_0 k T_e} = Ae^{i\frac{\omega_0}{\omega_e} k 2\pi}$$

If the external frequency is related to the internal frequency by a rational multiple m/n , the symmetry requirement becomes $A \rightarrow Ae^{i(km/n)2\pi}$. We will thus have to Eq.(3-4) terms which have this symmetry. For a given n , these can be shown to be of the form \bar{A}^{n-1} , so we have:

$$\partial_T A = (\mu + iv)A - (1 + i\beta)|A|^2 A + (1 + i\alpha)\nabla^2 A + \gamma_n \bar{A}^{n-1} \quad (3-5)$$

Which is the normal form valid for resonance of order $n < 5$.

From the previous analysis of the weakly nonlinear oscillator we can interpret the parameter of Eq.(3-5) simply. The parameter μ corresponds to the damping, the oscillator being damped for $\mu < 0$. The parameter v is simply the detuning, i.e. the deviation of the frequency ratio from being a rational. The real part of the cubic coefficient describes the nonlinear character of the damping, while the imaginary part accounts for the amplitude dependence of the natural frequency. As such the latter acts in a similar way as the detuning. The spatial term accounts for diffusion and dispersion respectively and finally γ which is directly related to the amplitude of the external forcing.

3.5 NOTE ON AVERAGING

A word of caution is due, in what regards the interpretation of the above amplitude equations as normal forms for a given resonance. The possible confusion arises from the act of averaging involved for example in the multi-scale analysis. Indeed, we have already seen in section 3.1 what the normal forms are for the loss of stability of a limit cycle. But these normal forms are *mappings*, corresponding exactly to the behavior of the Poincaré map of the original cycle, and as such they cannot be interpreted as flows simply by dropping the iteration index.

To clarify this, it is instructive to recall the basis of the averaging method [42]. Supposing that we have a system of the form:

$$\dot{x} = \epsilon f(x, t, \epsilon) \quad x \in \mathbb{R}^n \quad \epsilon \ll 1$$

where f is T -periodic. It is then possible to define the averaged system:

$$\dot{y} = \epsilon \frac{1}{T} \int_0^T f(y, t, 0) dt$$

and it can be shown that this system is qualitatively equivalent to the Poincaré map of the original system. One thus gets a continuous system which reflects the behavior of a discrete map, notably on questions of stability of fixed points.

The danger lies in the fact that in the case of resonances, the averaging is performed over the shortest common period. In the case of a resonance of order n , the resulting averaged system is thus not an approximation of the Poincaré map of the original, but of its n -th iterate.

This distinction is quite relevant when comparing the mechanism of period doubling and parametric forcing. For the period doubling the emphasis is on a limit cycle with frequency ω_0 which bifurcates to a cycle with frequency $\omega_0/2$. In the forcing case, the emphasis is on a self-oscillation with frequency ω_0 perturbed by a forcing at $2\omega_0$. Mathematically this is equivalent, but the approach will be different, at least for a physicist.

With these words of caution in mind, we can finally state that the averaged equations, approximating the n -th iterate of the Poincaré map for a resonance of order n are indeed given by Eq.(3-5) (omitting spatial terms).

3.6 RESONANCE TONGUES AND PHASE DIAGRAMS

We have seen in the previous section how we can derive the normal form for a strong resonances and we have also seen that this normal form (in the case of finite-dimensional systems) and its resulting flow can be interpreted as the approximation of the corresponding Poincaré map. Now in view of the qualitative arguments given in the first chapter, where it was shown that many interesting spatial features of reaction-diffusion equations can be inferred from the flow of the reaction part, it is of interest to make a detailed analysis of the phase space for each resonance, as a function of parameters.

The essential feature of a resonance is its Arnold tongue or resonance horn, which can be interpreted as the possible values of the detuning such that a phase locking occurs for a given amplitude of the forcing. We are thus interested in the bifurcation set in the (v, γ) space. The task of fully determining this bifurcation set turns out to be quite feasible, except in the case $n = 4$, which is subtler. Here, we will analyze the first three cases, the first two being maybe the most physically relevant.

3.6.1 Stationary solutions

The starting point of this analysis is to obtain the fixed points of the system Eq.(3-5) (without spatial terms of course). We begin by writing the system in polar coordinates $A = Re^{i\varphi}$:

$$\begin{aligned}\partial_T R &= R - R^3 + \gamma_n R^{n-1} \cos(n\varphi) \\ R \partial_T \varphi &= vR - \beta R^3 - \gamma_n R^{n-1} \sin(n\varphi)\end{aligned}\tag{3-6}$$

solving for stationary solutions yields:

$$\begin{aligned}\gamma_n^2 R_0^{2(n-1)} \cos^2(n\varphi_0) &= (R_0^3 - R_0)^2 \\ \gamma_n^2 R_0^{2(n-1)} \sin^2(n\varphi_0) &= (vR_0 - \beta R_0^3)^2\end{aligned}$$

i.e.:

$$(R_0^3 - R_0)^2 + (vR_0 - \beta R_0^3)^2 - \gamma_n^2 R_0^{2(n-1)} = 0$$

and the phase:

$$\tan(n\varphi_0) = \frac{\nu - \beta R_0^2}{R_0^2 - 1}$$

Inserting this into Eq.(3-5) and linearizing, yields the linearized operator:

$$L_0 = \begin{bmatrix} -2R_0^2 & 2(\beta R_0^2 - \nu) \\ -2\beta R_0^2 & 2(1 - R_0^2) \end{bmatrix}$$

The eigenvalues of this matrix will thus determine the stability type of the stationary solutions, and they are given by:

$$\sigma_{\pm} = 1 - 2R_0^2 \pm \sqrt{1 - 4\beta^2 R_0^4 + 4\beta\nu R_0^2}$$

and eigenvectors:

$$\xi_{\pm} = \begin{pmatrix} 1 \mp (\sigma_{\pm} - 1 + 2R_0^2) \\ 2\beta R_0^2 \\ 1 \end{pmatrix}$$

This is enough to determine all local bifurcations of the dynamical system. We will now analyze each case separately.

3.6.2 Case $n = 1$

In this case the equation reads:

$$(R_0^3 - R_0)^2 + (\nu R_0 - \beta R_0^3)^2 - \gamma^2 = 0$$

Which we can rewrite as:

$$X^3 - \frac{2(1 + \nu\beta)}{1 + \beta^2} X^2 + \frac{1 + \nu^2}{1 + \beta^2} X - \frac{\gamma^2}{1 + \beta^2} = 0$$

By now defining:

$$b = -\frac{2(1 + \nu\beta)}{1 + \beta^2}, \quad c = \frac{1 + \nu^2}{1 + \beta^2}, \quad d = -\frac{\gamma^2}{1 + \beta^2} = 0$$

and:

$$q = \frac{2b^3 - 9bc + 27d}{54}, \quad p = \frac{3c - b^2}{9}, \quad r = \text{sgn}(q)\sqrt{|p|}$$

and making the change of variable $Y = X + b/3$, we can analyze all the possible solutions.

The first characteristic is given by $p = 0$, which in terms of the original parameters reads:

$$\nu^2(3 - \beta^2) - 8\beta\nu + \beta^2 - 1 = 0$$

Except for the special case $\beta = \sqrt{3}$, this has always two solutions ν_{\pm} . For $\nu < \nu_-$ or $\nu > \nu_+$ we have only one solution, given by:

$$R_0^2 = -2r \sinh \log \left(\frac{q}{r^3} + \sqrt{\frac{q^2}{r^6 + 1}} \right)^{1/3} - \frac{b}{3}$$

In the other case $\nu \in [\nu_-, \nu_+]$, we have another characteristic, given by $q^2 + p^3 = 0$, which can be solved in terms of d , yielding:

$$\gamma^2 = \frac{2b^3}{27} - \frac{bc}{3} \pm \frac{2}{27} (b^2 - 3c)^{3/2}$$

This determines the resonance horn itself. Outside of this horn, we still have a unique solution, now given by:

$$R_0^2 = -2r \cosh \log \left(\frac{q}{r^3} + \sqrt{\frac{q^2}{r^6 + 1}} \right)^{1/3} - \frac{b}{3}$$

while inside the horn, we have three solutions given by:

$$R_0^2 = \begin{cases} -2r \cos(\Psi/3) - b/3 \\ 2r \cos(\pi/3 - \Psi/3) - b/3 \\ 2r \cos(\pi/3 + \Psi/3) - b/3 \end{cases}$$

Where $\Psi = \arccos(q/r^3)$.

We have thus determined all the possible stationary solutions. By using the expression for the eigenvalues that we found earlier, we can find all the bifurcation sets of these solutions (see Figure 9 and Figure 10). The corresponding phase portraits are shown in Figure 11 and Figure 12.

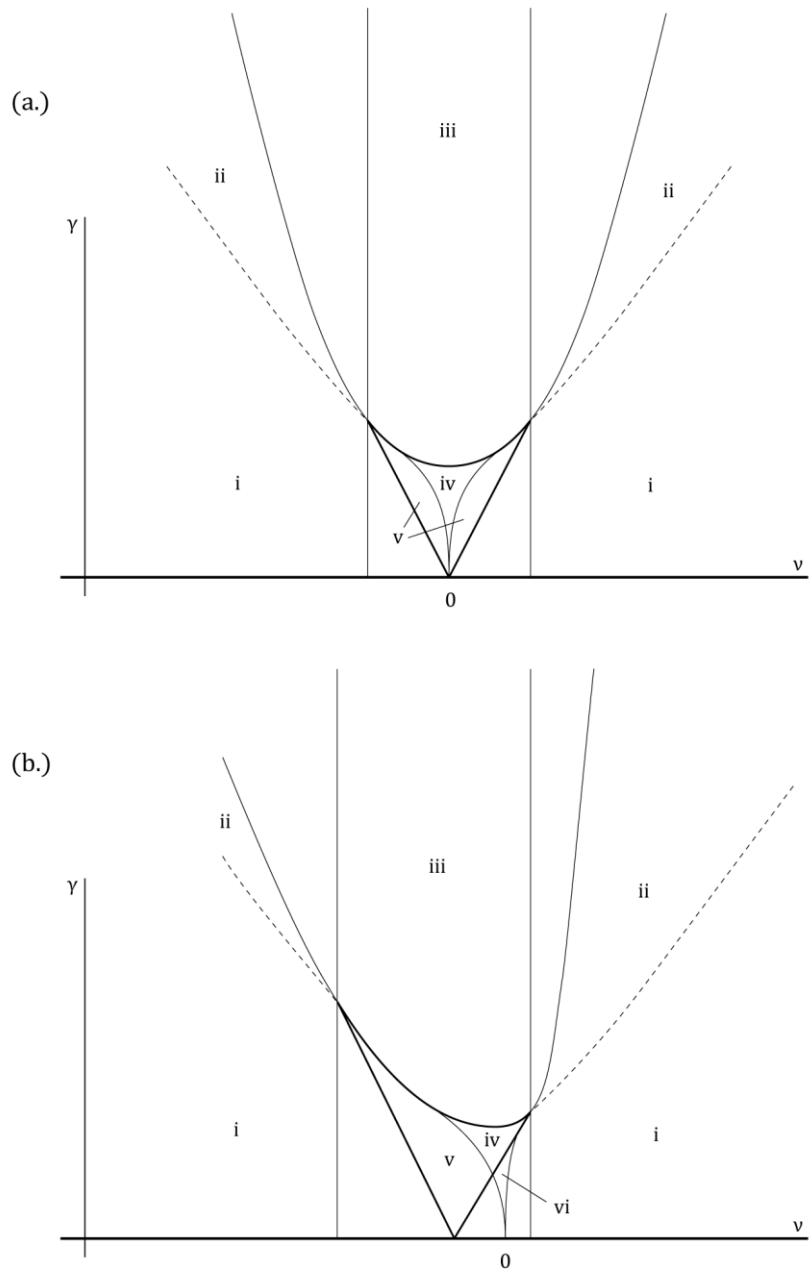


Figure 9: Resonance horns in the case $n = 1$ with $\beta = 0.0$ and $\beta = -0.36$ respectively. The thick lines delimit the existence of phase locked solutions, the thin lines correspond to local saddle node bifurcations of the various fixed points and the dotted line corresponds to a Hopf bifurcation. Roman numerals refer to phase diagrams shown below.

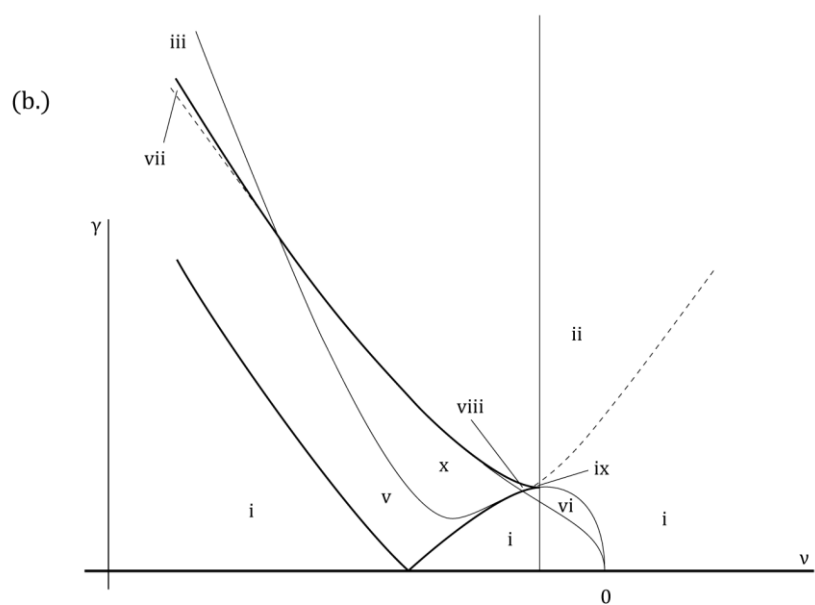
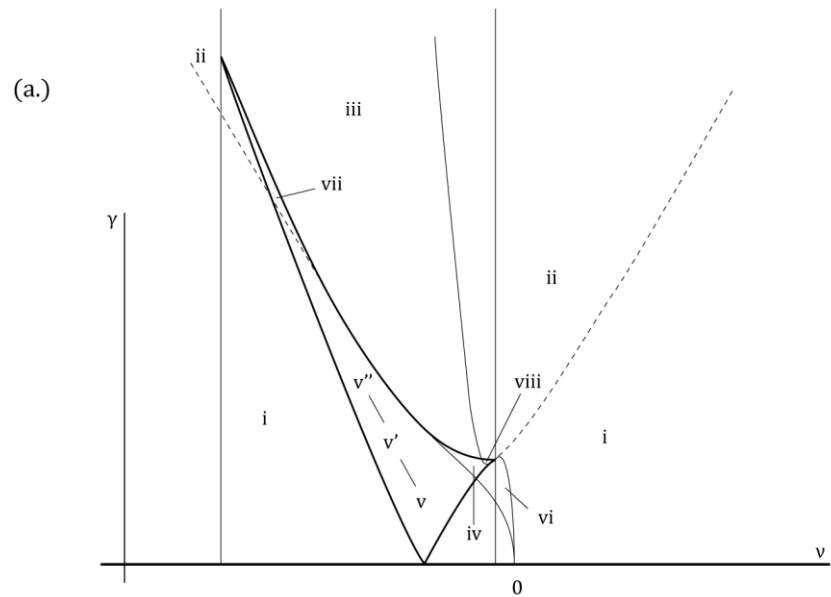


Figure 10: Same as in previous figure for $\beta = -0.8$ and $\beta = -1.8$ respectively.

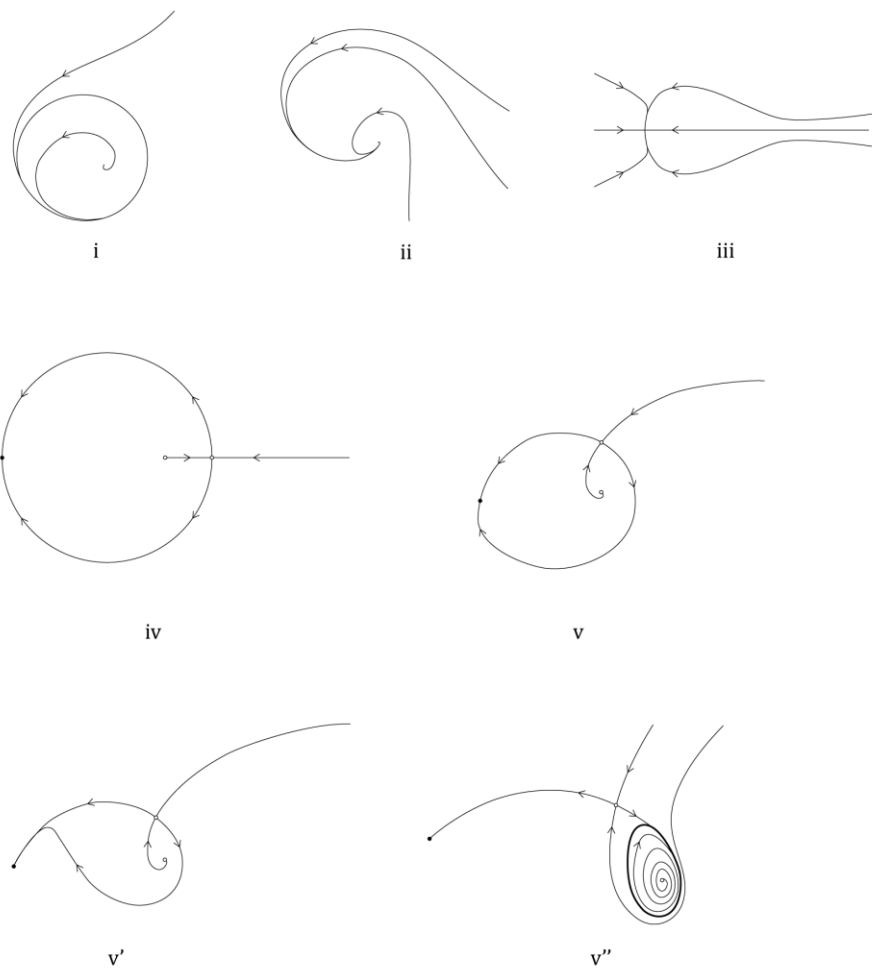
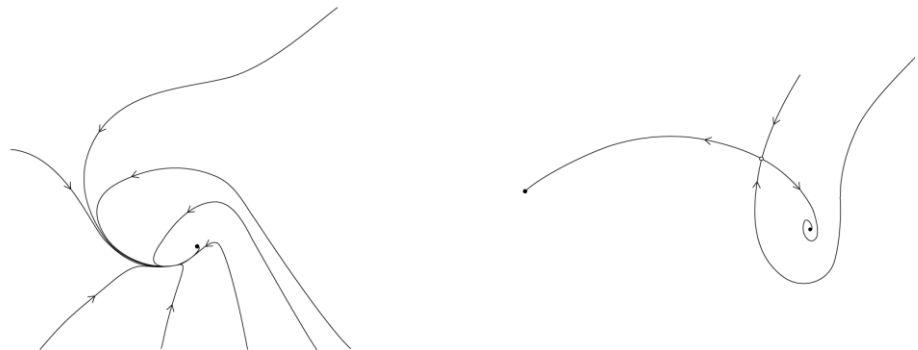
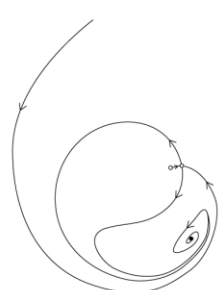


Figure 11: Phase diagrams for the case $n = 1$

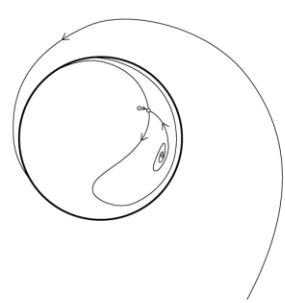


vi

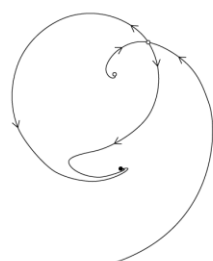
vii



viii



ix



x

Figure 12: Phase diagrams for the case $n = 1$. (continued)

3.6.3 Case $n = 2$

In this case the equation reads:

$$(R_0^3 - R_0)^2 + (\nu R_0 - \beta R_0^3)^2 - \gamma^2 R_0^2 = 0$$

Thus $R_0 = 0$ is always a solution. For the other two, we get:

$$R_0^2 = \frac{1 + \nu\beta \pm \sqrt{\gamma^2(1 + \beta^2) - (\mu\beta - \nu)^2}}{1 + \beta^2}$$

The solution with the plus sign always exists, while the other one may disappear. Note that when solving for the phase, we get a total of four non-trivial fixed points, each pair differing by a phase of π .

A necessary condition for the existence of these solutions is:

$$|\gamma| \geq \frac{|\beta - \nu|}{\sqrt{1 + \beta^2}}$$

Which shows that β acts a kind of detuning, in the same way as ν . A second necessary condition is $R_0^2 > 0$, which is important only for the negative root. This condition gives:

$$|\gamma| \leq \sqrt{1 + \nu^2}$$

This determines the resonance horn fully. Again by using the eigenvalues found earlier, we can determine the bifurcation sets for all solutions (see Figure 13 - Figure 15).

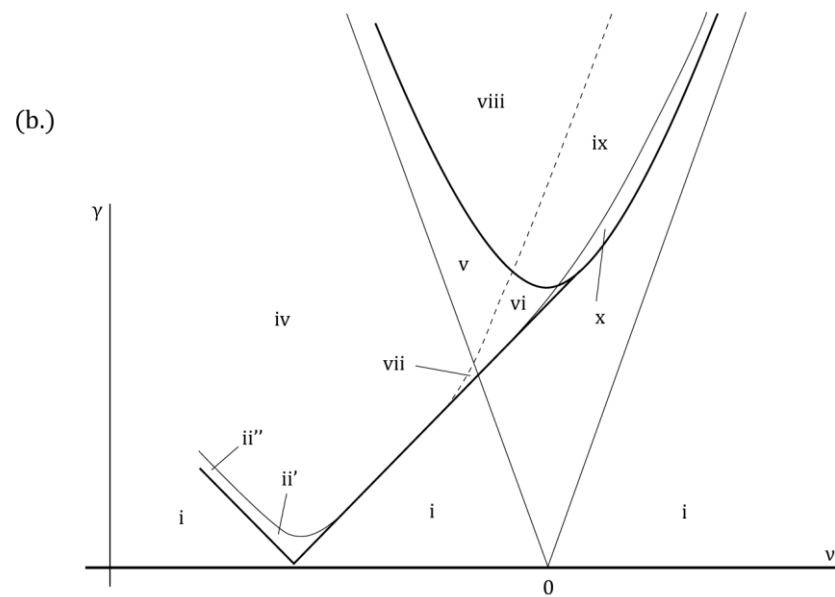
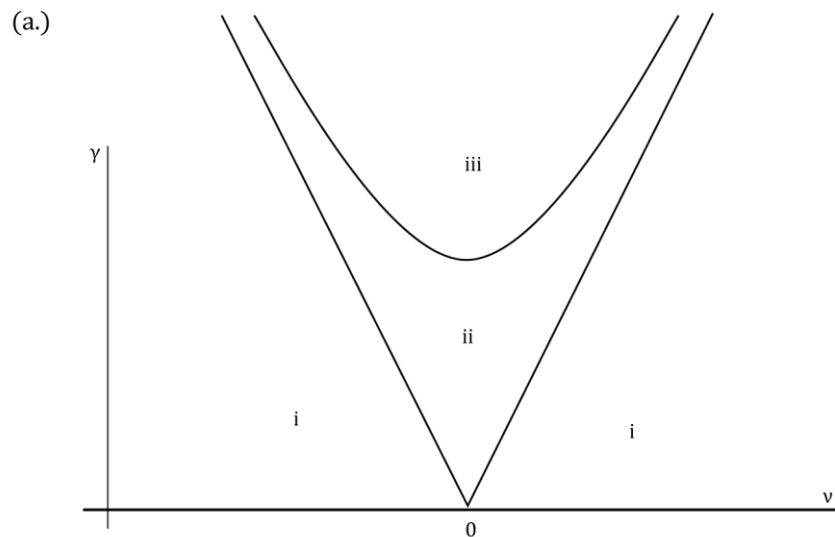


Figure 13: Resonance horn in the case $n = 2$ with $\beta = 0$ and $\beta < 0$ respectively. The thick line delimits the existence of phase locked solutions, the thin lines correspond to local saddle node bifurcations of the various fixed points and the dotted line corresponds to a Hopf bifurcation.

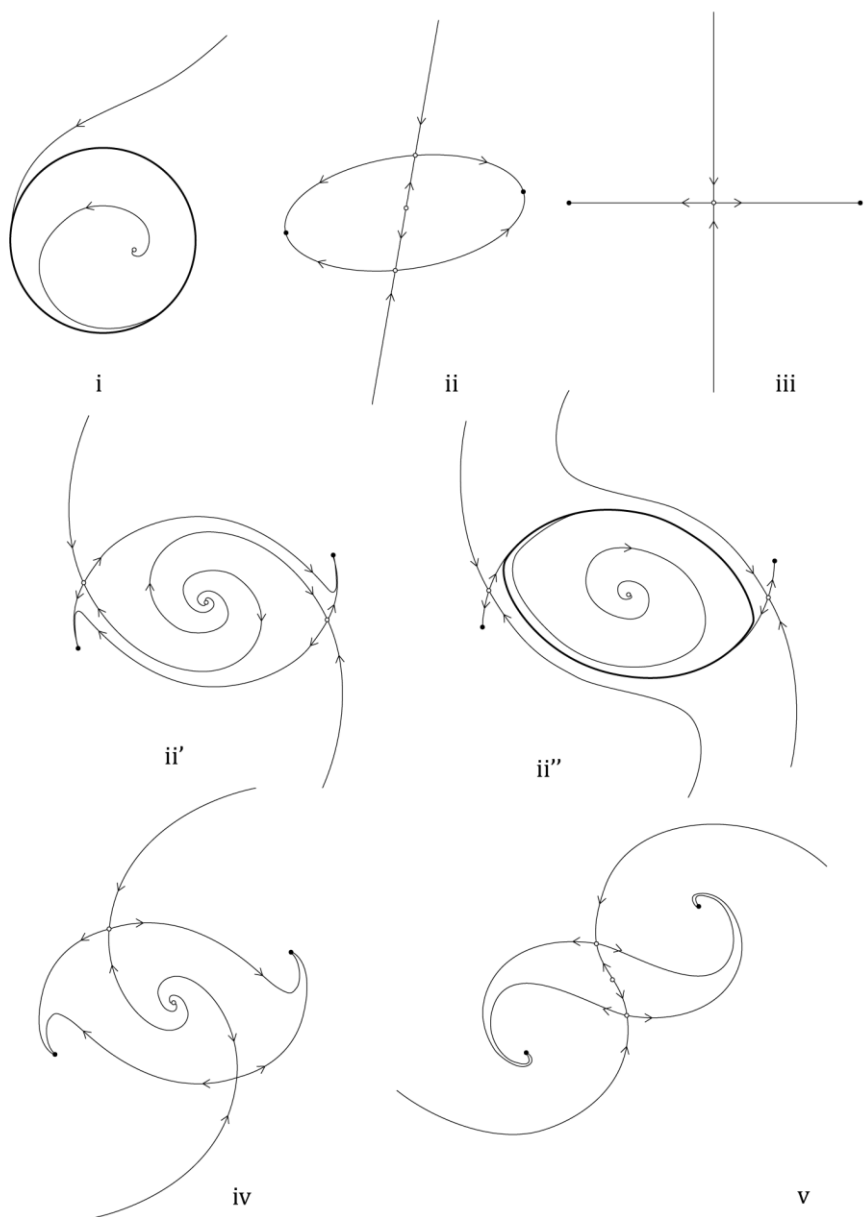
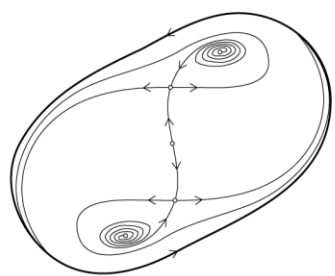
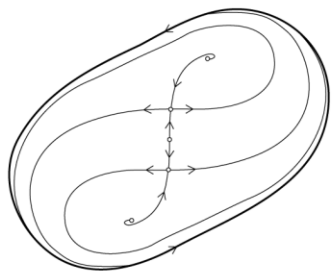


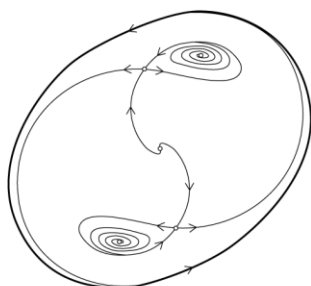
Figure 14: Phase diagrams for the case $n = 2$



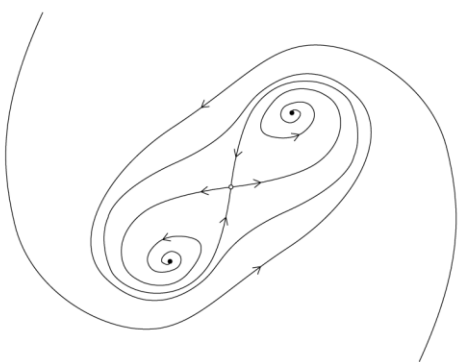
v'



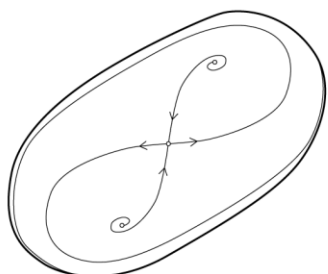
vi



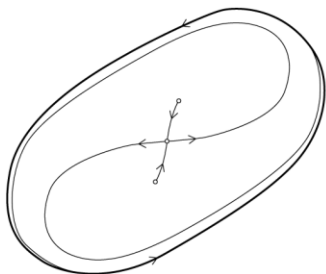
vii



viii



ix



x

Figure 15: Phase diagrams for the case $n = 2$ (continued)

Case $n = 3$

In this case the equation reads:

$$(R_0^3 - R_0)^2 + (\nu R_0 - \beta R_0^3)^2 - \gamma^2 R_0^4 = 0$$

Again we see that $R_0 = 0$ is always a solution. For the other two, we get:

$$R_0^2 = \frac{2(1 + \beta\nu) + \gamma^2 \pm \sqrt{\gamma^2(\gamma^2 + 4(1 + \beta\nu)) - 4(\nu - \beta)^2}}{2(1 + \beta^2)}$$

A necessary condition of existence is given by:

$$|\gamma| \geq \sqrt{2\sqrt{(1 + \beta^2)(1 + \nu^2)} - 2(1 + \beta\nu)}$$

Which is in fact a sufficient condition, as the roots are always positive, thus the above expression delimits the resonance horn. The bifurcation sets can then be found as before (see Figure 16 - Figure 18).

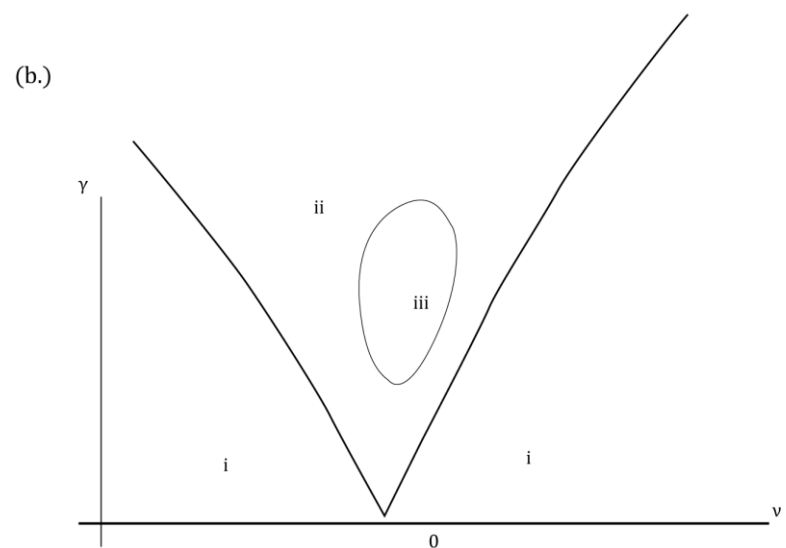
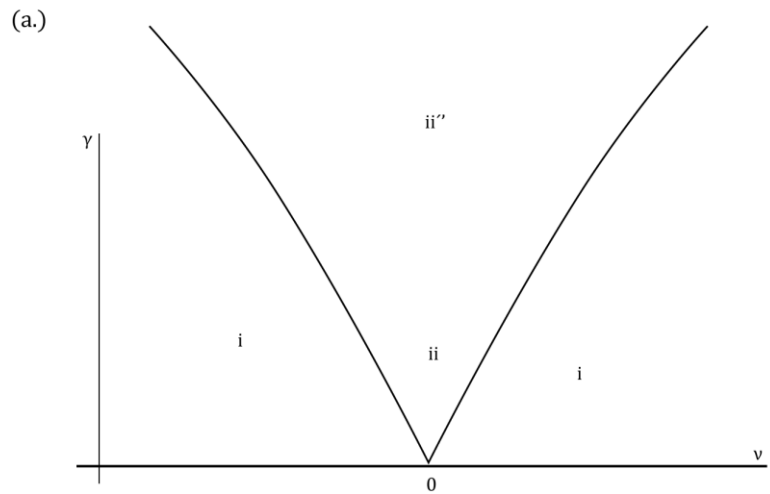


Figure 16: Resonance horns in the case $n = 3$ with $\beta = 0$ and $\beta < 0$ respectively. The thick line delimits the existence of phase locked solutions, the thin lines correspond to local saddle node bifurcations.

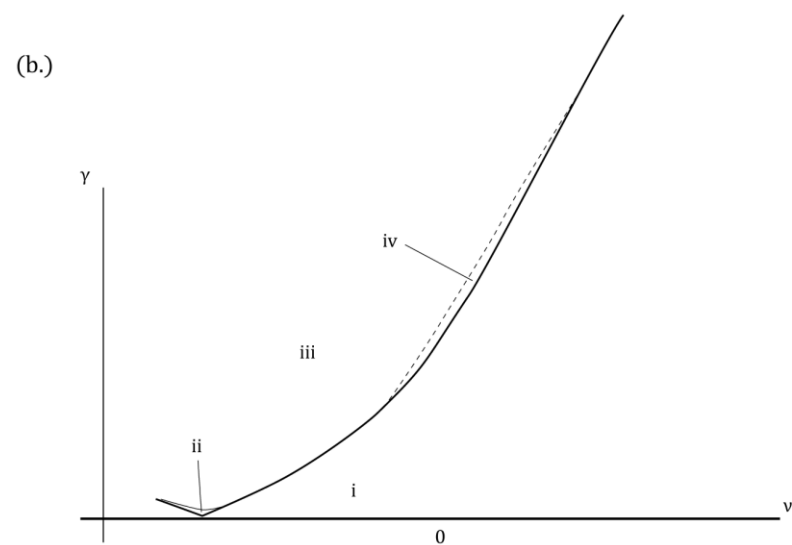
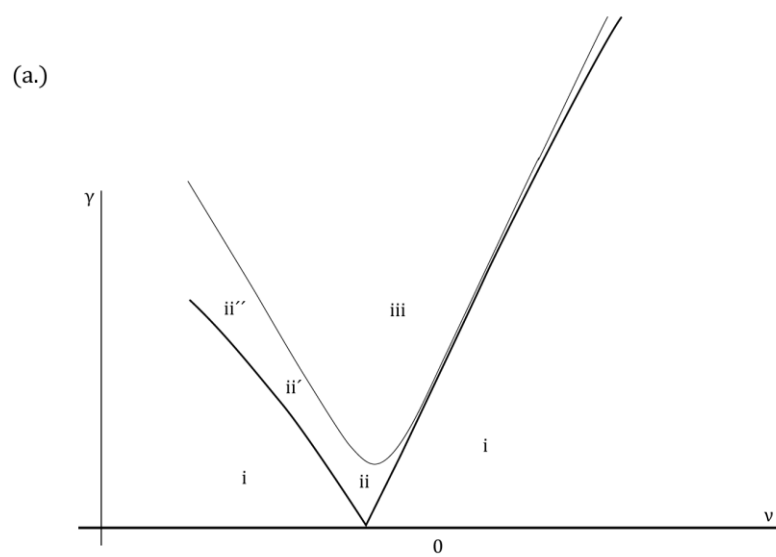


Figure 17: Same as in previous figure for lower values of β . The thick lines delimit the existence of phase locked solutions, the thin lines correspond to local saddle node bifurcations, and the dotted line corresponds to a Hopf bifurcation.

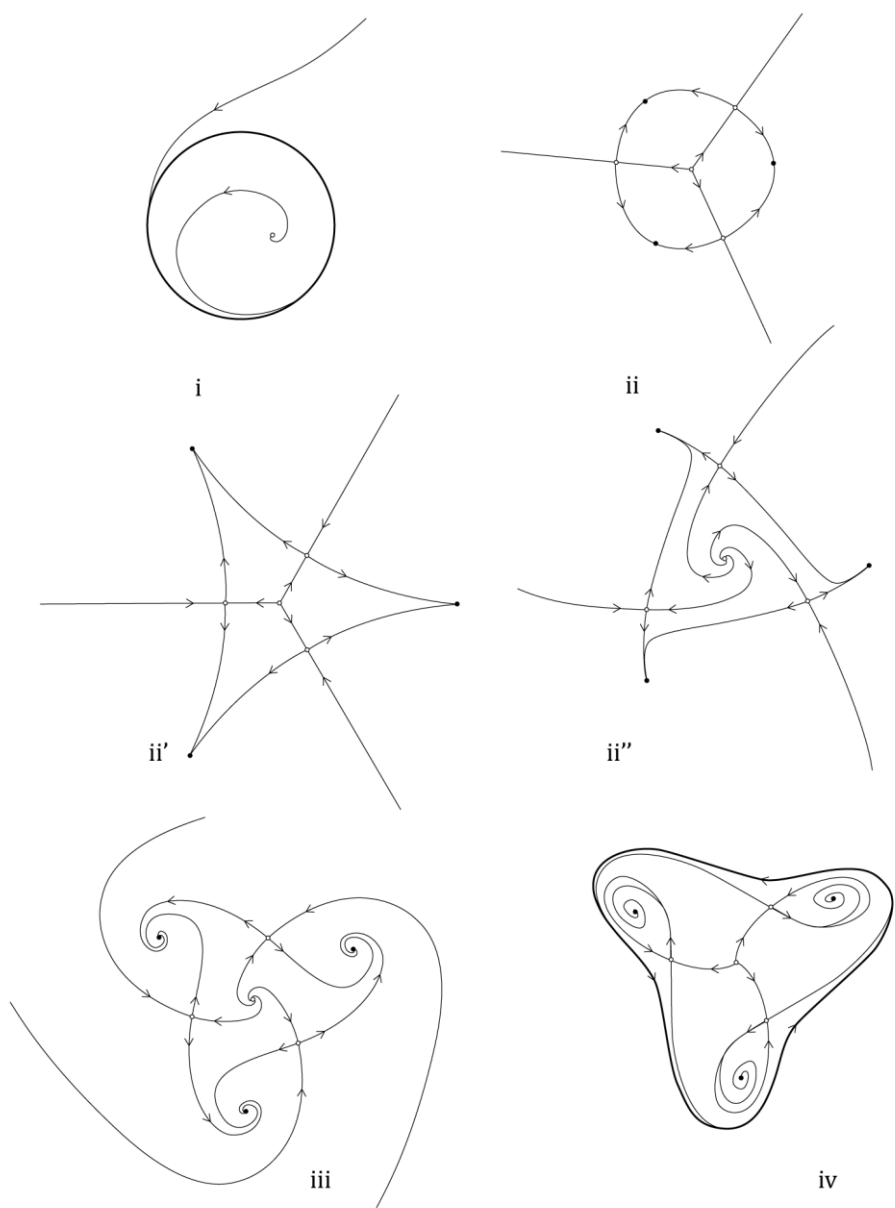


Figure 18: Phase diagrams for the case $n = 3$

4 INSTABILITIES OF PHASE-LOCKED STATES

4.1 REDUCTION TO A DYNAMIC OF PHASE ONLY

An interesting limit of Eq.(3-5) is when we can reduce the dynamic to an equation for the phase only [9, 8]. This can be done in the limit when the *effective detuning*, defined as the cumulative effect of detuning itself characterized by ν and the ‘nonlinear’ detuning characterized by β , is small.

4.1.1 Stable phase limit

The linearized operator around a given equilibrium point $R_0 e^{i\varphi_0}$ written in the (R, φ) base was found to be:

$$L_0 = \begin{bmatrix} -2R_0^2 & 2(\beta R_0^2 - \nu) \\ -2\beta R_0^2 & 2(1 - R_0^2) \end{bmatrix} \quad (4-1)$$

It is then reasonable to expect that when the radial mode is strongly damped while the phase mode becomes marginal, a reduction to a phase dynamic is possible. This suggests the following scaling:

$$R_0^2 \sim O(1), \quad (\beta - \nu) \sim \gamma \sim O(\epsilon)$$

Using this scaling, we consider a solution of the form $A = (1 + \rho)e^{i\varphi}$, where we further assume that:

$$\rho \sim \nabla^2 \sim O(\epsilon)$$

By inserting into Eq.(3-5), we obtain up to order 3:

$$\begin{aligned} \partial_t \rho &= -2\rho - 3\rho^2 - \rho^3 + \gamma(1 + \rho)^{n-1} \cos(n\varphi) + \nabla^2 \rho - (1 + \rho)(\nabla \varphi)^2 \\ &\quad - \alpha(2\nabla \rho \nabla \varphi + (1 + \rho)\nabla^2 \varphi) \\ \partial_t \varphi &= (1 - \rho + \rho^2) \left[\nu(1 + \rho) - \beta(1 + 3\rho^2 + 3\rho + \rho^3) - \gamma(1 + \rho)^{n-1} \sin(n\varphi) \right] \\ &\quad + 2\nabla \rho \nabla \varphi + (1 + \rho)\nabla^2 \varphi + \alpha(\nabla^2 \rho - (1 + \rho)(\nabla \varphi)^2) \end{aligned} \quad (4-2)$$

At order 1 we thus get:

$$\begin{aligned} \partial_t \rho &= -2\rho + \gamma \cos(n\varphi) - (\nabla \varphi)^2 - \alpha \nabla^2 \varphi \\ \partial_t \varphi &= \nu - \beta - 2\beta\rho - \gamma \sin(n\varphi) - \alpha(\nabla \varphi)^2 + \nabla^2 \varphi \end{aligned} \quad (4-3)$$

Introducing the coordinate change $\varphi = \psi + u_1 \rho$, we obtain:

$$\begin{aligned} \partial_t \psi &= \nu - \beta - 2\beta\rho + 2u_1\rho + \nabla^2 \psi - \alpha(\nabla \psi)^2 + u_1(\nabla \psi)^2 + u_1 \alpha \nabla^2 \psi \\ &\quad - \gamma \sin(n(\psi + u_1 \rho)) - u_1 \gamma \cos(n(\psi + u_1 \rho)) \end{aligned}$$

After developing the sinus and cosine, we get:

$$\begin{aligned} \partial_t \psi &= \nu - \beta - 2(u_1 - \beta)\rho - \gamma[\sin(n\psi) + u_1 \cos(n\psi)] - (\alpha - u_1)(\nabla \psi)^2 \\ &\quad + \alpha u_1 \nabla^2 \psi \end{aligned}$$

So we can decouple ρ from the phase by choosing $u_1 = \beta$. So we finally obtain the desired phase equation:

$$\partial_t \psi = \nu - \beta - \gamma \sqrt{1 + \beta^2} \sin(n\psi + \arctan(\beta)) + (1 + \alpha\beta)\nabla^2\psi - (\alpha - \beta)(\nabla\psi)^2 \quad (4-4)$$

The equation for ρ now reads:

$$\partial_t \rho = -\rho + \gamma \cos(n\psi) - (\nabla\psi)^2 - \alpha\nabla^2\psi$$

Introducing the change of coordinate:

$$\rho = \xi + a_1 \cos(n\psi) + a_2(\nabla\psi)^2 + a_3\nabla^2\psi$$

And by choosing:

$$a_1 = \frac{\gamma}{2}, \quad a_2 = -\frac{1}{2}, \quad a_3 = -\frac{\alpha}{2}$$

We obtain:

$$\partial_t \xi = -2\xi$$

Which together with Eq.(4-4) describes the dynamic near the central manifold. On the central manifold ($\xi = 0$), ρ can be calculated explicitly by the expression:

$$\rho = \frac{\gamma}{2} \cos(n\psi) - \frac{1}{2}(\nabla\psi)^2 - \frac{\alpha}{2}\nabla^2\psi$$

This phase approximation is valid as long as phase gradients remain small. This is true for $1 + \alpha\beta > 0$.

Stationary solutions of the phase equation

By looking for homogeneous and stationary solutions of Eq.(4-4), we obtain:

$$\begin{aligned} \psi_i^+ &= \frac{1}{n} \left[\arcsin\left(\frac{\nu - \beta}{\gamma\sqrt{1 + \beta^2}}\right) - \arctan(\beta) + 2i\pi \right] & i = 0, \dots, n-1 \\ \psi_i^- &= \frac{1}{n} \left[\arctan(\beta) - \arcsin\left(\frac{\nu - \beta}{\gamma\sqrt{1 + \beta^2}}\right) + (2i+1)\pi \right] & i = 0, \dots, n-1 \end{aligned} \quad (4-5)$$

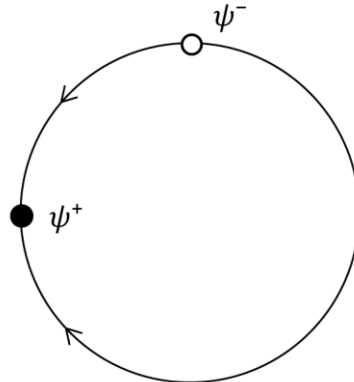


Figure 19: Fixed points of Eq.(4-4) in the variational case ($n = 1$)

In the variational case ($\nu = \beta = 0$) we find:

$$\begin{aligned}\psi_i^+ &= \frac{2\pi}{n}i, & i &= 0, \dots, n-1 \\ \psi_i^- &= \frac{(2i+1)\pi}{n}, & i &= 0, \dots, n-1\end{aligned}$$

where the ψ_i^+ are found to be stable, while the ψ_i^- are unstable (for $\gamma > 0$ otherwise it is the opposite). So we see that stable and unstable fixed points alternate on the circle. In this limit, we can also look for stationary solutions of Eq.(4-4):

$$\partial_x^2 \psi' = \gamma \sin(\psi')$$

By putting $\psi' = n\psi$, which is just the pendulum equation. We thus seek the separatrix solution which joins two stable fixed points, by imposing the boundary conditions:

$$\psi'(-\infty) = 0 \text{ and } \psi'(+\infty) = \pm 2\pi$$

With these boundary conditions we simply find the solutions of the classical pendulum:

$$\psi'_v(x) = \pm [2 \arctan(\sinh(\sqrt{n\gamma}x)) - \pi]$$

This solution corresponds to a stationary pulse or soliton, joining two symmetrically equivalent states.

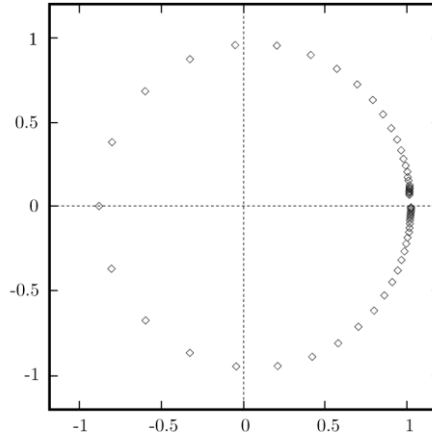


Figure 20: Stationary soliton solution in the case $n = 1$. Figure shows the distribution of the spatial solution in the phase space (U, V) where $A = U + iV$.

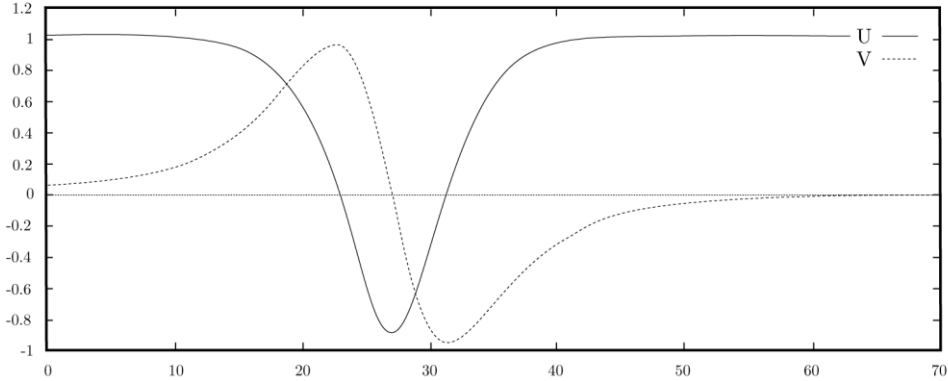


Figure 21: Same as in previous figure, showing U and V as a function of space ($\alpha = \beta = \nu = 0$ and $\gamma = 0.032787$)

Non-variational effects on the soliton solution

We can now study the effect of small non-variational terms on the phase equation. We assume that $\nu \sim \beta \ll 1$. We then obtain at order 1:

$$\begin{aligned}\psi_i^+ &= \frac{1}{n} \left[\frac{\nu - \beta}{\gamma} - \beta + i2\pi \right] \\ \psi_i^- &= \frac{1}{n} \left[\frac{\beta - \nu}{\gamma} + \beta + (2i + 1)\pi \right]\end{aligned}$$

By looking at the phase difference between the two adjacent fixed points, we see that the effect of ν and β is to desymmetrize the balance between the stable and unstable fixed points, so they tend to group in pair, eventually disappearing in a saddle-node bifurcation.

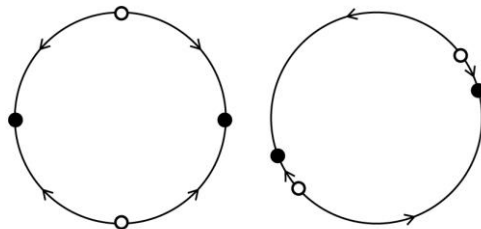


Figure 22: Effects of non-variational terms on the phase space ($n = 2$). First figure is without non-variational terms. In the second we have non-variational terms and we see that hyperbolic and stable points converge.

To investigate the non-variational effect on the soliton solution, we first note that from a qualitative point of view we expect this solution to move. This is because without the non-variational terms the stability of the soliton can be understood as a particle in a sinusoidal potential which has exactly the right speed to join two extremes.

With the non-variational terms, the potential becomes tilted and is thus non-symmetric. For the solution to exist we must thus add a friction, which compensates exactly the dissymmetry. A friction term is of the form $\partial_x \psi$, which

can be simply interpreted as a speed, in the context of our original amplitude equations.

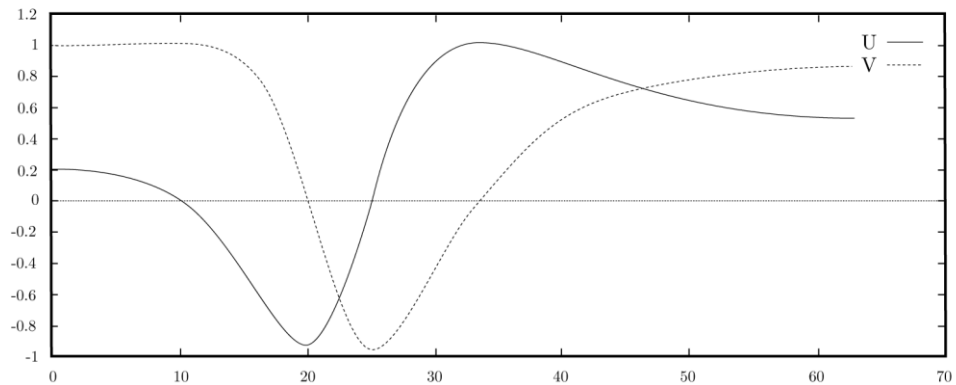


Figure 23: Real and imaginary part of the pulse solution as a function of space in the non-variational case. The pulse moves from right to left ($\alpha = \beta = 0$, $\nu = 0.031$ and $\gamma = 0.032787$)

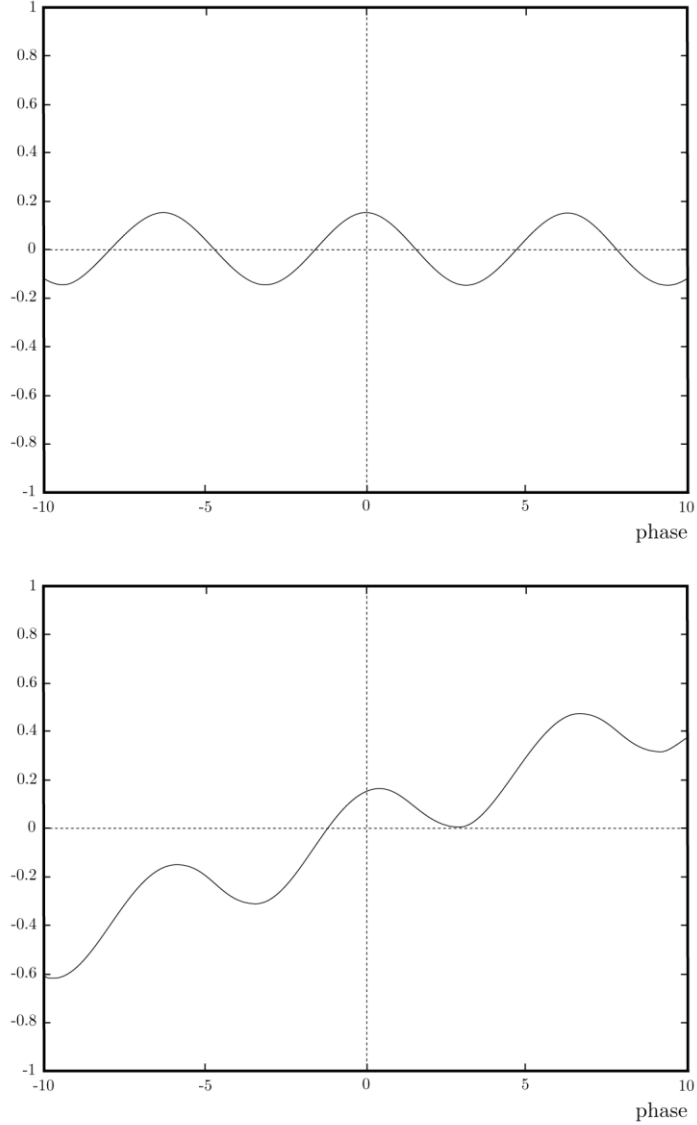


Figure 24: Potential of Eq.(4-4) ($n = 1$) without and with non-variational terms. Maxima correspond to stable fixed points. Figures correspond to $v = 0$ and $v = 0.05$ respectively, with $\beta = 0$ and $\gamma = 0.15$

To find an estimate for the speed, we assume non-variational terms to be small, and we write the perturbed solution as:

$$\Psi = \psi'_v(x - c_n t) + \epsilon \Phi_1(x - c_n t) + \dots$$

With $c_n = \epsilon c_{1,n} + \epsilon^2 c_{2,n} + \dots$. This we insert into:

$$\begin{aligned} \partial_t \psi' &= n(\nu - \beta) - n\gamma\sqrt{1 + \beta^2} \sin(\psi' + \arctan(\beta)) + (1 + \alpha\beta)\partial_x^2 \psi' \\ &\quad - \frac{(\alpha - \beta)}{n} (\partial_x \psi')^2 \end{aligned}$$

At order 1, we simply obtain the equation for the variational pulse. At order ϵ we obtain:

$$-c_{1,n} \partial_x \psi'_v = n(\nu - \beta) - n\gamma(\Phi_1 + \beta) \cos(\psi'_v) + \partial_x^2 \Phi_1 - \frac{(\alpha - \beta)}{n} (\partial_x \psi'_v)^2$$

The ‘solvability’ condition thus reads:

$$-c_{1,n} \partial_x \psi'_v = n(\nu - \beta) - n\gamma\beta \cos(\psi'_v) - \frac{(\alpha - \beta)}{n} (\partial_x \psi'_v)^2$$

Multiplying this with $\partial_x \psi'_v$ and integrating over space yields:

$$c_{1,n} = \frac{\pi}{4n\sqrt{n\gamma}} \left[2(\alpha - \beta)n\gamma - n^2(\nu - \beta) - \frac{n^2\gamma\beta}{2} \right] \quad (4-6)$$

Which is in good agreement with numerical simulations.

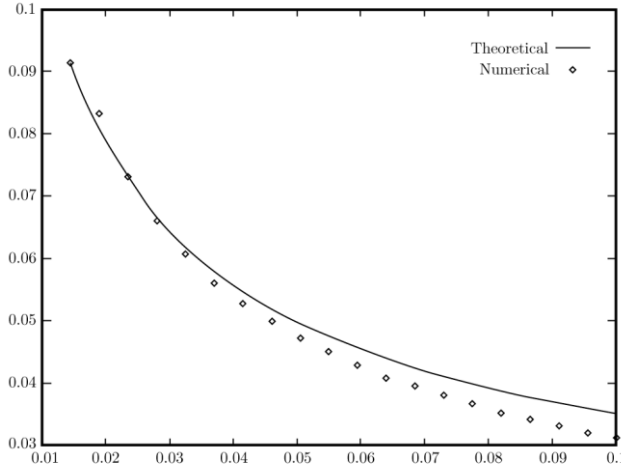


Figure 25: Speed of pulse as a function of γ with $\nu = 0.01$ fixed ($\alpha = \beta = 0$). Solid line shows speed according to Eq.(4-6), while the markers shows numerical results.

Excitability

The existence of these moving solitons leads to an interesting interpretation of the dynamic in this phase limit. As we have said before the effect of the non-variational terms (at least for β and ν) is equivalent to a particle moving in a slanted sinusoidal potential. It is thus clear that there exist values of γ , ν and β

such that the domains of attraction of the stable positions become small and eventually vanish.

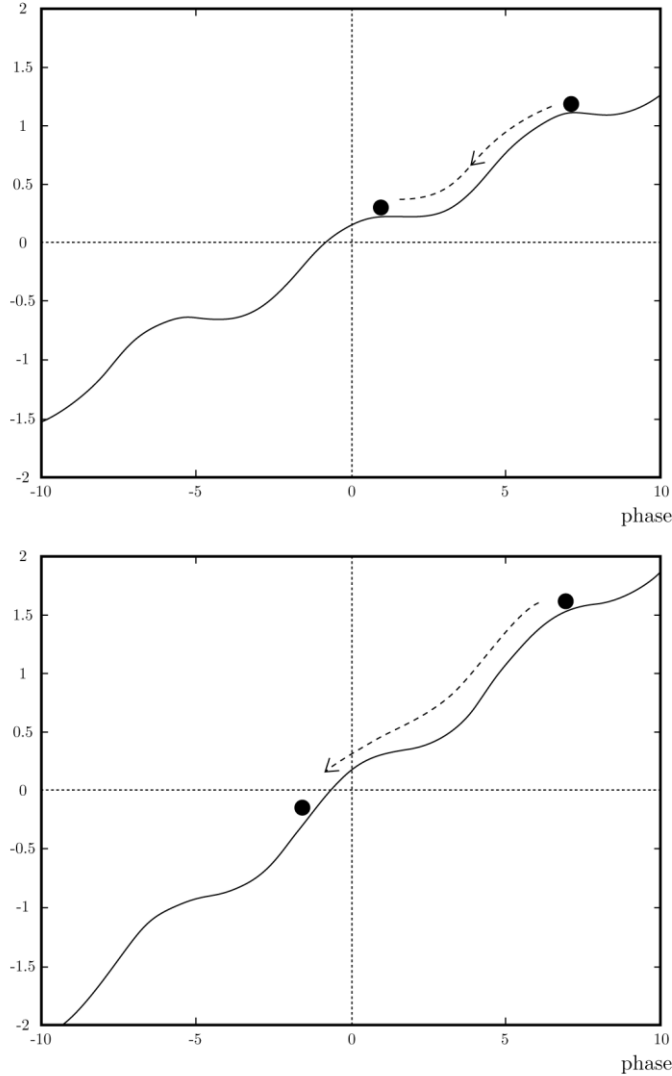


Figure 26: Potential of Eq.(4-4) ($n = 1$) in the excitable limit, and in the oscillatory limit. Maxima correspond to stable fixed points. Figures corresponds to $v = 0.14$ and $v = 0.20$ respectively, with $\beta = 0$ and $\gamma = 0.15$.

We thus see that in this situation, a small perturbation can send a particle down one step in the potential ladder. In terms of our original system this will correspond to a situation where we have a homogeneous state in one phase-locked position and a small localized perturbation of this state will then lead to the existence of pulses propagating from the loci of the perturbation. These pulses propagate from one stable phase-locked state to the next symmetrically equivalent state. For $n = 1$ for example, the pulse can be seen as a localized and moving excitation of the ground state.

Such a behavior is characteristic of *excitable* systems [43]. Such systems include for example the propagation of nerve impulses along synapses and muscle tissues in biological systems [12]. In this phase limit of Eq.(3-5), we can thus interpret the phase-locked states as being excitable. We note that this phenomenon is not strictly comparable with the notion of meta-stability in

sub-critical bifurcations, as the new equilibrium position is symmetrically equivalent to the previous one.

N-armed spirals

In two spatial dimensions we note that from a qualitative point of view, an arbitrary initial condition will generically have a point trapped at the origin ($A = 0$). Though this is not caught in the phase approximation, we can state that this leads naturally to the existence of pulses joining all the successive stable fixed points ($\psi_1 \rightarrow \psi_2 \rightarrow \dots \rightarrow \psi_n$). In the presence of non-variational terms these pulses will move. In two dimensions we will thus observe the existence of moving fronts. But as the origin is a topologically stable point of the field, the complex zero will not disappear and the pulses will thus always exist. No static equilibrium state is thus reached, but we observe the formation of n -armed spirals winding around the zero, where each arm is in one of the phase-locked states. Such spirals are known to exist in excitable media, e.g. in chemical reactions and in heart tissues [9, 43]. A similar mechanism of spiral formation is analyzed in more details later, in the context of Bloch/Ising transition. In fact, in the case $n = 2$, the excitable pulses can be considered to be a limit of the Bloch wall solutions.



Figure 27: 3-armed excitable spiral for the resonances $n = 3$. Figure shows real part of A .

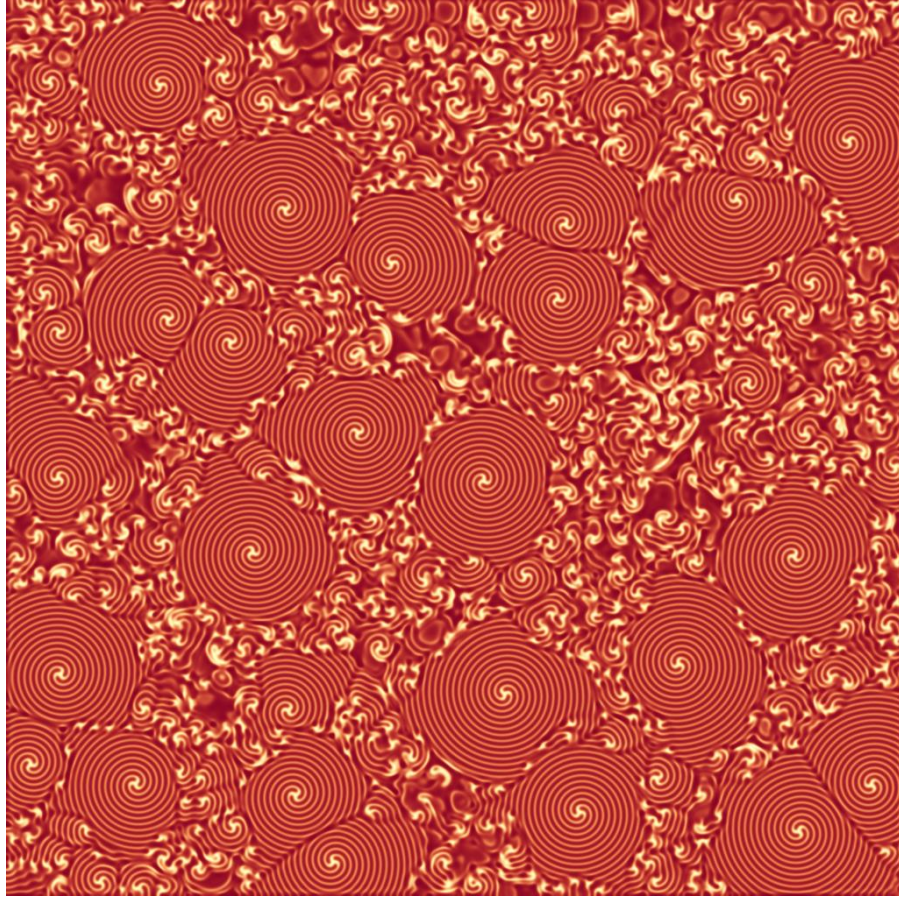


Figure 28: 3-armed excitable spirals for the resonance $n = 3$. Figure shows modulus of A .

Unstable phase limit

As we saw in the previous section, the reduction to the phase equation given by Eq.(4-4) is valid only while $1 + \alpha\beta > 0$. To find the correct equation describing the phase behavior for $1 + \alpha\beta < 0$, we must pursue our reduction to a higher order. To do this we assume the following scaling:

$$1 + \alpha\beta \sim \epsilon(\nu - \beta) \sim \epsilon^3 \gamma \sim \epsilon^2$$

With this scaling, the existence of the phase locked states is guaranteed. We will thus assume a solution of the form: $A = (1 + \rho)e^{\varphi_0 + \varphi}$, i.e. centered around the phase-locked state.

What we expect is the following: We know that for an unforced homogeneous Hopf bifurcation, when $1 + \alpha\beta$ is negative, the system develops a kind of weak turbulence. This is because the phase mode, which was marginal, acquires unstable long period modes.

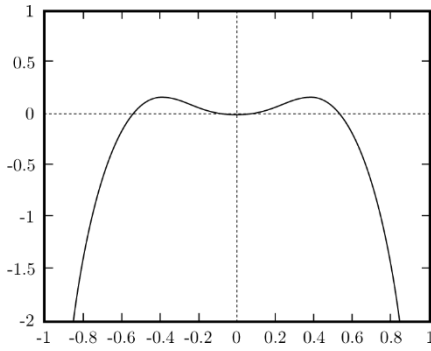


Figure 29: Growth rate of phase nodes as a function of wave vector in the case $\gamma = 0$, when $1 + \alpha\beta < 0$. ($\alpha = -2.0$ and $\beta = 1.5$)

The characteristic of this state is an evolution to spatiotemporal intermittency (in one dimension), and to a state called *defect mediated turbulence* in two dimensions, where a continuous creating and annihilation of vortex pairs occurs [22, 23].

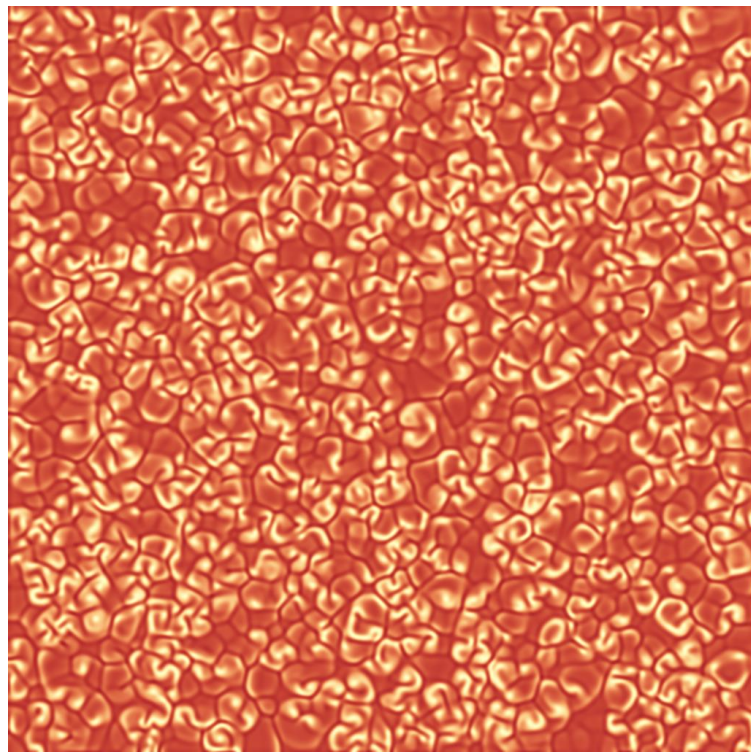


Figure 30: Defect mediated turbulence in the unforced Ginzburg-Landau equation when $1 + \alpha\beta < 0$. Figure shows the modulus of the field A.

In the case of resonances, the effect of the forcing is to stabilize the phase, or more precisely the locked phase. As the forcing is decreased though, the growth rate of the phase modes will acquire a marginal mode at $k \neq 0$, thus leading to the formation of structures. For a lower value of γ , we expect this structure to become unstable, eventually leading to its destruction, either by amplitude instabilities or the disappearance of the locked phase through a saddle-node bifurcation.

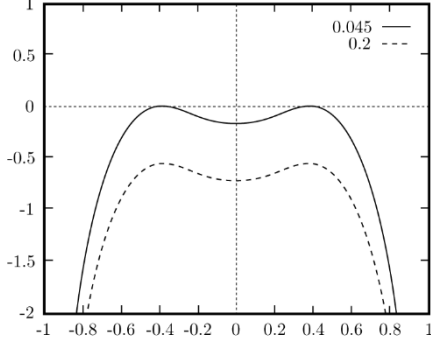


Figure 31: Growth rate of phase modes with temporal forcing as a function of wave vector. ($\alpha = -2.0$ and $\beta = 1.5$, with $\gamma = 0.045$ (solid) and 0.2 (dashed))

To derive the phase equation, we note simply that with the orders that we chose, the new terms which will have to be added to Eq.(4-4) are the same as for the phase equation for the unforced Hopf bifurcation. We thus get directly the phase equation as:

$$\partial_t \varphi = -n\gamma\sqrt{1+\beta^2}\varphi + (1+\alpha\beta)\nabla^2\varphi - (\alpha-\beta)(\nabla\varphi)^2 - \frac{\alpha^2(1+\beta^2)}{2}\nabla^4\varphi \quad (4-7)$$

with:

$$\psi = \frac{\nu - \beta}{n\gamma\sqrt{1+\beta^2}} + \varphi$$

Which is known as the damped Kuramoto-Shivashinsky equation [44]. It can be rewritten by doing the following scaling:

$$Y = -(\alpha - \beta)\sqrt{\frac{2}{\alpha^2(1+\beta^2)}}\varphi$$

and:

$$x = X \left[\frac{\alpha^2(1+\beta^2)}{2} \right]^{1/4}$$

The phase equation then reads:

$$\partial_t Y = [\delta - (\nabla^2 + k_0^2)^2]Y + (\nabla Y)^2$$

with:

$$\delta = \frac{1}{2}(1+\alpha\beta)^2 \frac{1}{\alpha^2(1+\beta^2)} - n\gamma$$

and:

$$k_0^2 = -\frac{1}{2}(1+\alpha\beta)\sqrt{\frac{2}{\alpha^2(1+\beta^2)}}$$

For $\delta = 0$, we have the appearance of a marginal phase mode with $k = k_0$. We can make a weakly nonlinear analysis of this pattern formation to investigate the further evolution of this instability.

One dimensional multi-scale analysis: super-critical k

We consider the equation:

$$\partial_t \varphi = -n\gamma\sqrt{1+\beta^2}\varphi + (1+\alpha\beta)\partial_x^2\varphi - (\alpha-\beta)(\partial_x\varphi)^2 - \frac{\alpha^2(1+\beta^2)}{2}\partial_x^4\varphi$$

We now introduce the scaling:

$$\partial_x \rightarrow \partial_x + \epsilon\partial_X \text{ and } \partial_t \rightarrow \partial_t + \epsilon^2\partial_T$$

and write φ as:

$$\varphi = \epsilon\varphi_0 + \epsilon^2\varphi_1 + \epsilon^3\varphi_2 + \dots$$

and assuming that we can write γ as $\gamma = \gamma_c - \epsilon^2\delta$. After insertion, we obtain the linear operator:

$$L_0 = -\partial_t - n\gamma_c\sqrt{1+\beta^2} + (1+\alpha\beta)\partial_x^2 - \frac{\alpha^2(1+\beta^2)}{2}\partial_x^4$$

By now identifying orders we obtain:

ϵ :

$$L_0\varphi_0 = 0$$

ϵ^2 :

$$L_0\varphi_1 + 2(1+\alpha\beta)\partial_X\partial_x\varphi_0 - (\alpha-\beta)(\partial_x\varphi_0)^2 - 2\alpha^2(1+\beta^2)\partial_X\partial_x^3\varphi_0 = 0$$

ϵ^3 :

$$\begin{aligned} \partial_T\varphi_0 &= L_0\varphi_2 + n\delta\sqrt{1+\beta^2}\varphi_0 + (1+\alpha\beta)\partial_X^2\varphi_0 \\ &\quad - 2(\alpha-\beta)\partial_x\varphi_0(\partial_x\varphi_1 + \partial_X\varphi_0) + 2(1+\alpha\beta)\partial_X\partial_x\varphi_1 \\ &\quad - \alpha^2(1+\beta^2)(2\partial_X\partial_x^3\varphi_1 + 3\partial_X^2\partial_x^2\varphi_0) \end{aligned}$$

At order 1, we can choose $\varphi_0 = Ae^{ikx} + \bar{A}e^{-ikx}$. Solving for k , yields:

$$k^2 = \frac{-(1+\alpha\beta) \pm \sqrt{(1+\alpha\beta)^2 - 2\alpha^2(1+\beta^2)n\gamma_c\sqrt{1+\beta^2}}}{\alpha^2(1+\beta^2)}$$

which is marginal when:

$$\gamma_c = \frac{(1+\alpha\beta)^2}{2n\alpha^2(1+\beta^2)^{3/2}}$$

with critical wave vector:

$$k_c^2 = -\frac{(1+\alpha\beta)}{\alpha^2(1+\beta^2)}$$

At order 2, the resonant part, corresponding to terms proportional to e^{ikx} and e^{-ikx} , is found to be:

$$2(1 + \alpha\beta)\partial_x(i k_c A e^{ik_c x} - i k_c \bar{A} e^{-ik_c x}) - 2\alpha^2(1 + \beta^2)\partial_x(-i k_c^3 A e^{ik_c x} + i k_c^3 \bar{A} e^{-ik_c x}) = 0$$

Which is identically true. The non-resonant part can then be written as:

$$L_0\varphi_1 + (\alpha - \beta)k_c^2(A^2 e^{2ik_c x} + \bar{A}^2 e^{-2ik_c x} - 2|A|^2) = 0$$

By putting $\varphi_1 = B e^{2ik_c x} + \bar{B} e^{-2ik_c x} + C$, and identifying terms of like power, we obtain:

$$B = -\frac{2(\alpha - \beta)}{9(1 + \alpha\beta)}A^2$$

and:

$$C = \frac{4(\alpha - \beta)}{(1 + \alpha\beta)}|A|^2$$

It is at order 3 that we obtain the normal form governing the dynamics of the complex amplitude A , which is found as a solvability condition to make the resonant part zero. The normal form is directly found to be:

$$\partial_T A = n\delta\sqrt{1 + \beta^2}A - 2(1 + \alpha\beta)\partial_X^2 A - \frac{8}{9}\frac{(\alpha - \beta)^2}{\alpha^2(1 + \beta^2)}|A|^2 A \quad (4-8)$$

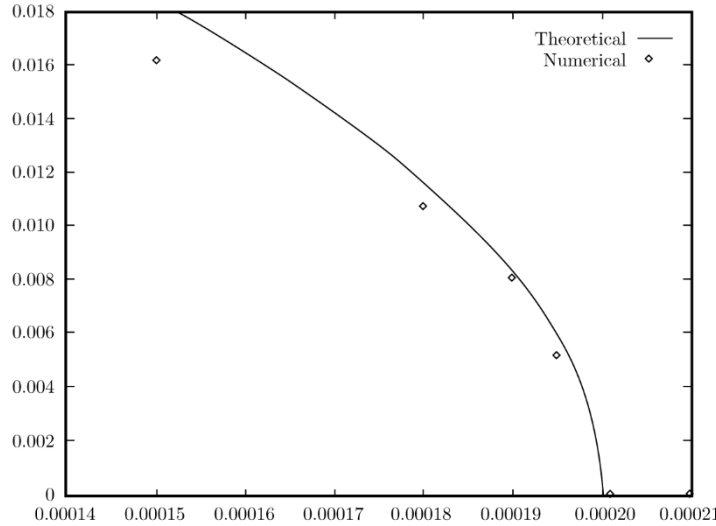


Figure 32: Bifurcation diagram for the amplitude of the modulated phase A . The thick line shows theoretical values, while dots show numerical results ($\beta = v = 1.0$ and $\alpha = -1.05$).

We thus see that in one dimension we have a super-critical transition towards a modulated pattern with wave vector k_c , and stationary amplitude given by:

$$|A| = \frac{3}{4} \left| \frac{1 + \alpha\beta}{\alpha - \beta} \right| \sqrt{1 - \frac{\gamma}{\gamma_c}}$$

For γ low enough, we expect the destruction of these periodic patterns through spatiotemporal intermittency [44], which is indeed observed numerically.

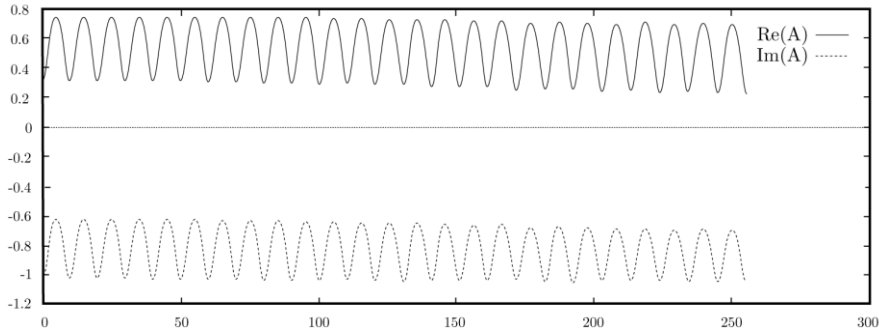


Figure 33: Real and imaginary part of A as a function of space for $\alpha = -1.29$, $\beta = 1.5$, $\nu = 1.45$ and $\gamma = 0.066$ in the case $n = 1$.

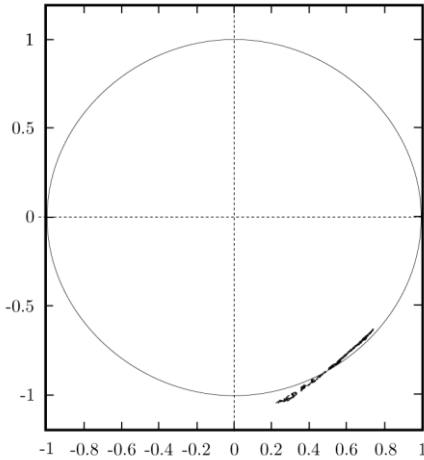


Figure 34: Same as in previous figure, except plotted in the phase space of A . The spatial manifold winds around the phase-locked state, along the marginal direction.

Two dimensional multi-scale analysis: sub-critical hexagons

In two dimensions we also have the possibility of a transition towards a hexagonal pattern. In the same way as in the previous section, we can make a multi-scale analysis, but as we are really only interested in the stability of the hexagons, we will not carry the analysis up to the description of the slow spatial modulations, make the calculations more straightforward.

Considering the same phase equation as in the previous section, we introduce the timescales:

$$\partial_t \rightarrow \partial_t + \epsilon \partial_{T_1} + \epsilon^2 \partial_{T_2}$$

and we develop φ and γ in the same way as before. After insertion we obtain the linear operator:

$$L_0 = -\partial_t - n\gamma_c \sqrt{1 + \beta^2} + (1 + \alpha\beta)(\partial_x^2 + \partial_y^2) - \frac{\alpha^2(1 + \beta^2)}{2}(\partial_x^4 + \partial_y^4 + 2\partial_x^2\partial_y^2)$$

Identifying orders then yields:

ϵ :

$$L_0\varphi_0 = 0$$

ϵ^2 :

$$\partial_{T_1}\varphi_0 = L_0\varphi_1 - (\alpha - \beta)\left((\partial_x\varphi_0)^2 + (\partial_y\varphi_0)^2\right)$$

ϵ^3 :

$$\partial_{T_1}\varphi_1 + \partial_{T_2}\varphi_0 = L_0\varphi_2 + n\delta\sqrt{1 + \beta^2}\varphi_0 - 2(\alpha - \beta)(\partial_x\varphi_0\partial_x\varphi_1 + \partial_y\varphi_0\partial_y\varphi_1)$$

At order 1, we choose φ_0 to be of the form:

$$\varphi_0 = Ae^{-ikx} + Be^{-ik\left(\frac{1}{2}x - \frac{\sqrt{3}}{2}y\right)} + Ce^{-ik\left(\frac{1}{2}x + \frac{\sqrt{3}}{2}y\right)} + c.c.$$

where c.c denotes complex conjugation, and we have chosen a hexagonal pattern with one symmetry axis aligned along the x direction. Inserting this expression in the linear operator, we find that it is a solution provided the k is the same as in the linear case and $\gamma = \gamma_c$ as found in the previous section.

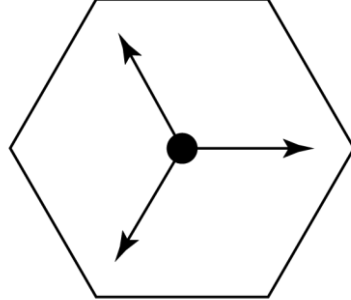


Figure 35: The fundamental modes of the hexagonal pattern

Turning to order 2, we easily see that resonant terms correspond to quadratic combinations of the amplitudes of the form:

$$AB, \bar{A}\bar{B}, AC, \bar{A}\bar{C}, BC, \bar{B}\bar{C}$$

sampling these together, we obtain the following solvability conditions:

$$\partial_{T_1}A = -(\alpha - \beta)k_c^2\bar{B}\bar{C}$$

$$\partial_{T_1}B = -(\alpha - \beta)k_c^2\bar{A}\bar{C}$$

$$\partial_{T_1}C = -(\alpha - \beta)k_c^2\bar{A}\bar{B}$$

We now have to solve for φ_1 . To do this we introduce a solution of the form:

$$\begin{aligned}\varphi_1 = & f_1 \cdot (2,0) + f_2 \cdot (-1, \sqrt{3}) + f_3 \cdot (-1, -\sqrt{3}) + f_4 \cdot \left(\frac{3}{2}, \frac{-\sqrt{3}}{2}\right) + f_5 \cdot \left(\frac{3}{2}, \frac{\sqrt{3}}{2}\right) \\ & + f_6 \cdot (0, \sqrt{3}) + f_7 \cdot (0,0) + c.c.\end{aligned}$$

where we have introduced the notation $f \cdot (a, b) = f e^{ik_c(ax+by)}$. For each such term, we have to solve:

$$\begin{aligned}\left[-n\gamma_c \sqrt{1+\beta^2} - (1+\alpha\beta)k_c^2(a^2+b^2) - \frac{\alpha^2(1+\beta^2)}{2}k_c^4(a^4+b^4+2a^2b^2) \right] f \\ = \chi(a, b)\end{aligned}$$

Where $\chi(a, b)$ represents the nonlinear contribution of that mode at that order.

For f_1 we have $\chi(2,0) = (\alpha-\beta)k_c^2 A^2 e^{2ik_c x}$, and we obtain:

$$f_1 = -\frac{2(\alpha-\beta)}{9(1+\alpha\beta)} A^2$$

The terms f_2 and f_3 are then found to be the same, with A replaced with B and C respectively.

We next consider f_4 , for which we have $\chi\left(\frac{3}{2}, \frac{-\sqrt{3}}{2}\right) = -(\alpha-\beta)k_c^2 A \bar{B} e^{ik_c(3x-\sqrt{3}y)/2}$, and we obtain directly:

$$f_4 = -\frac{(\alpha-\beta)}{2(1+\alpha\beta)} A \bar{B}$$

and we obtain the same for f_5 and f_6 , with $A \bar{B}$ replaced by $A \bar{C}$ and $B \bar{C}$ respectively.

The last term is the constant term f_7 , which is found to be:

$$f_7 = \frac{4(\alpha-\beta)}{(1+\alpha\beta)} (|A|^2 + |B|^2 + |C|^2)$$

We have thus determined the form of φ_1 , and we can go on to order 3. Here we get a second solvability condition to eliminate resonant terms. These have the form:

$$|A|^2 A, |B|^2 A, |C|^2 A$$

for the $e^{ik_c x}$ mode, the other terms being obtained by cyclic permutations of A, B, C. Inserting the expression for φ_0 and φ_1 , we finally obtain the solvability condition:

$$\partial_{T_2} A = n\delta \sqrt{1+\beta^2} A - \frac{8}{9} \frac{(\alpha-\beta)^2}{\alpha^2(1+\beta^2)} |A|^2 A - \frac{3}{2} \frac{(\alpha-\beta)^2}{\alpha^2(1+\beta^2)} (|B|^2 A + |C|^2 A)$$

and the equivalent for B and C. We can now combine the solvability conditions at order 2 and 3 to obtain the normal form for the hexagonal pattern:

$$\begin{aligned}\partial_T A = n\delta\sqrt{1+\beta^2}A + \frac{(\alpha-\beta)(1+\alpha\beta)}{\alpha^2(1+\beta^2)}\bar{B}\bar{C} \\ - \frac{(\alpha-\beta)^2}{\alpha^2(1+\beta^2)}\left[\frac{8}{9}|A|^2A + \frac{3}{2}(|B|^2A + |C|^2A)\right]\end{aligned}\quad (4-9)$$

The equations for B and C being obtained by cyclical permutations. Rescaling the amplitudes by the factor $3\alpha\sqrt{(1+\beta^2)}/\sqrt{8}(\alpha-\beta)$, we can put the equations into the form:

$$\partial_T A = n\delta\sqrt{1+\beta^2}A + \frac{3}{\sqrt{8}}\frac{(1+\alpha\beta)}{\alpha\sqrt{(1+\beta^2)}}\bar{B}\bar{C} - \left[|A|^2A + \frac{27}{16}(|B|^2A + |C|^2A)\right]\quad (4-10)$$

Stability analysis of the different possible stationary solutions of these equations then yields that the steady state (all amplitudes zero) is stable for:

$$\gamma > \gamma_c$$

and unstable otherwise. Hexagons become metastable for:

$$\gamma = \frac{79}{70}\gamma_c$$

and stable for $\gamma < \gamma_c$ up to the theoretical point:

$$\gamma = -\frac{455}{121}\gamma_c$$

where hexagons should lose their stability in favor of rolls [5]. This critical point should be taken with caution, as our local analysis is strictly speaking not valid in this range. But in our case this value can though never be attained, as γ would then have to cross zero, where our phase approximation is no longer valid. In fact, we observe numerically that the phase approximation breaks down before that due to the early onset of phase instability. We conclude that the pattern formation due to the quenching of the phase instability in two-dimensions leads exclusively to hexagonal structures. We also note that γ_c is proportional to $(1+\alpha\beta)^2$, which we had assumed small, so the hexagons should be weakly sub-critical. This result is in good agreement with numerical evidence.

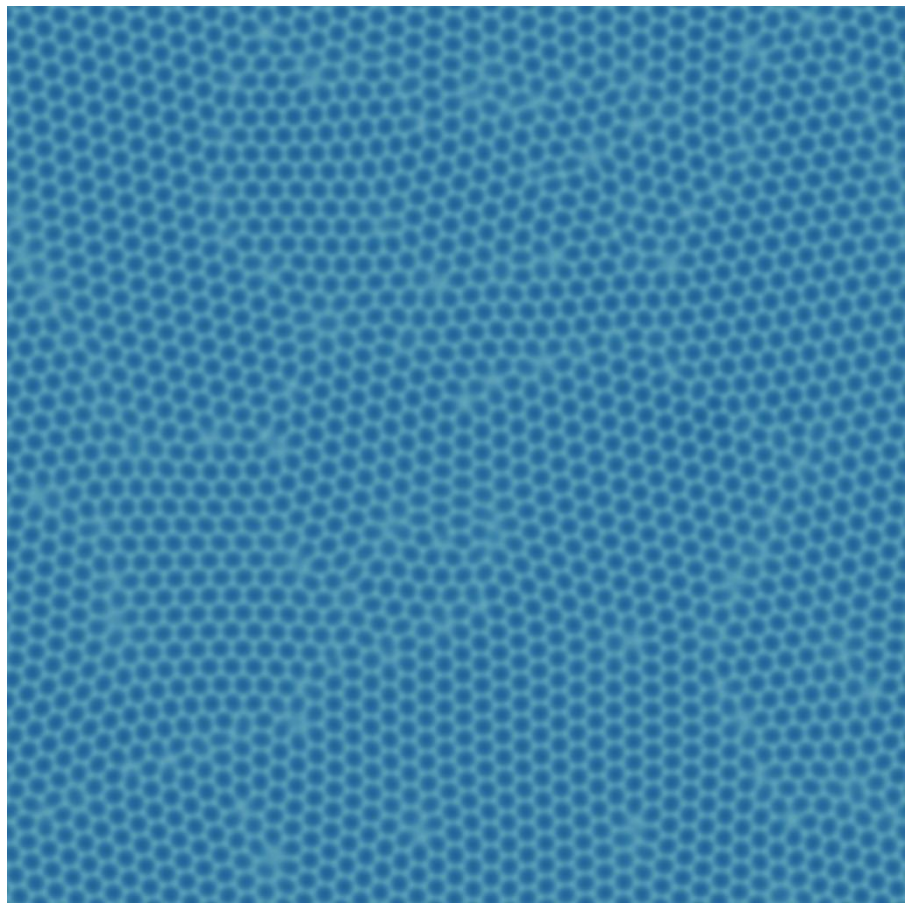


Figure 36: Hexagons around a phase locked state for $n = 2$. Figure showing the real part of the field A . ($\alpha = -1.29$, $\beta = 1.5$, $\nu = 1.45$ and $\gamma = 0.06$)

5 AMPLITUDE INSTABILITIES AND DEFECT BIFURCATIONS

Up to now, we have focused our attention on phase limits of Eq.(3-5). In this limit, the phenomena found are essentially the same for all resonances. This is because when the phase space reduces to a circle, there is no real qualitative difference between the various cases.

For amplitude instabilities, the situation is different, because now the origin is brought into the picture in a non-trivial manner and its behavior is qualitatively different for all cases. This has a great effect on the nature of defects, because most of them live on or close to this unstable solution and their behavior will thus depend on the underlying dynamic. To reduce the scope of our analysis, we will focus our attention on the parametric resonance, i.e. the case $n = 2$.

A quick glance at the bifurcation diagram of that system (see section 3.6.3), shows that we expect the generic existence of kink-like structures, joining the two phase locked states, with the core of the kink lying on or close to the origin. We also see that the origin can have four different stability types: hyperbolic, unstable node, unstable spiral and Hopf (through homoclinisation). This will affect the behavior of the kink greatly leading to a variety of phenomena in 1D and 2D. In most cases, it is only the behavior of the core which changes, as the phase locked states remain qualitatively the same. We can thus really consider all these phenomena as being bifurcations of the kink solution. The core being essentially 0-dimensional (in one space dimension), this again leads to a behavior characteristic of finite dynamical systems.

In this chapter we will study these phenomena, using analytical results when possible, but otherwise be trying to understand the qualitative mechanism underlying the various instabilities.

To begin with, we will develop the analogy between Eq.(3-5) for $n = 2$, and the dynamic of spins in magnetism, thus yielding some physical insight in the interpretation of kink-like structures.

5.1 BLOCH AND ISING DOMAIN WALLS IN MAGNETISM

In magnetism, a model where the spin is constrained to move in a plane is called the X-Y model. The free energy for such a model is given by [45]:

$$F = F_0 + |\nabla M_x|^2 + |\nabla M_y|^2 - a \frac{T - T_c}{T_c} (M_x^2 + M_y^2) + \frac{1}{2} D (M_x^2 + M_y^2)^2 \quad (5-1)$$

where $M = (M_x, M_y, M_z)$ is the magnetization and T_c is the Curie temperature. Writing $A = M_x + iM_y$, we can express the dynamic by a variational principle as:

$$\partial_t A = -\frac{\delta \int F dx}{\delta \bar{A}} = a \frac{T - T_c}{T_c} A - |A|^2 A + \nabla^2 A$$

Which describes the second order phase transition in which the magnet acquires a magnetization for $T > T_c$, with an arbitrary orientation in the X-Y

plane. Typically, this will create domains of magnetization, which eventually disappear in favor of a homogeneous magnetization, thereby minimizing the free energy.

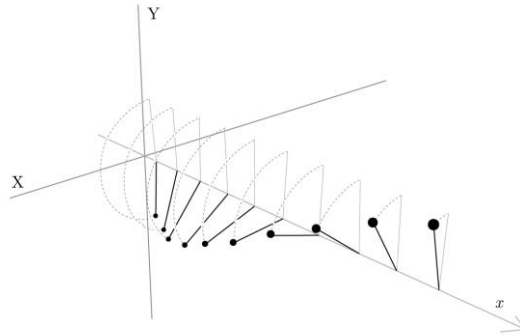


Figure 37: The X-Y spin model. This shows a configuration of spin coupled along a line.

In the presence of anisotropy of the original system, this behavior is quite different. An anisotropy in this case is anything which favors a given orientation in the X-Y plane. This could be due to crystalline anisotropy or the presence of an external magnetic field. In the case where one axis is favored (that we can take to be the X-axis), a new term must be added to the free energy: $-K(M_x^2 - M_y^2)$. This leads to the evolution equation [35]:

$$\partial_t A = \alpha \frac{T - T_c}{T_c} A - |A|^2 A + \nabla^2 A + K \bar{A} \quad (5-2)$$

Which is seen to be equivalent to the $q = 2$ parametric resonance, without non-variational terms. We can thus interpret the phase locked solution of Eq.(3-5) as being the preferred orientation of magnetization of an easy-axis ferrimagnet.

We note that there is no difference of energy between the two diametrically opposed states. This has the consequence that above the transition point we generically have domains of 'up' and 'down' magnetization separated by domain walls. Such walls are known in the solid state literature as Bloch and Ising domain walls.

The exact nature of these walls depends on the equilibrium between the anisotropy torque and the exchange torque. Intuitively we expect that when the anisotropy is strong compared to spin interaction, then spins with orientation not parallel to the preferred axis will be energetically disfavored. This gives rise to Ising walls, where the magnetization flips from one state to the other, while lying exclusively along the easy axis. This has the consequence that the magnetization goes down to zero in the core of the wall. But this again is a compromise, as the state of zero magnetization is an unstable one. This is a typical example on how core of defects lie through unstable solutions of the system.

When the anisotropy becomes comparable with the spin interaction, a transition in the nature of the domain wall is observed. The energy cost involved in making a transition between up and down states by going through an unstable solution becomes comparable with the energy cost of having spins

lying outside of the preferred axis. This gives rise to Bloch walls, where the magnetization transits from one state to the other by rotating in the X-Y plane.

An interesting characteristic of Bloch walls is that they are inherently chiral, in the sense that they have two distinct direction of rotation: they can transit clockwise or anti-clockwise. We can thus interpret the transition between Ising and Bloch walls as a break of the chiral symmetry.

5.2 THE ISING/BLOCH TRANSITION IN THE PARAMETRIC RESONANCE CASE

In terms of the parametric resonance, the analogy is that Ising walls correspond to regions separating oscillators running in phase and anti-phase with the forcing, where the connection is mad with a phase jump, while Bloch walls correspond to a transition where the phase changes smoothly from one to the other over a finite region.

For the magnetism model described by Eq.(5-2), the exact solutions are known [46, 47, 48]. They correspond to solutions of Eq.(3-5), where the non-variational parameters ν, β and α are set to zero. In one dimension, these solutions can be written as:

$$X_I = \pm\sqrt{1+\gamma} \tanh\left(\sqrt{\frac{1+\gamma}{2}}x\right) \quad (5-3)$$

$$Y_I = 0$$

for the Ising wall, the Bloch wall being given by:

$$X_B = \pm\sqrt{1+\gamma} \tanh(\sqrt{2\gamma}x) \quad (5-4)$$

$$Y_B = \pm \frac{\sqrt{1-3\gamma}}{\cosh(\sqrt{2\gamma}x)}$$

Where we have put $A = X + iY$.

But we can in fact seek more general solutions, of the form $A = R(x)e^{i\varphi}$, including the non-variational terms. After insertion, this yields:

$$\partial_t R = R - R^3 + \gamma R \cos(2\varphi) + \partial_x^2 R$$

$$0 = \nu R - \beta R^3 - \gamma R \sin(2\varphi) + \alpha \partial_x^2 R$$

By now using the ansatz: $R = c_1 \tanh(c_2 x)$, and inserting into the above expressions, we obtain:

$$0 = (2c_1 c_2^2 - c_1^3) \tanh(c_2 x)^3 + (c_1 - 2c_1 c_2^2 + \gamma c_1 \cos(2\varphi)) \tanh(c_2 x)$$

$$0 = (2\alpha c_1 c_2^2 - \beta c_1^3) \tanh(c_2 x)^3 + (\nu c_1 - 2\alpha c_1 c_2^2 - \gamma c_1 \sin(2\varphi)) \tanh(c_2 x)$$

Solving for c_2 yields:

$$c_2^2 = \frac{1 + \alpha\nu \pm \sqrt{\gamma^2(1 + \alpha^2) - (\alpha - \nu)^2}}{2(1 + \alpha^2)}$$

To solve for c_1 we must assume that $\beta = \alpha$, which gives:

$$c_1^2 = \frac{1 + \alpha\nu \pm \sqrt{\gamma^2(1 + \alpha^2) - (\alpha - \nu)^2}}{1 + \alpha^2}$$

Which corresponds exactly to the amplitude squared of the locked states. The angle of rotation φ can be found as:

$$\varphi = \frac{1}{2} \arctan \left(\frac{\nu - 2\alpha c_2^2}{2c_2^2 - 1} \right)$$

The simple interpretation of this solution is that it corresponds to the Ising wall solution Eq.(5-3), rotated by a complex constant. This is basically due to the fact that the detuning ν simply rotates the phase locked states in the complex plane. It also appears that α cancels the effect of β on the solution. We also note that we have two possible values for the constant c_2 , but the solution with the minus sign in the expression for c_2 simply corresponds to an Ising solution joining the hyperbolic fixed points, and is thus unstable.

To simplify things, we can rotate Eq.(3-5) by $e^{-i\varphi}$, and take $\alpha = \beta = 0$. We then have the solution in the rotated coordinates:

$$X_I = \sqrt{\gamma^2 - \nu^2} \sqrt{1 + \sqrt{\gamma^2 - \nu^2}} \tanh \left(\sqrt{\frac{1 + \sqrt{\gamma^2 - \nu^2}}{2}} x \right) \quad (5-5)$$

$$Y_I = 0$$

and in the original system they become:

$$X_I = \frac{\sqrt{\gamma^2 - \nu^2} \sqrt{1 + \sqrt{\gamma^2 - \nu^2}}}{\gamma} \tanh \left(\sqrt{\frac{1 + \sqrt{\gamma^2 - \nu^2}}{2}} x \right) \quad (5-6)$$

$$Y_I = \frac{\nu \sqrt{\gamma^2 - \nu^2} \sqrt{1 + \sqrt{\gamma^2 - \nu^2}}}{\gamma} \tanh \left(\sqrt{\frac{1 + \sqrt{\gamma^2 - \nu^2}}{2}} x \right)$$

where we see that the effect of ν is simply to renormalize γ .

In exactly the same manner, we can derive a similar expression for the Bloch wall, with the same renormalization of γ .

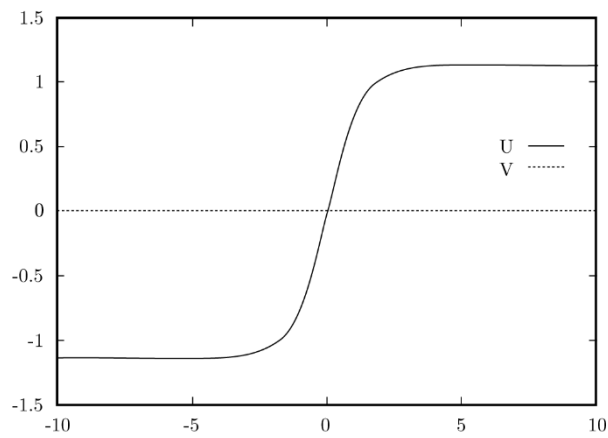


Figure 38: A sketch of the analytical Ising wall for $\gamma = 0.35$.

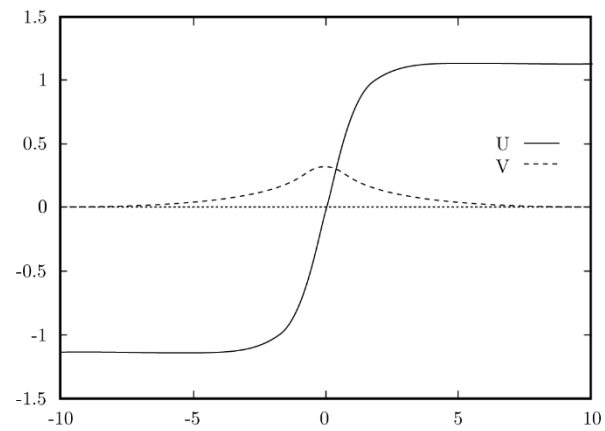


Figure 39: A sketch of the analytical Bloch wall for $\gamma = 0.3$.

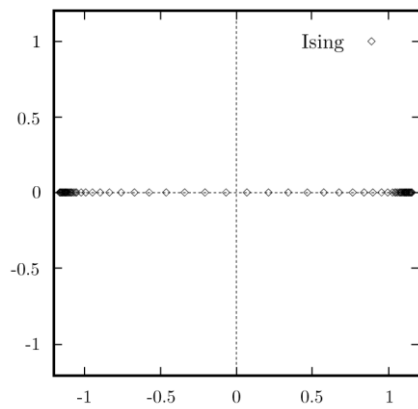


Figure 40: Numerical simulation in the variational case with $\gamma = 0.35$. Figure shows the spatial manifold in the phase space of A . The Ising wall goes through the origin.

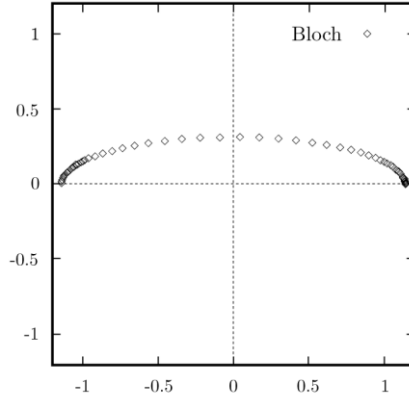


Figure 41: Same as in previous with $\gamma = 0.3$. The Bloch wall avoids the origin.

5.2.1 Qualitative stability analysis of Bloch and Ising walls

The stability of Eq.(5-3) and Eq.(5-4) can be calculated explicitly with a linear stability analysis, or from an energy point of view [23, 27], but it can also be inferred from a qualitative analysis (it should also be noted that all the stability results applying to the solutions, also apply to the rotated solution $v \neq 0$, simply by making the transformation $\gamma \rightarrow \sqrt{\gamma^2 - v^2}$).

First of all, we observe that the phase space of Eq.(5-2) has two attracting fixed points, which domains of attraction are separated by stable manifolds of unstable points. The existence of an Ising like solution is then seen to be generic when $\gamma > 1$, because then the origin is hyperbolic, and any initial condition crossing the stable manifold of the origin will necessarily be trapped on it.

For $\gamma < 1$ the situation is subtler, as we then have two new fixed hyperbolic points bifurcating from the origin which is now an unstable node. A naïve qualitative argument would suggest that we now should generically have solution trapped on the stable manifold of the new hyperbolic point. This is not quite so, because the flow is not symmetric around the hyperbolic point.

A simple argument consists in comparing the eigenvalue with which a solution leaves the origin towards the hyperbolic point, and the eigenvalue which the latter has in the direction of the stable fixed points. The idea is to compare the tendency to avoid the origin with the tendency to avoid the origin with the tendency to align along the anisotropy axis. The two antagonist ‘forces’ are equal when:

$$1 - \gamma = 2\gamma \rightarrow \gamma = \frac{1}{3}$$

This is precisely the result of a detailed stability analysis which gives that Ising walls are stable solutions for $\gamma > 1/3$, but else they exchange stability with Bloch wall solutions.

If we define the chirality of the wall as being:

$$\chi = \int_{-\infty}^{\infty} (Y \partial_x X - X \partial_x Y) dx \quad (5-7)$$

We can draw the bifurcation diagram, describing the breaking of the chiral symmetry of the domain wall. From now on we will call any domain wall with non-zero chirality a Bloch-like wall, or simply a Bloch wall, regardless of whether their form is given by Eq.(5-4). In the same manner we will call non-chiral walls, Ising walls.

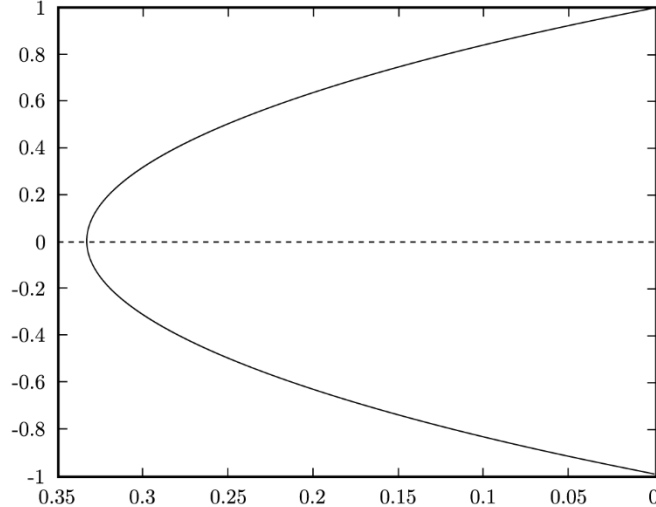


Figure 42: Bifurcation diagram for the chiral parameter as a function of γ .

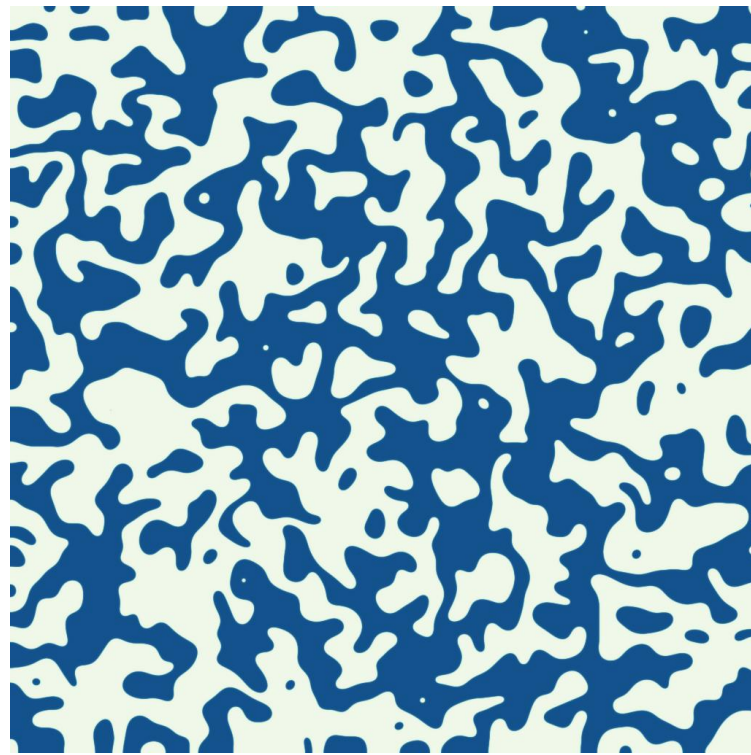


Figure 43: Ising domains in two dimensions. Figure shows real part of A .

This example of transition between Bloch and Ising walls is a good example of a defect bifurcation. The defect exists due to topological constraints in phase space and its core is strung across an unstable solution, or its stable and unstable manifolds. Any change in the stability or topology of this unstable solution will thus be reflected in the core of the defect. This is an important

conclusion, as it is often the case that the core of the defect is responsible for pattern selection mechanisms, and as such it has an influence on the whole spatial structure. A bifurcation in the core can thus drastically change the nature of the system. We will see in the next section how this can happen for the Ising/Bloch solutions.

5.3 NON-VARIATIONAL EFFECTS ON BLOCH AND ISING WALLS

Up to now, our discussion on Bloch and Ising walls has been in analogy to the transition of spins in ferromagnets. This model can be derived from a free energy by a variational principle, and will thus always evolve into an equilibrium state

The introduction of complex parameters into equation Eq.(5-2), yielding in fact Eq.(3-5), radically changes this picture. As we can no longer define a free energy, then there is no guarantee of existence of static equilibrium solutions. The system thus becomes a non-variational or out-of-equilibrium system, where non-static solutions can be maintained by a continuous energy input, balancing the stabilizing effect of diffusive terms.

We can investigate what happens to our domain wall solutions in the limit of small non-variational terms (ν , β and α in Eq.(3-5)). Qualitatively there is no drastic change in the stability of fixed points, so we do not expect the wall solution to disappear. On the other hand, there is (for ν and β) a change in the symmetry of the system as seen from the defect, characterized by the convergence of the stable and hyperbolic solutions. For the Ising wall this is of no consequence, but for the Bloch wall there is a change. In the variational case, the core of the wall was equally distributed between the two domains of attraction of the fixed points. But with the addition of the non-variational terms, there is now a larger fraction in one domain compared to the other. This dissymmetrizes the wall and we can expect that the stable solution around the fixed point with the larger domain of attraction will win over the other one, thus making the wall move. This is purely a non-variational effect, as there is absolutely no dynamical difference between the two stable states, and the movement of the wall only depends on the chirality, as can be seen from the fact that when the chirality is close to zero, the equilibrium between the domains is restored. We thus have an interesting change of Bloch walls due to non-variational terms, which can be summarized in that Bloch walls move with a speed proportional to their chirality [23, 36].

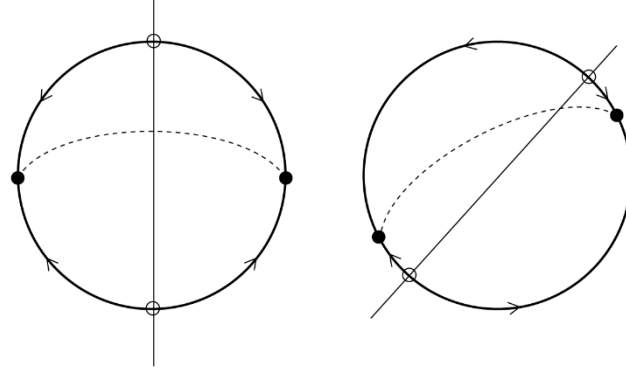


Figure 44: Domains of attraction of the stable points in the variational and non-variational case. The dashed line represents a Bloch wall solution. Notice how asymmetric the domains of attraction are with regard to the Bloch solutions.

This result is more rigorously shown by considering the non-variational terms as a small perturbation, and the domain wall solution as homoclinic orbits connecting the two stationary solutions. By using Melnikov's method to check the persistence of this orbit, we obtain the Melnikov function:

$$M = \int_{-\infty}^{\infty} \left(\Re(G(A_0)) \frac{\partial \Re(A_0)}{\partial x} + \Im(G(A_0)) \frac{\partial \Im(A_0)}{\partial x} \right) dx$$

Where G is the non-variational part of Eq.(3-5), and $A_0(x)$ is the wall solution. For Ising walls, $M = 0$, so they do persist under small non-variational perturbations. For Bloch walls the $M = 0$ condition is inconclusive. It can be made conclusive by allowing the wall to move, i.e. by considering a perturbed solution of the form: $A(x) = A_0(x + s(t)) + \epsilon a(x + s(t))$. The solvability condition then yields in the case $\nu \neq 0$:

$$\partial_t s \approx \frac{3\pi}{2\sqrt{2}} \frac{\nu\chi}{1 + \sqrt{\gamma^2 - \nu^2}} \quad (5-8)$$

Where $\chi = \sqrt{1 - 3\sqrt{\gamma^2 - \nu^2}}$ is the chirality.

This new effect has a small but interesting consequence in one dimension in what concerns asymptotic behavior. Indeed, for an arbitrary initial condition in a regime where Ising walls are stable, we will end up with a spatially chaotic array of Ising walls, which is stable for very long times. On the other hand, in a Bloch regime with non-variational terms, the mobility of defects is greatly increased, thus boosting up the rate of kink/anti-kink annihilations. This has a direct consequence that for asymptotic times, one of the phase locked solution will be chosen, given any arbitrary initial condition. This is an example of where when putting a system out of equilibrium actually leads to a 'cleaner' defect-free state.

In two spatial dimensions, the situation is not the same, but nevertheless, the bifurcation of the Ising wall leads to a remarkable phenomenon. This is the subject of the next section.

5.3.1 Néel spirals

In two dimensions, Bloch and Ising walls still exist, now forming a line defect. We thus observe the existence of domains of arbitrary shape and size. These domain will either shrink or expand in the non-variational Bloch regime.

A new phenomenon arises though, which is directly related to the dimension of space and the discrete nature of the broken chiral symmetry of Bloch walls. In a qualitative description, we see that if some arbitrary initial condition is mapped into phase space, it can have a generic intersection with the origin due to its two-dimensional nature. In the Ising regime this is of no consequence, as the evolution will eventually lead to the formation of lines of complex zeros, corresponding to the Ising wall line defect.

In the Bloch regime things are different, as part of the system can evolve to a right-winding Bloch wall, while another part can evolve to a left-winding Bloch wall. In other words, as the chirality is a real order parameter, describing the appearance of a discrete symmetry, we can have Ising like kinks of chirality *along* the Bloch wall, where the chirality goes from right to left over a finite region. Such a defect appears as point defect in a two-dimensional system, and is known under the name of Néel point in magnetism.

In the variational regime, this new defect can be considered as a mere curiosity, as it has no consequence on the global structure. In the non-variational case, the Néel point becomes the center of a remarkable pattern formation.

Indeed, if we focus our attention on the core of the Néel point, then it is reasonable to assume that the chirality varies in a linear manner. Knowing that the speed of a Bloch wall is proportional to the chirality, we have at the core a straight wall segment where the speed varies linearly from $-v_0$ to v_0 , where v_0 is the asymptotic value of the speed along the chirality kink. Assuming the speed is always perpendicular to the wall, this segment will tend to rotate uniformly. Far from the core, the speed of the wall is at its asymptotic value, so it moves uniformly.

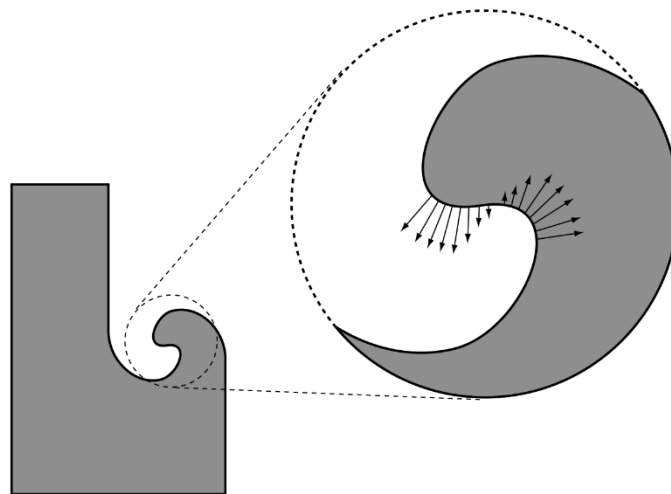


Figure 45: Detail of the core of the excitable spiral. Chirality changes sign at the core, thus yielding a kink-like velocity profile.

In a way we can think that the tips of the rotating wall segment are constantly generating Bloch walls in the azimuthal direction, moving at asymptotic speed. It is not hard to see that this generates a two-armed spiral centered around the Néel point. We can even estimate the wavelength, as it will be the distance travelled by one spiral arm while the core performs one full rotation. This yields directly:

$$\lambda = \pi\Delta$$

where Δ is the width of the chirality kink. It can be estimated as: $\Delta = 4/\sqrt{1 - 3\gamma}$. We thus have:

$$\lambda = 2 \frac{2\pi}{\sqrt{1 - 3\gamma}}$$

which is valid for small values of the non-variational terms. For large value of ν we can put the renormalized value of γ in this expression to get a better estimate.

To summarize, we observe how in two dimensions, the bifurcation of a point defect leads to the appearance of a complicated spatial behavior, characterized by the existence of a static distribution of rotating spirals with fixed wavelength. This is quite different from the one-dimensional case, where we eventually had a defect free state in the non-variational system. This is of course simply due to the fact that in two-dimensions, the point defects have practically no mobility and can thus not disappear easily. Such a spiral has recently been observed in nematic liquid crystals in a rotating field [38], and a reduction from microscopic equations for this system does indeed yield Eq.(5-2).



Figure 46: Early dynamic of a Neel point in the non-variational case. Figure shows the real part of A.

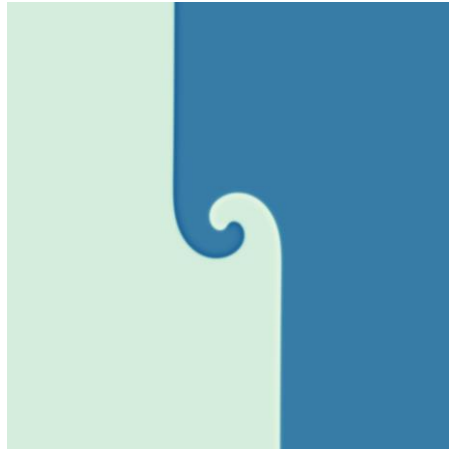


Figure 47: Same as in previous figure a little later.

5.4 OSCILLATORY INSTABILITY OF ISING WALLS

The Bloch/Ising transition is not the only possible bifurcation of the kink defect. Another important transition occurs for $\beta \neq 0$. In that case, the analytical solution for the kink is not known (except for $\alpha = \beta$), so we will have to make a qualitative description of this.

5.4.1 The ‘twist’ instability

We have already seen that for small values of β , we will have persistence of the Bloch solution, except that it will now move. For larger values of β , it is still clear that for large enough forcing, an Ising-like solution will still exist. The interesting consequences of $\beta \neq 0$ on the phase space of Eq.(3-5) is amongst others that there is now a possibility for the origin to be an unstable foci instead of being an unstable node. As the core of the kink lies through the origin, we expect a change in the nature of the kink for that situation.

By looking at the difference between the attractor on which the spatial manifold relaxes in phase space for $\beta = 0$ and $\beta \neq 0$, and when we put ourselves in a region where the origin has unstable imaginary eigenvalues, we see that there occurs a twist at the core. This twist increases as we go further away from the middle of the resonance tongue.

For a certain amount of twist, an instability occurs, which can be explained as follows. We can estimate that the two respective domains of attraction of the phase-locked states can be roughly delimited by the line joining the two unstable hyperbolic points (more rigorously they are delimited by the stable manifold of the hyperbolic point which joins the origin for $t \rightarrow -\infty$), and the line joining the two stable states. We see that for small enough twist, the kink attractor is divided in two connex halves, each lying entirely in the domain of attraction of a stable state, the two halves being separated at the origin.

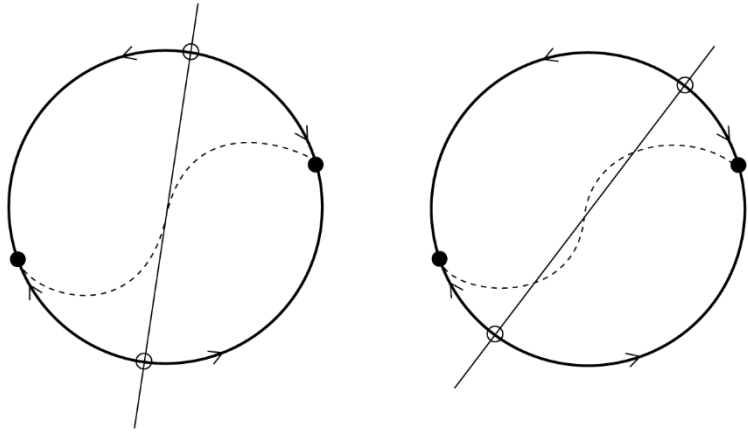


Figure 48: The twist instability of the core of the kink. Figure shows the kink solution (dashed), and how its core becomes unstable when we get near the resonance boundary.

If the twist becomes large enough, we see that a small part of the kink around the origin can cross the domain boundary and finds itself attracted to the opposite fixed point. The spatial manifold can no longer be separated in two connex halves belonging to the domain of attraction of the respective stable points.

What is observed is that the core of the kink then develops two new small kinks, which evolve towards being independent kinks, i.e. a kind of knot or folding of the original kink occurs around the origin. If we are just above threshold of that instability, the new kinks never actually make it, and eventually the knot unfolds, thus restoring the original kink. The unfolding though is a complicated process, so the kink loses its appearance while it happens. In these cases, the folding and unfolding process is observed to be roughly periodic in time. Apparently, the kink will also move as a result of this instability, which can be understood because while in the folding and unfolding process, the kink has a non-zero chirality, so it will have a tendency to move. In fact, in the case when dispersion is also present, we observe a similar instability, which can be understood as a Hopf bifurcation of the chirality parameter. This is the subject of the next section.

5.4.2 Hopf bifurcation of chirality

The most remarkable aspect of this instability of the core of the kink occurs for non-zero values of the dispersion α . As we have seen in the case of the Ising walls, then if α is close to β , the effect of the dispersion is to undo the effect of β . We are thus interested in the instability of the kink for a dispersion with the opposite sign of that of β (The effect of the dispersion in this case must be understood as a kind of spatially dependent non-linear detuning).

We fix α and β in Eq.(3-5), such that $\alpha\beta < 0$, and we vary the forcing γ . For large enough γ , the usual Ising-like kink is observed. As we lower γ , and we come to a configuration of phase space such that the twist instability can develop, the core of the kink starts to oscillate around the origin. The difference between the previous description of the twist instability is thus that the core

does not fold around the origin like before, but rather it oscillates as a whole, so no new kinks are formed. In fact, an ansatz of the form:

$$A = A_I(x) + B(x)e^{i\omega_0 t}$$

where $A_I(x)$ is the stable Ising-like solution and $B(x)$ is the envelope of the amplitude, and is such that it vanishes far from the core, should describe this structure approximately. We have thus our basic Ising-like kink, which develops an oscillatory component with mean value zero. This form suggests immediately an interpretation of this phenomenon. Indeed, in the case of the Ising/Bloch transition described earlier, the most natural way to analyze that bifurcation was to study the stability of the Ising wall solution with regards to small perturbations. This leads to an equation of the form:

$$\partial_x^2 B + f(x)B = \sigma B$$

where B represents the perturbation of the kink solution. In the Ising case, this equation turns out to be solvable, leading to an eigenvalue problem with one discrete real eigenvalue, the rest being a continuous spectrum. The discrete eigenvalue has a corresponding eigenfunction which corresponds to the chirality breaking part of the Bloch solution. We thus have in that case a pitchfork bifurcation of the chirality, as described earlier.

It is thus extremely likely that this oscillatory bifurcation corresponds to a similar transition from a non-chiral wall towards a chiral wall, but with a complex eigenvalue. This would thus be a Hopf bifurcation of the chirality of the kink. Unfortunately, as the analytical form of the kink for arbitrary α and β is not known, this analysis cannot be pursued here.

The effect of this Hopf bifurcation on the behavior of the kink turns out to have far reaching consequences. Indeed, as the chirality oscillates, the kink moves with a velocity proportional to the chirality. It thus starts to move back and forth in a regular manner. But as the forcing is decreased, a transition occurs, which can be interpreted as the Ising/Bloch transition of the underlying kink. What is observed is that the chirality now acquires a non-zero mean value, which can be positive or negative. This has the net result that the kink will no migrate in one give direction, in an oscillatory manner.

To analyze what happens next, it is best to build an observable which gives us some information about the exact oscillatory behavior of the kink. The simplest is to define a position independent measure, which can for example be taken to be the chirality itself:

$$\chi = \int_{-\infty}^{\infty} (Y\partial_x X - X\partial_x Y)dx$$

Where we have written $A = X + iY$. By looking at a return map of this variable, i.e. looking at points $(\chi(t), \chi(t + \tau))$, for some conveniently chosen delay time τ , we observe at the onset of the oscillation a limit-cycle which appears supercritically.

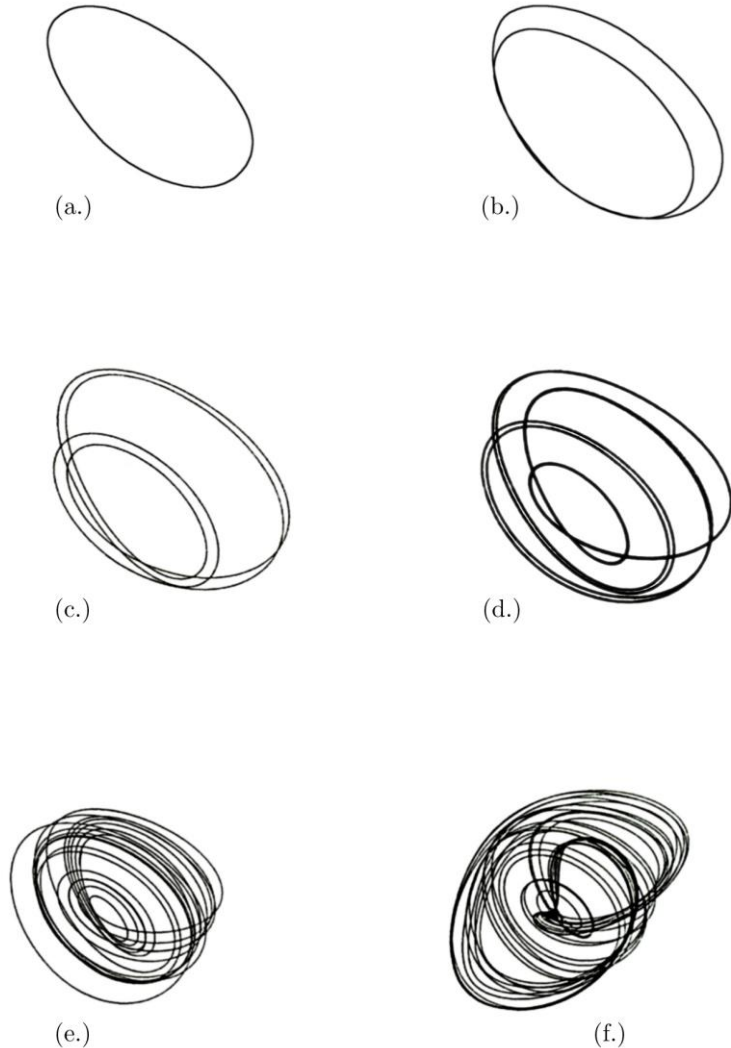


Figure 49: Period doubling cascade of the core of the kink. Figures show a simple Hopf bifurcation of chirality, period doubling, period quadrupling, period octupling, strange attractor and strange symmetric attractor, respectively ($\alpha = -1.3, \beta = 1.5, v = 1.55$ and $\gamma = 0.455, 0.445, 0.428, 0.422, 0.415, 0.370$) Delay time $\tau = 0.033$.

For lower values of γ , a period doubling transition occurs, and then successively a whole cascade of period doublings, eventually ending on a strange attractor.

At this stage the kink migrates in a chaotic fashion, going in one way for some time, then changing direction at arbitrary times, but still with a global trend in some direction. For a lower value of γ , a qualitative change of the attractor is observed, which can be interpreted as the symmetrization of the strange attractor [49]. The kink then has no longer any trend in one given direction, and its position effectively diffuses in the system.

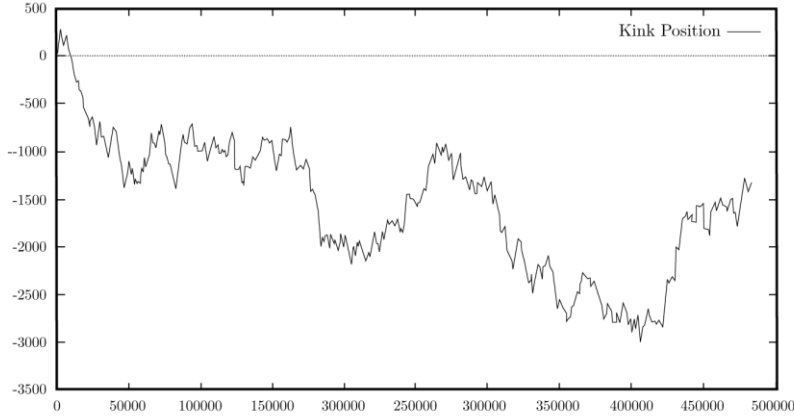


Figure 50: Position of the kink defect as a function of time ($dt = 0.3$, $v = 1.55$, $\beta = 1.5$, $\alpha = -1.3$ and $\gamma = 0.370$)

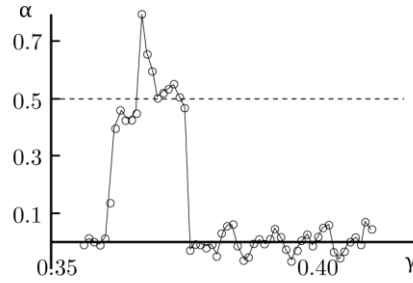


Figure 51: Diffusion rate of defect as a function of γ . Fit values of α for the dispersion of defect position $P(t)$ in $\langle P(t)^2 \rangle - \langle P(t) \rangle^2 = Ct^{2\alpha}$ as a function of γ . The dashed line corresponds to Brownian motion. ($dx=1.0$, $dt=0.3$).

The interpretation of this phenomenon is the following. We know that the origin is unstable for these values of parameters, and we also know that in the limit that γ goes to zero, we would be in a situation of instability characterized by an unstable phase. Now all these instabilities cannot manifest themselves while the stable states exist, but in the kink, one part of the system lies through the unstable solution, and thus senses these instabilities before they actually can develop in the whole system. In the case that the dispersion is zero, these instabilities manifest themselves as strong amplitude instabilities originating from the core of the kink, eventually leading to the formation of new kinks. In the case where $\alpha\beta < 0$, the situation is more subtle and the core actually behaves as it was a discrete dynamical system. This could be understood in the following manner: when we lower the forcing, we get closer to the instabilities linked with the origin. As the core of the kink lies through the origin, these instabilities will have a tendency to manifest themselves there first. But due to the spatial confinement of the core of the kink, imposed by the topology of phase space, the instabilities actually develop like they were in a bounded system. The unstable modes will thus be discretized, and will appear one by one in the core. In the limit where we have only a couple of modes in the core, the behavior of the core will be typical of a low-dimensional discrete dynamical system.

What is interesting is that though this instability is spatially confined, it leads, through the breaking of the chiral symmetry, to a spatial behavior. The defect has then at its core, a chaotic motor which drives it stochastically through the whole system.

For lower values of γ , various behavior is observed, including backwards period halving transitions, the exact scenario being extremely sensitive of the exact values of the parameters. For some critical value of γ , the instability of the core, which can be seen as a turbulent drop, finally invades the system, through two fronts which propagate at a given velocity [50, 51].

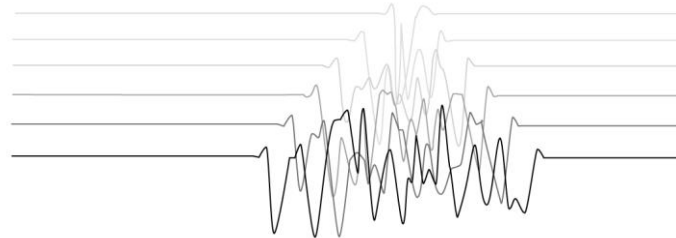


Figure 52: Spreading of a turbulent drop, as the width of the chaotic kink diverges. This shows the modulus of A , for different times.

5.4.3 Chaotic domains in two dimensions

In two dimensions, we can investigate what happens to Ising-like domain walls for these values of parameters. Though we can no longer, strictly speaking, talk of discrete dynamical behavior at its core, we do observe a behavior which can be understood as if the whole domain wall has a chaotic position in space. A typical evolution of a domain wall in these conditions is shown in Figure 53.

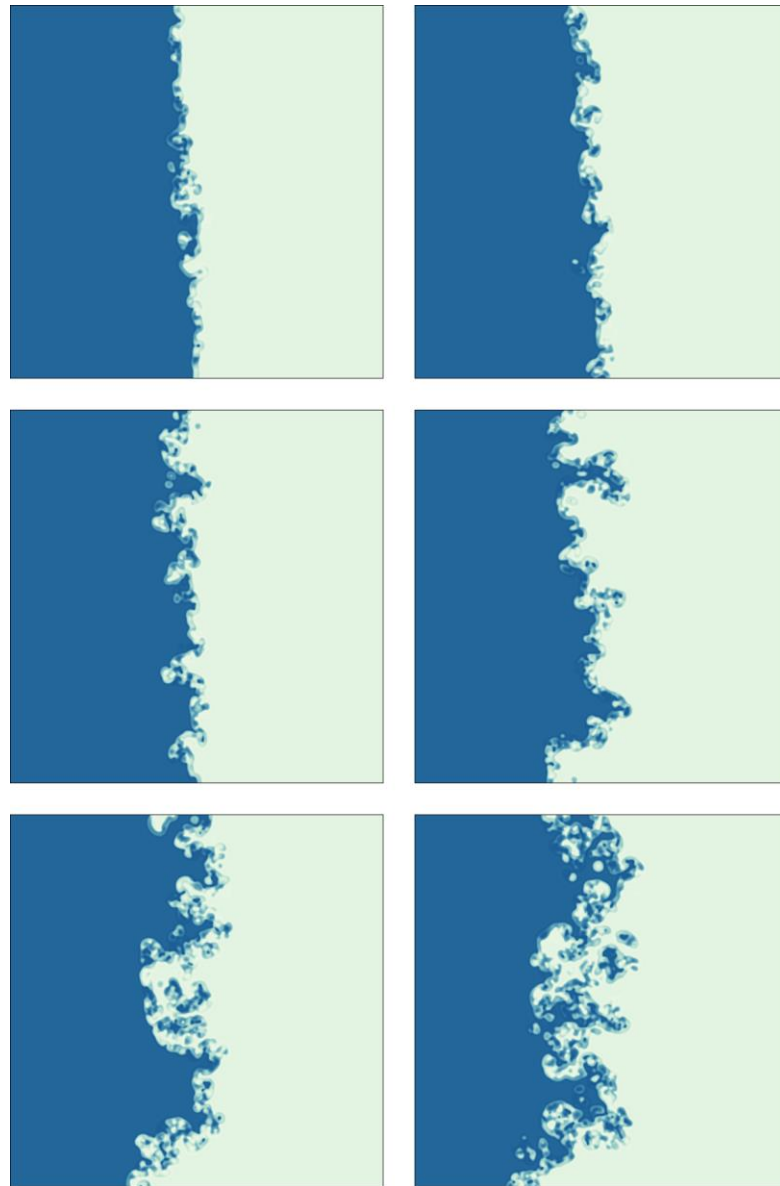


Figure 53: Evolution of a chaotic domain wall in two dimensions

5.5 INSTABILITIES LEADING TO SPATIAL STRUCTURATION

Up to now we have studied kink solutions joining phase locked states. But there exists another instability which doesn't necessarily involve the locked states, but is only due to the anisotropy of the flow around the origin.

For a wide range of parameters Eq.(3-5) evolves into a periodic structure, and often these structures evolve smoothly from states characterized by the existence of Ising-like kink solutions. This is why we are tempted to formulate a qualitative interpretation of these pattern forming instabilities, even though all such interpretations should be taken not too seriously, but only considered as an attempt to unify our vision of defect genericity with genericity of pattern forming instabilities. The idea is to link the existence of pattern instabilities with the existence of kink solutions or some other static attractor surrounded by a limit cycle.

5.5.1 The winding mechanism

We assume that there is a situation in phase space such that a kink solution exists, i.e. two stable states which can be joined by some spatial solution, or more generally some stable attractor on which the spatial solutions relax to. Let us consider the case where a global bifurcation occurs such that a Hopf cycle emerges, which encircles the two stable states which remain qualitatively unchanged.

In principle, the kink solution will still exist, as nothing has changed in the stability of the fixed points. The new phenomenon arises when there is an initial condition which has some part cutting the new limit cycle. Then there is one part of the system which wants to relax on the kink attractor, while another part tends to rotate around that attractor. The spatial manifold will thus be winded around the kink attractor, with a winding rate proportional to the frequency of the limit cycle. As a result of this a roughly periodic array of kinks will be built up. In this case, the dispersion, which is essentially a diffusion in Fourier space, will regularize the pattern, and effectively choose a single wavelength. That wavelength should be inversely proportional to the cycle frequency.

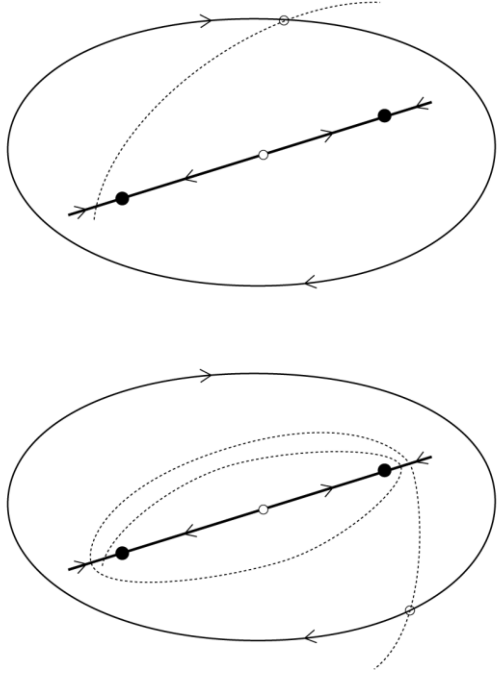


Figure 54: Principle of the winding mechanism. A spatial manifold intersects a limit cycle, while at the same time being attracted towards a stable attractor.

As a specific example, we consider instabilities happening at the onset of the phase locked states, i.e. when we have a transition between a limit cycle and the existence of phase locked states. This happens when we enter the resonance horn from one direction. We will take $\beta = 0$, and we assume that we are in the oscillatory regime.

In this region, there is of course no fixed point to lock on, but there is still an anisotropy in the oscillation rate, the rate being lower near the region where the fixed point will appear through a saddle node when crossing the resonance horn. If we do cross the tongue, we will in fact have an evolution towards a kink solution of the type Ising or Bloch.

Just outside the tongue, the oscillation rate is basically proportional to the distance from the tongue, i.e. $\sim \sqrt{\nu^2 + \gamma^2}$. But there is another effect which influences the frequency, at least from a point of view of the spatial solution, namely the dispersion α .

Indeed, the dispersion also induces a rotational effect in phase space, but it is much more difficult to interpret, as it represents a spatial effect not present in the dynamical system. As such, the qualitative theory presented in the first chapter does not apply to cases involving dispersive effects. But we have already seen cases in the context of Ising and Bloch walls, where the effect of α and β can be considered as similar (e.g. the Ising solution being valid for $\alpha = \beta$). So, we can sometimes look at α as being a kind of detuning, which depends on the spatial form.

In that context, we can conceive that for some value of α , the dispersion will have a reducing effect on the effective detuning as seen by the spatial solution,

and thus on the oscillation rate. In other words, from the point of view of the spatial solution, the system will be closer to the resonance tongue than the dynamical system predicts. We can even think that for some value of the dispersion and for a given shape of the spatial solution, the oscillation rate actually goes down to zero. If such is the case, this will naturally occur along the anisotropy axis, the oscillation rate being the lowest there. That region will behave in a similar manner as an attractor, or central manifold.

But even in that case, we still have a limit cycle encircling the origin. In view of the winding mechanism described above, there should be a possibility of a pattern formation, and that is exactly what is observed. This is of course all very speculative, but it turns out to be a consistent argument.

To analyze this instability more seriously, we can investigate the stability of the origin with regards to small perturbations. Putting $A = \epsilon A_0 \cos(kx) + \epsilon^2 A_1 + \dots$ into Eq.(3-5), we obtain at order 1, the following linear operator:

$$\begin{bmatrix} \mu + \gamma - k^2 & -\nu + \alpha k^2 \\ \nu - \alpha k^2 & \mu - \gamma - k^2 \end{bmatrix} \quad (5-9)$$

Which yields the following eigenvalues:

$$\sigma_{\pm} = \mu - k^2 \pm \sqrt{\gamma^2 - (\alpha k^2 - \nu)^2}$$

This shows that in the linear theory, the detuning for a sinusoidal solution is renormalized as $\nu \rightarrow \alpha k^2 - \nu$. Solving for zero eigenvalues in terms of k yields:

$$k^2 = \frac{\mu + \alpha\nu \pm \sqrt{\gamma^2(1 + \alpha^2) - (\alpha\mu - \nu)^2}}{1 + \alpha^2}$$

Note the similitude between this and the expression of the amplitude of phase locked states (see section 3.6.3). Solving for critical k in terms of γ yields:

$$\gamma_c^2 = \frac{(\mu\alpha - \nu)^2}{1 + \alpha^2} \quad (5-10)$$

Which again yields the critical k as:

$$k_c^2 = \frac{\alpha\nu + \mu}{1 + \alpha^2} \quad (5-11)$$

The corresponding eigenvalues being: $0, 2\alpha(\mu\alpha - \nu)/(1 + \alpha^2)$, with eigenvectors:

$$\left(\frac{1}{\alpha + \sqrt{1 + \alpha^2}}, \left(\sqrt{1 + \alpha^2} - \alpha \right) \right)$$

In comparison, the eigenvalue for $k = 0$ at criticality is given as:

$$\mu \pm i\alpha\nu/\sqrt{1 + \alpha^2}$$

For $\mu > 0$ the transition to the stable pattern is implicitly sub-critical, as we then have also as a solution the simple oscillatory regime. For the pattern to be created we must have some part of the initial condition crossing the anisotropy axis inside the limit cycle. For $\mu = 0$, the origin is marginal, and we then observe a super-critical transition towards the pattern.

This linear analysis is in qualitative agreement with the mechanism described earlier. The pattern appears along an axis close to the anisotropy axis, and numerically we observe that it ends up by merging exactly with the kink solutions when crossing the resonance horn, the wavelength effectively diverging to infinity.

To make a fully non-linear analysis of this instability would require a reduction to a normal form of codimension 2. Indeed, we have two competing instabilities: a Hopf bifurcation of the origin for $\mu \sim 0$ and a saddle-node for $\gamma = \gamma_c$. We should then develop A in one complex amplitude C , describing the amplitude of the spatial structure, and another amplitude B , describing the Hopf bifurcation at the origin. We could do this at the doubly critical point ($\mu = 0, \gamma = \gamma_c$), so we could write:

$$A = (Ce^{ikx} + \bar{C}e^{-ikx})\xi_k + Be^{i\omega_0 t}\xi_0 + \bar{B}e^{-i\omega_0 t}\bar{\xi}_0 + \dots$$

Where ξ_k is the eigenvector for the marginal mode $k = k_c$ and ξ_0 is the eigenvector for the Hopf bifurcation of the origin. The normal form for such a codimension 2 situation can be shown to be of the form:

$$\begin{aligned} \partial_t C &= Cf(|C|^2, |B|^2) \\ \partial_t B &= Bg(|C|^2, |B|^2) \end{aligned} \quad (5-12)$$

This analysis is detailed in section 5.5.2, but we can note that one possible bifurcation of the system described by Eq.(5-12), is the following: There exists a fixed point of C which is hyperbolic. For $\mu > 0$ a supercritical Hopf cycle emerges at the origin, its amplitude following μ . For some value of $\mu = \mu_c$, the cycle meets the hyperbolic point and changes to a heteroclinic orbit. There is then a transition from an oscillatory state to a steady state represented by the amplitude C . This is without doubt the ‘mathematically correct’ interpretation of the winding mechanism described earlier.

One remarkable feature of this transition is that it exhibits the same behavior as the Ising kink, which can be easily comprehended in view of the fact that the pattern is actually built up of Ising walls. In particular, a transition from Ising-like pattern towards Bloch-like pattern is observed when γ is lowered, the pattern thus breaking its parity. We then can observe for some values of parameters, the movement of cells inside the pattern, which behave like a moving inclusion.

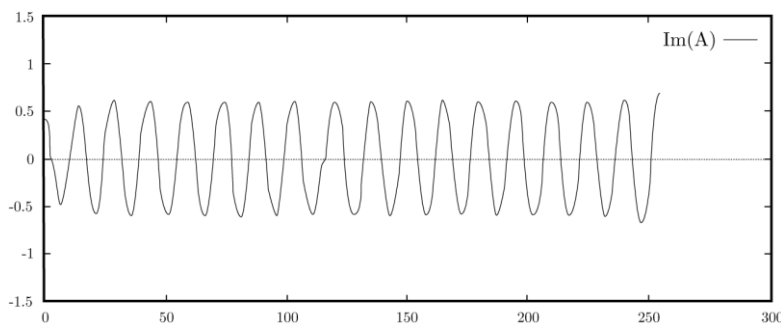


Figure 55: Imaginary part of A showing a pattern with broken chiral symmetry ($\nu = 0.13, \beta = 1.1, \alpha = -1.29$ and $\gamma = 0.327$).

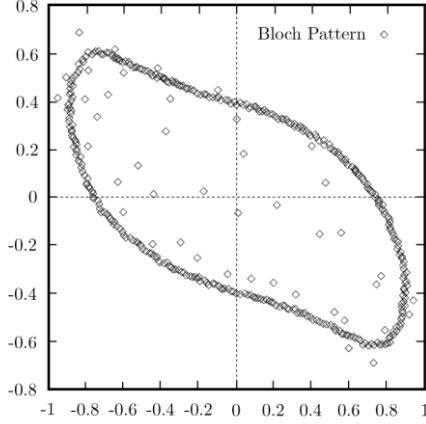


Figure 56: Same as in previous figure, showing the spatial manifold in phase space. We see that we have both right and left handed patterns.

5.5.2 Analysis of the codimension 2 instability

We wish to study the possible instabilities of the zero solution in Eq.(3-5). To do this we study the linearization of Eq.(3-5) around zero and we obtain the following linear operator written in the $A = U + iV$ basis:

$$\begin{bmatrix} -\partial_t + \mu + \gamma + \partial_x^2 & -\nu - \alpha \partial_x^2 \\ \nu + \alpha \partial_x^2 & -\partial_t + \mu - \gamma + \partial_x^2 \end{bmatrix}$$

We can then study the linear stability of modes of the form: $e^{\sigma_k t} e^{ikx} \Psi$. The eigenvalue problem then reads:

$$\begin{bmatrix} -\sigma_k + \mu + \gamma + k^2 & -\nu + \alpha k^2 \\ \nu - \alpha k^2 & -\sigma_k + \mu - \gamma - k^2 \end{bmatrix} \Psi = 0$$

Which gives the following expressions:

$$\sigma_k^\pm = \mu - k^2 \pm \sqrt{\gamma^2 - \nu^2 + 2\alpha\nu k^2 - \alpha^2 k^4}$$

Solving for zero eigenvalue in terms of k yields:

$$k^2 = \frac{\mu + \alpha\nu \pm \sqrt{\gamma^2(1 + \alpha^2) - (\alpha\mu - \nu)^2}}{1 + \alpha^2}$$

The mode is thus marginal with eigenvalue zero for $\gamma = \gamma_c$, which is given by:

$$\gamma_c^2 = \frac{(\alpha\mu - \nu)^2}{1 + \alpha^2}$$

With critical wave vector:

$$k_c^2 = \frac{\mu + \alpha\nu}{1 + \alpha^2}$$

The eigenvalues at this point are given by:

$$\sigma_{k_c}^- = \frac{2\alpha(\alpha\mu - \nu)}{1 + \alpha^2} \text{ and } \sigma_{k_c}^+ = 0$$

We can thus control this instability with the parameter γ . This would yield a straightforward evolution towards a spatially modulated pattern (assuming σ^+ to be negavite), if there wasn't another instability which can compete, namely the homogeneous Hopf bifurcation. By looking at the expression for eigenvalues, we see that for $k = 0$, we have:

$$\sigma_0^\pm = \mu \pm \sqrt{\gamma^2 - \nu^2}$$

We thus see that for $\mu \sim 0$ and $\gamma < \nu$ we have a marginal mode with a Hopf bifurcation. This instability is directly governed by the parameter μ . By adjusting our two control parameters, we can obtain simultaneous marginality of the two instabilities. The system is then in a situation of a codimension 2 bifurcation.

To study this bifurcation, we decompose A in the marginal modes as follow:

$$\begin{pmatrix} U \\ V \end{pmatrix} = (Ce^{ik_c x} + \bar{C}e^{-ik_c x})\Phi + Be^{i\omega_0 t}\Psi + \bar{B}e^{-i\omega_0 t}\bar{\Psi} + \dots \quad (5-13)$$

Where C and B are slowly variable amplitudes in space and time, which we assume to be small of order ϵ . The dots correspond to higher order terms and Φ and Ψ are the eigenvectors at the critical point. We then write our control parameters as:

$$\mu = \mu_c + \epsilon^2 \mu' \text{ and } \gamma = \mu \gamma_c + \epsilon^2 \mu \gamma'$$

With:

$$\mu_c = 0 \text{ and } \gamma_c = \frac{|\nu|}{\sqrt{1 + \alpha^2}}$$

(we choose γ_c to be positive). The eigenvectors and eigenvalues of the two modes at this point are then given by:

$$\sigma_{k_c}^- = -\frac{2\alpha\nu}{1 + \alpha^2} \text{ and } \sigma_{k_c}^+ = 0$$

For the spatial mode. The corresponding eigenvectors are:

$$\Phi^- = \begin{pmatrix} 1 \\ \alpha + \sqrt{1 + \alpha^2} \end{pmatrix} \text{ and } \Phi^+ = \begin{pmatrix} 1 \\ \sqrt{1 + \alpha^2} - \alpha \end{pmatrix}$$

Where we further assume that $\alpha\nu > 0$ to insure the existence of a wavevector. For the temporal mode, we obtain the eigenvalues:

$$\sigma_0^\pm = \pm i \frac{\alpha\nu}{\sqrt{1 + \alpha^2}}$$

And eigenvectors:

$$\Psi^\pm = \begin{pmatrix} 1 \\ \frac{1 \pm i\alpha}{\sqrt{1 + \alpha^2}} \end{pmatrix}$$

We can now go on to perform a multiple scale analysis of the instabilities. We introduce slow times scales with the scaling: $\partial_t \rightarrow \partial_t + \epsilon^2 \partial_T$ and slow spatial scales: $\partial_x \rightarrow \partial_x + \epsilon \partial_X$. With these scalings we get at order 1 the solution of the

linear problem we just found. At order 2, we will get terms from the Laplacian, but these are non-resonant and can thus be incorporated as second order corrections. At order 3, we obtain an expression containing resonant terms. To eliminate them, we introduce the inner product:

$$(f \cdot e^{i(kx+\sigma t)} \Phi) = \frac{k_c \omega_0}{4\pi^2} \frac{1}{(\Phi, \bar{\Phi})} \int_{-\pi/\omega_0}^{\pi/\omega_0} \int_{-\pi/k_c}^{\pi/k_c} (f, e^{-i(kx+\sigma t)} \bar{\Phi}) dx dt$$

Where (a, b) denotes the usual vector inner product.

Using this vector product, we obtain as a solvability condition the normal forms governing the evolution of the amplitudes C and B as:

$$\begin{aligned} \partial_T C &= \left(\frac{\mu' + \gamma' + (\mu' - \gamma') \& (\sqrt{1 + \alpha^2} - \alpha)^2}{1 + (\sqrt{1 + \alpha^2} - \alpha)^2} \right) C - 6(1 + \alpha^2 - \alpha\sqrt{1 + \alpha^2}) |C|^2 C \\ &\quad + \partial_X^2 C - 4 \left(\frac{3 + 2\alpha^2 - \alpha\beta}{1 + \alpha^2} \right) |B|^2 C \end{aligned} \quad (5-14)$$

And:

$$\begin{aligned} \partial_T B &= \mu' B - 2 \left(\frac{3 + 2\alpha^2}{1 + \alpha^2} + i \frac{2\alpha\beta}{\sqrt{1 + \alpha^2}} \right) |B|^2 B + \left(1 + i \frac{\alpha^2}{\sqrt{1 + \alpha^2}} \right) \partial_X^2 B \\ &\quad - 4 \left(\frac{(1 + \alpha^2 - \alpha\sqrt{1 + \alpha^2})(3 + 2\alpha^2 + \alpha\beta)}{1 + \alpha^2} - 2i\alpha\beta (\alpha - \sqrt{1 + \alpha^2}) \right) |C|^2 B \end{aligned} \quad (5-15)$$

5.5.3 Other spatial structuration cases

We have seen how a sub-critical pattern is built up around an attractor surrounded by a limit cycle. In this case, the locked states did not exist, but the presence of dispersion effectively created a stable spatial solution.

In view of this we can now look for other similar situations in phase space where such a winding mechanism could be effective. By looking at the bifurcation set and phase space diagrams in section 3.6.3, we can identify two essential situations.

The first is when the two phase locked states undergo a Hopf bifurcation, while at the same time a global limit cycle appears.

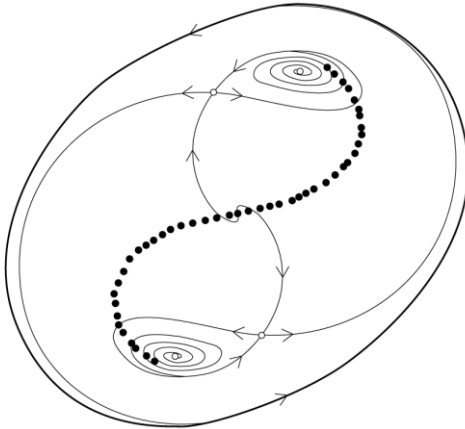


Figure 57: Global Hopf cycle with Hopf bifurcation of phase locked states. Dots show the attractor on which the spatial manifold relaxes.

The other is a transition where a global Hopf cycle appears, surrounding the phase locked states and the hyperbolic points.

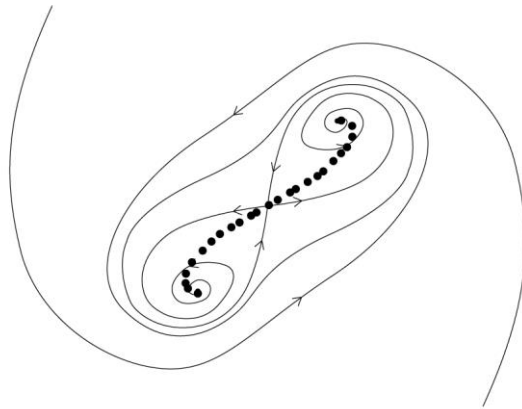


Figure 58: Global Hopf cycle with hyperbolic points. Dots show the attractor on which the spatial manifold relaxes.

In both cases, we numerically observe that for $\alpha \neq 0$, a regular pattern is built up for parameters around the onset of the global cycle.

5.6 PHENOMENOLOGY IN TWO DIMENSIONS

In two spatial dimensions, the pattern forming instability leads to the formation of stripes and hexagons. This transition is generically sub-critical. A typical situation in the case of the instability described in section 5.5.2 is when we have a value of γ such that the Ising-like kinks exist (we can for example take $\mu = 1$, $\nu = 0$, $\beta = 1.5$, $\alpha = -1.2$ and γ ranging from 1.5 down to zero). When lowering γ we eventually come to a regime where hexagons are stable. As they are strongly sub-critical we can then observe the isolated hexagons, by perturbing the stable solution locally. For lower values of γ , these will be the seed for hexagonal paving, which eventually invades all the system.

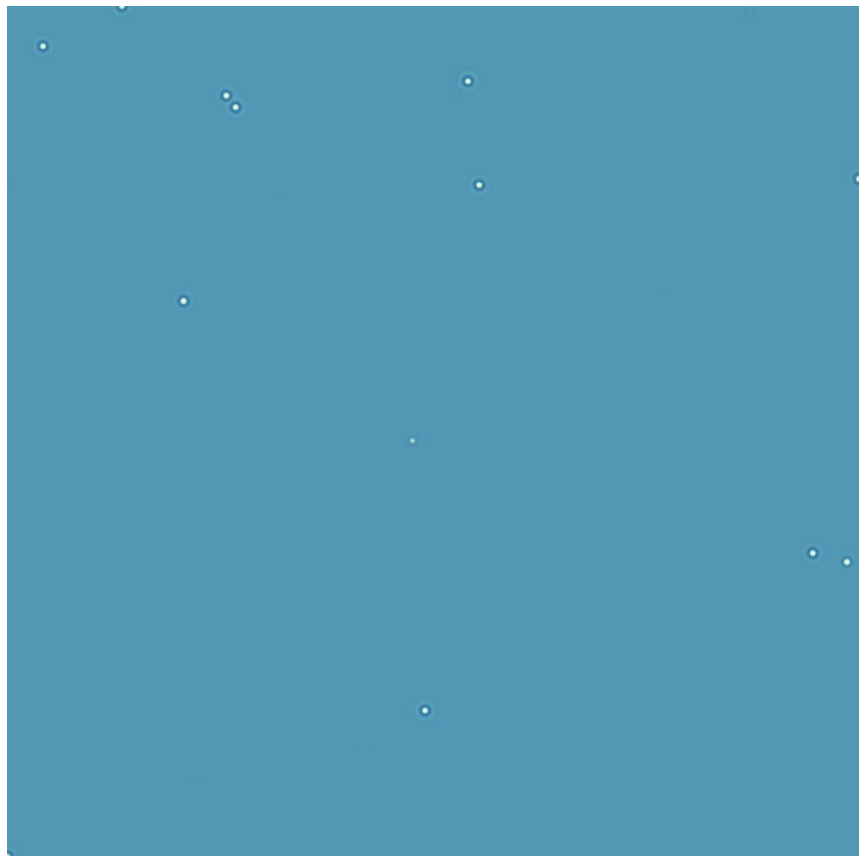


Figure 59: Isolated hexagons in the sub-critical regime.

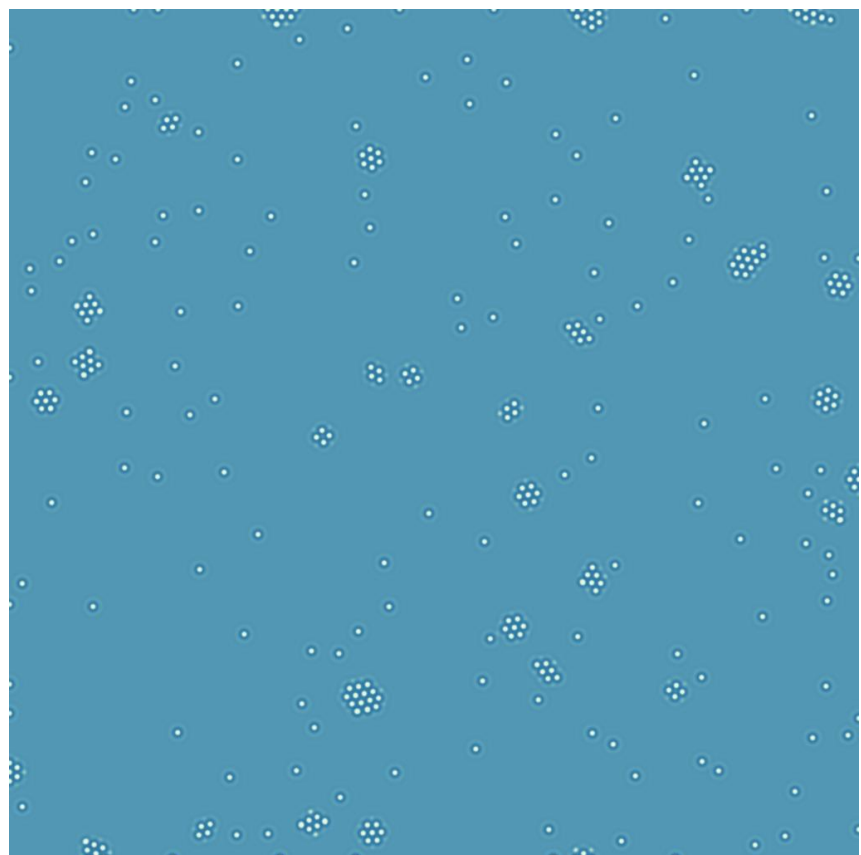


Figure 60: Build-up of the hexagonal pattern around the initials seeds

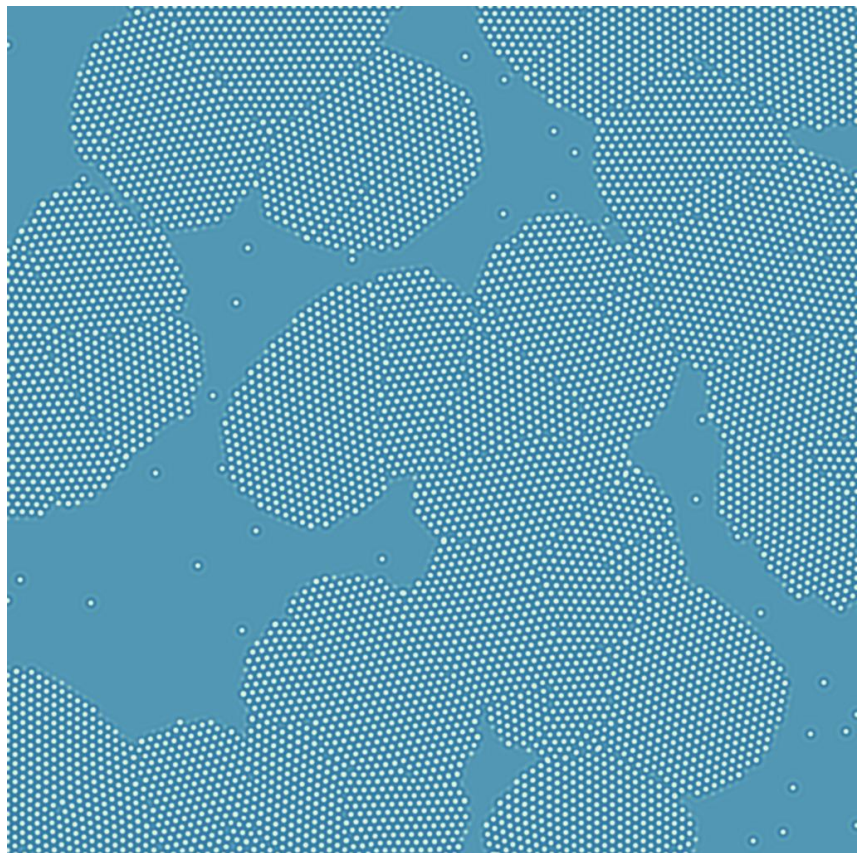


Figure 61: Same as in previous figure

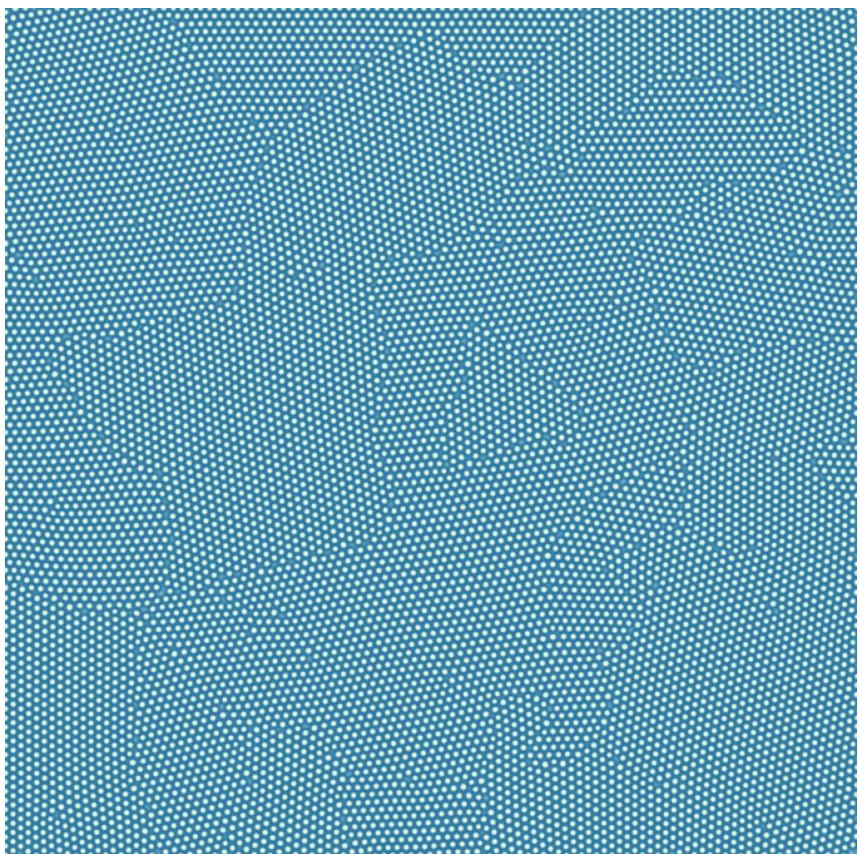


Figure 62: Complete hexagonal pattern

At some critical value of γ , the hexagons lose their stability in favor of stripes. This transition occurs in such a way that neighboring hexagons merge to form a stripe, and these stripes then continue to grow by their tip. We then have a system with stripes forming domains of arbitrary orientations separated by grain boundaries.

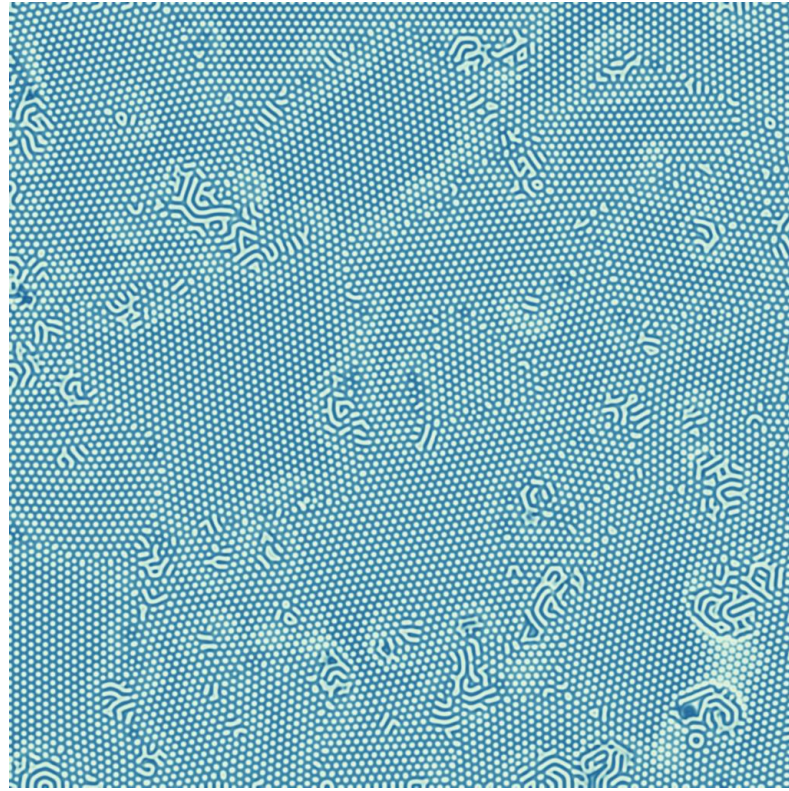


Figure 63: Transition from the hexagonal pattern to the striped pattern

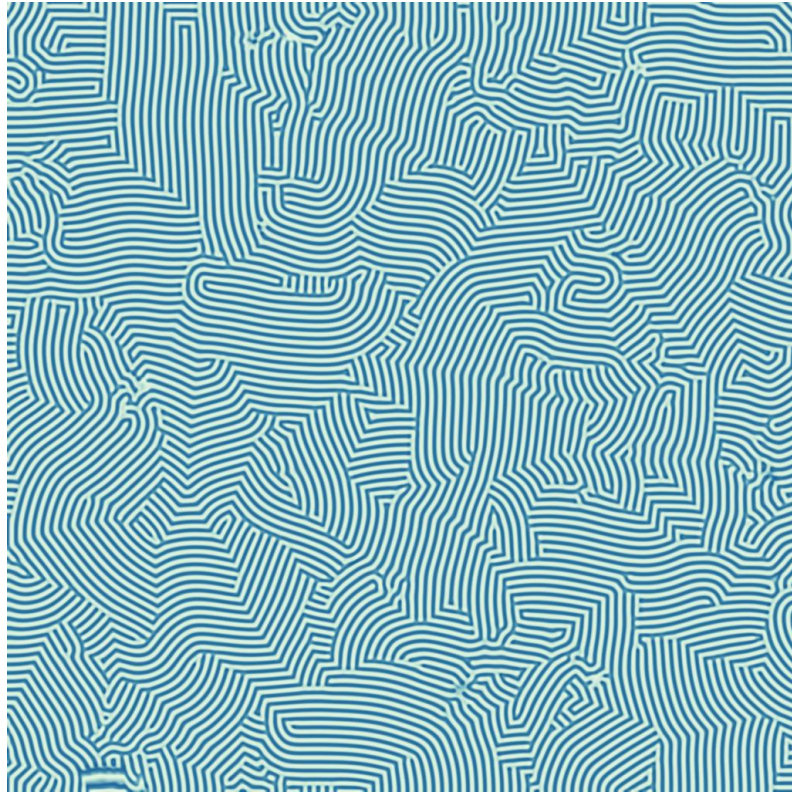


Figure 64: Striped pattern

For some value of γ , the Bloch like pattern becomes favorable. We then have a situation where the stripes have an increased mobility, in the same manner as for usual Bloch walls. This leads to the *cleaning* of the pattern, all grain boundaries being quickly advected to the boundary. Eventually we will come to a situation where the oscillatory regime will be favored, thus leading to the destruction of the pattern. The oscillatory instability effectively invading the system through grain boundaries.

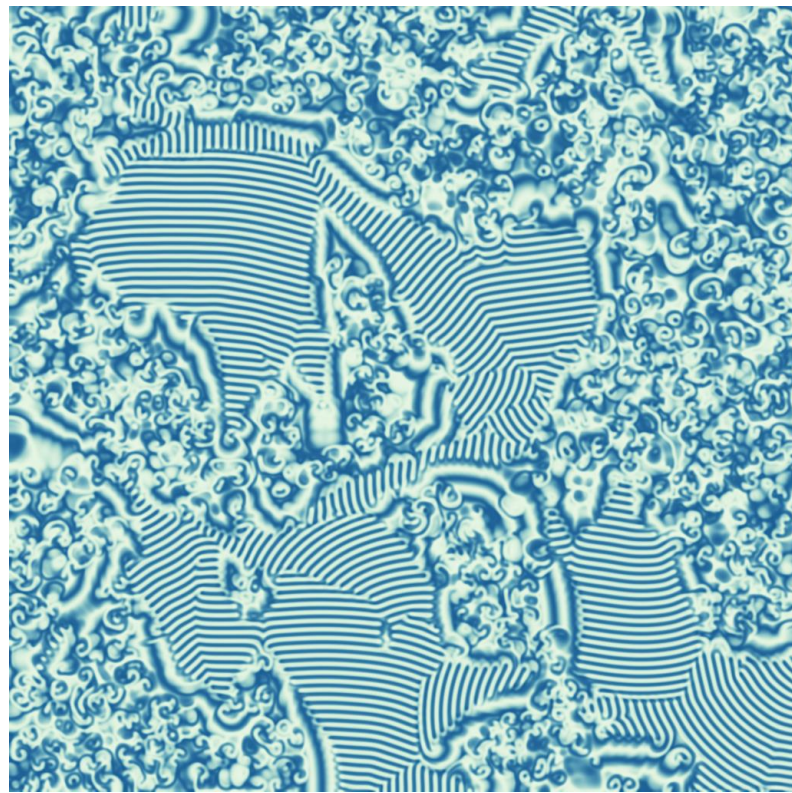


Figure 65: Oscillatory instability of the striped pattern

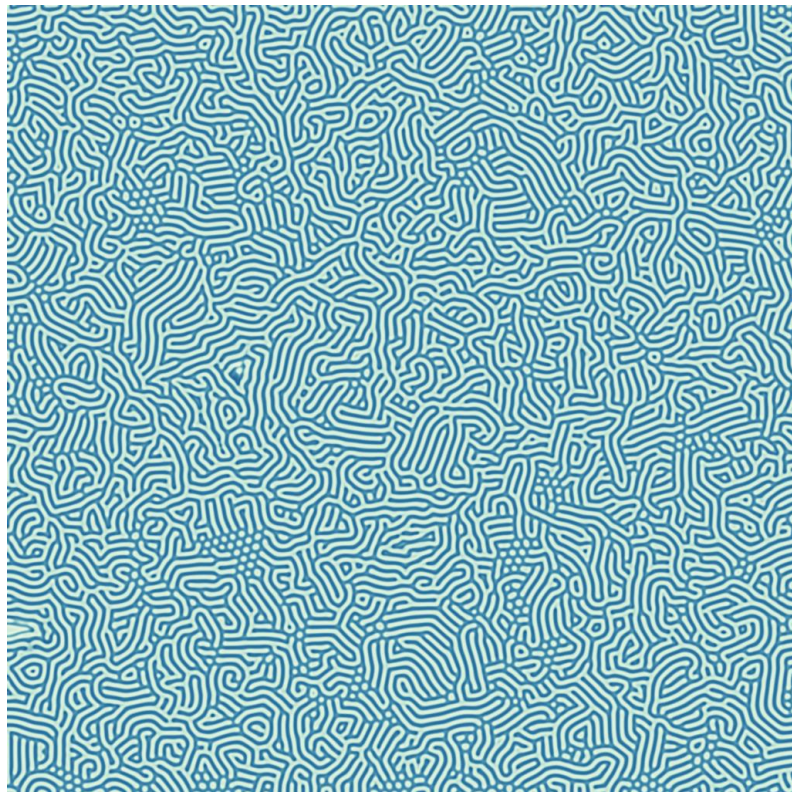


Figure 66: Labyrinthine pattern obtained by a rapid quenching from the oscillatory regime down to the striped regime.

BIBLIOGRAPHY

- [1] L. D. Landau, "On The Theory of Phase Transitions," in *Collected Papers of L.d. Landau*, Pergamon Press, 1965.
- [2] A. C. Newell and J. A. Whitehead, "Finite bandwidth, finite amplitude convection," *Journal of Fluid Mechanics*, vol. 38, p. 279–303, 1969.
- [3] A. C. Newell, "Envelope Equations," in *Lectures in Applied Mathematics, Nonlinear Wave Motion*, vol. 15, Providence, Rhode Island: American Mathematical Society, 1974, pp. 157-163.
- [4] M. J. Feigenbaum, "Quantitative universality for a class of nonlinear transformations," *Journal of Statistical Physics*, vol. 19, p. 25–52, 1978.
- [5] S. Ciliberto, P. Coullet, J. Lega, E. Pampaloni and C. Perez-Garcia, "Defects in roll-hexagon competition," *Physical Review Letters*, vol. 65, no. 19, p. 2370, 1990.
- [6] L. A. Segel, "Distant side-walls cause slow amplitude modulation of cellular convection," *Journal of Fluid Mechanics*, vol. 38, pp. 203-224, 1969.
- [7] A. C. Newell and J. A. Whitehead, "Review of the Finite Bandwidth Concept," in *Instability of Continuous Systems*, H. Leipholz, Ed., Berlin, Springer-Verlag, 1971, pp. 284-289.
- [8] Y. Pomeau and P. Manneville, "Stability and fluctuations of a spatially periodic convective flow," *Journal de Physique Lettres*, vol. 40, no. 23, pp. 609-612, 1979.
- [9] Y. Kuramoto, *Chemical Oscillations, Waves, and Turbulence*, Berlin: Springer-Verlag, 1984.
- [10] L. Kramer, F. Hynne, P. Graae Sorenson and D. Walgraef, "The Ginzburg-Landau approach to oscillatory media," *Chaos*, vol. 4, pp. 443-452, 1994.
- [11] N. B. Abraham and W. J. Firth, "Overview of transverse effects in nonlinear-optical systems," *Journal of the Optical Society of America B*, vol. 7, no. 6, pp. 951-962, 1990.
- [12] H. Meinhardt, "Pattern formation in biology: a comparison of models and experiments," *Reports on Progress in Physics*, vol. 55, no. 6, p. 797, 1992.
- [13] J. E. Wesfried, H. R. Brand, P. Manneville, G. Albinet and N. Boccara, Eds., *Propagation in Systems Far From Equilibrium*, Springer-Verlag, 1988.
- [14] P. Coullet and P. Huerre, Eds., *New Trends in Nonlinear Dynamics and Pattern-Forming Phenomena: The Geometry of Nonequilibrium*, Plenum Press, 1991.

- [15] D. Walgraef, Ed., *Patterns, Defects and Microstructures in Nonequilibrium Systems*, Dordrecht: Martinus Nijhoff, 1987.
- [16] F. Busse and L. Kramer, Eds., *Nonlinear Evolution of Spatio-Temporal Structures in Dissipative Continuous Systems*, New York: Plenum Press, 1990.
- [17] M. C. Cross and P. C. Hohenberg, "Pattern formation outside of equilibrium," *Reviews of Modern Physics*, vol. 65, no. 3, pp. 851-1112, 1993.
- [18] A. C. Newell, T. Passot and J. Lega, "Order Parameter Equations for Patterns," *Annual Review of Fluid Mechanics*, vol. 25, pp. 399-453, 1993.
- [19] H. R. Brand, P. S. Lomdahl and A. C. Newell, "Benjamin-Feir turbulence in convective binary fluid mixtures," *Physica D: Nonlinear Phenomena*, vol. 23, no. 1-3, pp. 345-361, 1986.
- [20] H. R. Brand, P. S. Lomdahl and A. C. Newell, "Evolution of the order parameter in situations with broken rotational symmetry," *Physics Letters A*, vol. 118, no. 2, pp. 67-73, 1986.
- [21] P. Coullet and G. Iooss, "Instabilities of one-dimensional cellular patterns," *Physical Review Letters*, vol. 64, p. 866, 1990.
- [22] P. Coullet, L. Gil and J. Lega, "A form of turbulence associated with defects," *Physica D*, vol. 37, pp. 91-103, 1989.
- [23] P. Coullet and J. Lega, "Defect-mediated turbulence in wave patterns," *Europhysics Letters*, vol. 7, pp. 511-516, 1988.
- [24] D. Rogula, "Large Deformation of Crystals, Homotopy and Defects," in *Trends in Application of Pure Mathematics to Mechanics*, G. Fichera, Ed., New York, Pitman, 1976.
- [25] G. Toulouse and M. Kléman, "Principles of a classification of defects in ordered media," *Journal de Physique Lettres*, vol. 37, no. 6, pp. 149-151, 1976.
- [26] G. Volovik and V. Mineev, "Line and point singularities in superfluid He3," *JETP Letters*, vol. 24, no. 11, p. 561, 1976.
- [27] N. D. Mermin, "The topological theory of defects in ordered media," *Reviews of Modern Physics*, vol. 51, no. 3, p. 591, 1979.
- [28] P. Coullet, C. Elphick, L. Gil and J. Lega, "Topological defects of wave patterns," *Physical Review Letters*, vol. 59, no. 8, p. 884, 1987.
- [29] P. Coullet, L. Gil and D. Repaux, "The Role of Topological Defects in Subcritical Bifurcations," in *Instabilities and Nonequilibrium Structures II*, vol. 50, E. Tirapegui and D. Villarroel, Eds., Springer, 1989, pp. 189-205.

- [30] D. Walgraef and N. M. Ghoniem, Eds., Patterns, Defects and Materials Instabilities, vol. 183, Springer, 1990.
- [31] D. Repaux, "Transition commensurable-incommensurable pour des systèmes macroscopiques hors d'équilibre," Thèse de doctorat, Université de Nice, Nice, 1987.
- [32] P. Coullet, "Commensurate-incommensurate transition in nonequilibrium systems," *Physical Review Letters*, vol. 56, no. 7, p. 724, 1986.
- [33] J. M. Gambaudo, "Perturbation of a Hopf bifurcation by an external time-periodic forcing," *Journal of Differential Equations*, vol. 57, no. 2, pp. 172-199, 1985.
- [34] V. I. Arnold, Chapitres supplémentaires de la théorie des équations différentielles ordinaires, MIR, 1980.
- [35] P. Coullet, J. Lega and Y. Pomeau, "Dynamics of Bloch Walls in a Rotating Magnetic Field: a Model," *Europhysics Letters*, vol. 15, no. 2, p. 221, 1991.
- [36] P. Coullet, J. Lega, B. Houchmandzadeh and J. Lajzerowicz, "Breaking chirality in nonequilibrium systems," *Physical Review Letters*, vol. 65, no. 11, p. 1352, 1990.
- [37] T. Frisch, P. Coullet, S. Rica and J. M. Gilli, "Spiral waves in liquid crystal," *Physical review letters*, vol. 72, no. 10, p. 1471, 1994.
- [38] J. M. Gilli, M. Morabito and T. Frisch, "Ising-Bloch transition in a nematic liquid crystal," *Journal de Physique II*, vol. 4, no. 2, pp. 319-331, 1994.
- [39] K. B. Migler and R. B. Meyer, "Solitons and pattern formation in liquid crystals in a rotating magnetic field," *Physical Review Letters*, vol. 66, no. 11, p. 1485, 1991.
- [40] T. Frisch, "Spiral waves in nematic and cholesteric liquid crystals," *Physica D*, vol. 84, no. 3-4, pp. 601-614, 1995.
- [41] P. Coullet, K. P. Eriksson and F. Plaza, "Qualitative Theory of Defects in Non-Equilibrium Systems," in *Instabilities and Nonequilibrium Structures III*, vol. 64, E. Tirapegui and W. Zeller, Eds., Springer, 1991, pp. 357-363.
- [42] J. Guckenheimer and P. J. Holmes, Nonlinear Oscillations, Dynamical Systems, and Bifurcations of Vector Fields, New York: Springer Verlag, 1983.
- [43] V. S. Zykov, Simulation of Wave Processes in Excitable Media, A. T. Winfree and P. Nandapurkar, Eds., Manchester: Manchester University Press, 1988.

- [44] H. Chaté, "Transition vers la turbulence via intermittence spatiotemporelle," Phd Thesis, Université Pierre et Marie Curie, Paris, 1989.
- [45] M. Le Bellac, Quantum and Statistical Field Theory, Oxford: Oxford University Press, 1992.
- [46] L. N. Bulaevskii and V. L. Ginzburg, "Temperature Dependence of the Shape of the Domain Wall in Ferromagnetics and Ferroelectrics," *JETP*, vol. 18, no. 2, p. 530, 1964.
- [47] S. Sarker, S. E. Trullinger and A. R. Bishop, "Solitary-wave solution for a complex one-dimensional field," *Physics Letters A*, vol. 59, no. 4, pp. 255-258, 1976.
- [48] J. Lajzerowicz and J. J. Niez, "Phase transition in a domain wall," *Journal de Physique Lettres*, vol. 40, no. 7, pp. 165-169, 1979.
- [49] A. Arneodo, P. Coullet and C. Tresser, "Oscillators with chaotic behavior: an illustration of a theorem by Shil'nikov," *Journal of Statistical Physics*, vol. 27, no. 1, pp. 171-182, 1982.
- [50] B. Houchmandzadeh, "Phd Thesis," Université de Grenoble, 1992.
- [51] Y. Pomeau, "Front motion, metastability and subcritical bifurcations in hydrodynamics," *Physica D: Nonlinear Phenomena*, vol. 23, no. 1-3, pp. 3-11, 1986.
- [52] P. Coullet and C. Tresser, "Itérations d'endomorphismes et groupe de renormalisation," in *Comptes rendus de Académie des sciences*, vol. A287, 1978, p. 577-580.